Experimental and Numerical Investigation of Residual Stress for Structural Integrity Assessment of Proximity Girth Welds

by

Sachin Bhardwaj

Thesis submitted in fulfilment of
the requirements for the degree of
PHILOSOPHIAE DOCTOR
(PhD)

Faculty of Science and Technology
Department of Mechanical and Structural Engineering and Materials Science
2022

University of Stavanger
NO-4036 Stavanger
NORWAY
www.uis.no

ISBN: 978-82-8439-143-4
ISSN: 1890-1387
PhD: Thesis UiS No. 679

"Dream, dream, dream. Dreams transform into thoughts and thoughts result in action."

Dr. APJ Abdul Kalam

"I seek refuge in Siva whose power is unequalled, whose glory spreads everywhere, who is Un-born!"

- Ramesh Menon, SIVA PURANA

Preface

This doctoral thesis is submitted in partial fulfilment of for the degree of Doctor of Philosophy (PhD) at the University of Stavanger (UiS), Norway. The research work has been carried out at the Department of Mechanical and Structural Engineering and Material Science, Faculty of Science and Technology, UiS, in the period from July 2019 to September 2022. During this period, the author also performed part-time teaching duties within the department in a 'Structural Integrity' course in Autumn 2020 where topics like different welding processes and Non-Destructive testing were covered. The author was also involved in supervising two master's theses during Spring 2021. The PhD project was mainly funded by the Norwegian Ministry of Education and Research.

Acknowledgements

First and foremost, I would like to express my gratitude to my supervisor, Prof. R. M. Chandima Ratnayake for providing his valued mentorship and support throughout this the project. I am greatly thankful for his periodic challenges and feedback for successful completion of this project. I greatly recognize his technical and professional knowledge and giving me the opportunity to work on this interesting project. His role and support for gathering experimental funding for this project is highly appreciated. I would also like to express my sincere gratitude to my co-supervisor, Prof. Morten Andre Langøy for providing his valuable and timely feedback during the evaluation stages of my PhD coursework.

Secondly, I would also like to thank Associate Professor Arvind Keprate and co-authors based at PSI and NTNU for providing me their constant support throughout this project. I would like to acknowledge the support of all the IMBM lab engineers and staff members, especially Jan-Tore Jakobsen, Emil S. Kristiansen and Belal Ghazei Alnajar without whom this experimental study would not have been possible. Special mention goes to Ole Jørgen Engelsvoll from Valide in providing their financial support for securing material and components for this experimental study. I would also like to thank Arve Hovland, Constantinos Tesfay and Petter Lunde from Rosenberg Worley and Q-Lab respectively, for providing industrial support in the fabrication and testing of samples. I would also like to acknowledge role of IFE (Institute for energiteknikk), Norway and UiScatt through which beam time for conducting neutron diffraction experiments at Paul Scherrer Institute (PSI), Switzerland was possible. Furthermore, the role of SINTEF is highly appreciated for receiving their extensive support in conducting X-ray diffraction experiments.

Lastly, I would like to thank my parents, my lovely wife, ‘Tapasya’, my beautiful niece, ‘Swara’, friends and family for providing their constant support and encouragement and being a part of this wonderful journey.

Abstract

Over the last decade, there has been a growing interest in the life extension of existing welded structures in offshore and renewable industry. During this phase of extension, maintaining minimum distance between welds in highly compact welds of piping's, pressure vessels etc, are highly debatable. Weld placement is a subject often contested by contractors and inspection engineers when deciding how to maintain a 'minimum distance' between repair and existing welds. International fabrication codes and standards are inconclusive in recommending minimum distance criteria between newly fabricated welds; however, it is completely lacking a description for this criterion for repair weld placement. This research investigates the challenges that are encountered due to proximity of welds on structural integrity of aging welded structures. Case study-based research method is used to perform this large-scale experimental study and its validation by use of non-destructive measurement results with numerical models for estimation of residual stresses in proximity girth welds.

Firstly, weld placement criteria for maintaining 'minimum distance between welds' was investigated across various domains of fabrication and repair codes in offshore structures, pipeline s & piping's. A clear lack of consensus was found when it comes to defining the criteria after assessment of various repair and fabrication codes and no reported technical justification was found in open literature. A detailed literature review for residual stress profile estimations at a distance away from the weld toe in defect assessment procedures of API 579, BS 7910, R6, etc., was conducted and which were found to be practically non-existent for girth weldments. Key parameters like pipe geometry (radius to diameter ratio), heat input per unit volume of weld area (J/mm^3), etc. have been identified as important parameters in determining full field residual stress profiles at a distance away from the weld toe.

Secondly, welding procedure qualification records and residual stresses profiles were established for proximity girth weld on S355 grade pipe weldments in a large-scale experimental study. The welding procedures qualification record (WPQR) for proximity joints was performed as per the EN 15614-1 & NORSOK M-101 code, which is a widely accepted welding qualification code. Sufficient mechanical test-based evidence was gathered to further investigate the effect of welding-induced residual stress profiles (beneficial or deleterious) developed between proximity welds. A non-destructive method of neutron diffraction (ND) was used to measure full field residual stresses between adjacent proximity welds at different depths, fabricated with two different welding processes.

Furthermore, an experimental based XRD study was performed to validate numerical base thermo-mechanical simulation as recommended in level three, defect assessment procedures of structural integrity, for assessing critical weld joints. The findings from this research study proposes thickness and transverse distribution region of harmful tensile residual stresses which are developed at weld root toe for proximity welds. These findings enable practitioners to understand the importance of residual stresses at a distance away from weld toe for proximity welds during pipe replacement procedures with due consideration given to component geometry and heat input of welding process.

Keywords: Offshore structures, piping girth welds, proximity welds, repair welds, welding-induced residual stress, neutron and X-ray diffraction, welding procedure qualification record, minimum distance between welds

List of Appended Articles

Paper I: Bhardwaj, Sachin; Ratnayake, R.M.C. (2020) Challenges due to welds fabricated at a close proximity on offshore structures' pipelines and piping: state of the art. I: *ASME 2020 39th International Conference on Ocean, Offshore and Arctic Engineering* - ISBN 978-0-7918-8434-8 DOI: 10.1115/OMAE2020-18586

Paper II: Bhardwaj, Sachin; Ratnayake, R.M.C. (2020) Residual stress estimation in defect assessment procedures at weld toe and away locations on girth welds: Review of key parameters. *Theoretical and Applied Fracture Mechanics Journal.* ISSN0167-8442.Volume111.DOI: 10.1016/j.tafmec.2020.102848

Paper III: Bhardwaj, Sachin; Ratnayake, R.M.C. (2021), Estimation of welding-induced plastic zone size and residual stress levels: Linear heat input approximation. I: *ASME 2021 40th International Conference on Ocean, Offshore and Arctic Engineering.* ISBN 978-0-7918-8519-2.DOI: 10.1115/OMAE2021-62843

Paper IV: Bhardwaj, Sachin; Ratnayake, R.M.C. (2022) Welding procedure qualification record (WPQR) for welds fabricated at proximity. *The International Journal of Advanced Manufacturing Technology.* ISSN 0268-3768. DOI: 10.1007/s00170-022-09022-5

Paper V: Bhardwaj, Sachin; Ratnayake, R.M.C; Polatidis, Efthymios; Capek, Jan (2022) Experimental investigation of residual stress distribution on girth welds fabricated at proximity using neutron diffraction technique. *The International Journal of Advanced Manufacturing Technology.* ISSN 0268-3768. DOI: 10.1007/s00170-022-09574-6

Paper VI: Bhardwaj, Sachin; Sigmund Kyrre Aas; Ratnayake, R.M.C. (2022) Experimental & Numerical investigation of residual stresses in proximity girth welds (*submitted to Journal*)

List of Non-Appended Articles

Paper I: Bhardwaj Sachin; Ratnayake, R.M.C.; Keprate, Arvind; Ficquet, Xavier (2020), Machine learning approach for estimating residual stresses in girth welds of topside piping. I: *ASME 2020 39th International Conference on Ocean, Offshore and Arctic Engineering.* ISBN 978-0-7918-8434-8.DOI: 10.1115/OMAE2020-18703

Paper II: Bhardwaj, Sachin; Ratnayake, R.M.C.; Keprate, Arvind (2020), Review of Weld Quality Classification Standard and Post Weld Fatigue Life Improvement Methods for Welded Joints. *Lecture Notes in Civil Engineering* ISSN 2366-2557.Volume 110.s.257-270. DOI: 10.1007/978-981-15-9121-1_20

Paper III: Bhardwaj, Sachin; Ratnayake, R.M.C. (2021), Comparison between shrinkage strain and FEM thermo-mechanical method for estimation of welding induced residual stresses. I: *ASME 2021 40th International Conference on Ocean, Offshore and Arctic Engineering.* ISBN 978-0-7918-8519-2.DOI: 10.1115/OMAE2021-62895

Paper IV: Bhardwaj, Sachin; Keprate, Arvin; Ratnayake, R.M.C. (2022), Residual Stress Prediction of Welded Joints Using Gradient Boosting Regression. *Intelligent Technologies and Applications. INTAP 2021. Communications in Computer and Information Science*, Volume 1616. Springer, Cham. https://doi.org/10.1007/978-3-031-10525-8_4

Abbreviations

EPRI	Electric Power Research Institute
FFS	Fitness for service
FEM	Finite element method
HAZ	Heat affected zones
JIP	Joint industry project
NDT	Non- destructive technique
ND	Neutron diffraction
NCS	Norwegian continental shelf
O&G	Oil & Gas
PWHT	Post weld heat treatment
PVRC	Pressure Vessel Research Council
SCC	Stress corrosion cracking
SCF	Stress concentration factor
TWI	The Welding Institute
WP	Weld proximity
WRS	Welding induced residual stresses
WPQR	Welding procedure qualification record
XRD	X-ray diffraction

Table of Contents

Preface iv

Acknowledgements v

Abstract vi

List of Appended Articles viii

List of Non-Appended Articles x

Abbreviations xi

Part 1: Thesis Summary xiv

1. Introduction 1

1.1 General Overview 1

1.2 Research Gaps 4

1.3 Research Aim 7

1.4 Research Limitations 7

1.5 Thesis Outline 8

2. Research Methodology 9

2.1 General 9

2.2 Research Methodology 10

3. Discussion and Conclusion 13

3.1 General 13

3.2 Overview of Appended Papers 15

Paper I: Challenges due to welds fabricated at a close proximity on offshore structures, pipelines and piping: state of the art 15

Paper II: Residual stress estimation in defect assessment procedures at weld toe and away locations on girth welds: Review of key parameters 17

Paper-III: Estimation of welding-induced plastic zone size and residual stress levels: Linear heat input approximation 18

Paper IV: Welding procedure qualification record (WPQR) for welds fabricated at close proximity 19

Paper V Experimental investigation of residual stress distribution on girth welds fabricated at close proximity using the neutron diffraction technique 20

Paper VI: Experimental and Numerical investigation of residual stresses in proximity girth welds 23
Research Contributions 26
Future Research 28
Appendices-1 29
References 30
Part II: Papers 35

Table of Figures

Figure 1 a) Average repair rates for different types of products, b) average repair rates considering commonly used material grades 2
Figure 2 – Research Plan - Multiple case study-based approach 12
Figure 3: Weld deposition area A_w: wp plastic zone width illustration 18
Figure 4: Neutron diffraction measurement points for proximity welds 20
Figure 5: WRS distribution at 6mm depth for different WPs in the a) hoop & b) axial direction 22
Figure 6: Axisymmetric FEM model of existing and repair welds reproduced from weld macrographs with XRD and ND measurement locations 23
Figure 7: Axial residual stress distribution a), through thickness at the existing weld toe b) decomposed stress components at the existing weld toe 25

List of Tables

Table 1 – Overview of international codes for defining criteria for the minimum distance between close proximity welds 16

Part 1: Thesis Summary

1. Introduction

1.1 General Overview

Welding is defined as the most common thermally driven joining process used in the fabrication of offshore and onshore structures [1]. Welding involves a phenomenon of a multi-physics interaction between thermal, mechanical, microstructure, phase transformations, etc. properties which make understanding it complicated in nature [2]. Various defects in welds in large steel structures are categorized in different quality levels for acceptance according to their nature of severity as per ISO 5817 [3]. The average repair rate of welds in the oil and gas (O&G) and power industries are found to be in the range of 2.3–3%, with the majority found in onshore pipelines and piping structures as shown in Fig.1a, as per The Welding Institute's (TWI) multi-industry survey [4]. As shown in Fig. 1b, average repair rates found in piping and pressure vessels are found to be maximum in low-alloy high-strength steels such as S355.

a)

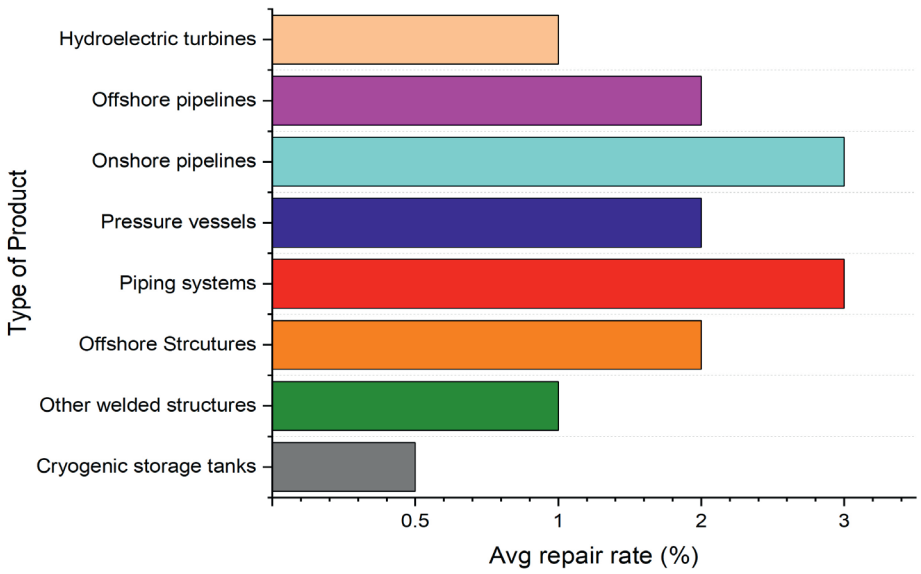

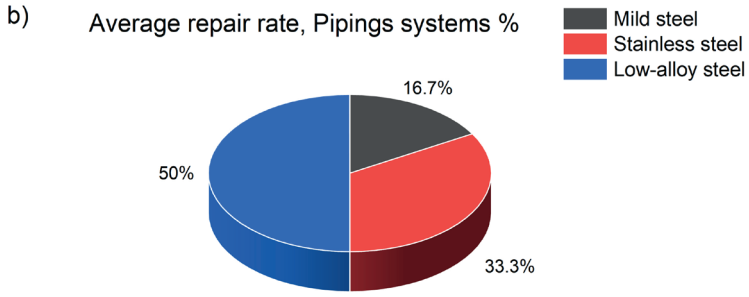

Figure 1 a) Average repair rates for different types of products, b) average repair rates considering commonly used material grades

As per a recent survey by the Electric Power Research Institute (EPRI) for power piping, 40% of the repair welds have resulted in failure due to cracking within the first year of service [5, 6] and 70% of failures of in-situ repair welds are due to no post-weld heat treatment (PWHT). Various factors are responsible for repairs in welds such as welding procedures [7, 8], the qualification of welders, material grade, etc., however poor/incorrect fit-up or inaccessibility to welds has been identified as a second major factor after welder's skill followed by welding procedures in determining the average rate of repair in welds [4].

Poor fit-ups or inaccessibility to welds are categorised as the major reasons for defects in welds that often lead to the replacement of entire lengths of pipes, e.g., in highly compact piping layouts [4]. Welds are identified as the most vulnerable sites for crack initiation due to the presence of geometric discontinuities, leading to high stress concentration at weld cap and root toe locations [3]. Weld proximity criteria as per ISO 19902 [9]& API RP 2A [10]-Code Petroleum and natural gas industries code — Fixed steel offshore structures, recommends an arbitrary distance to be maintained between adjacent braces weld toes without taking the thickness and diameter of joining members into consideration. Widely accepted process piping ASME B31.3 [11] code recommends no guidance regarding maintaining these

distances and is often left to engineering judgement. Due to cycles of heating and cooling of adjacent welds and complex interactions taking place between various physics domains such as thermal, metallurgical and mechanical during welding, proximity regions are prone to failures [12]. Various degradation mechanisms like corrosion, residual stress, fatigue and fracture are well-associated with causing major accidents in large offshore floating structures in the past and still pose a greater challenge in present day in-service structures [13].

Various experimental studies have been performed by researchers in the past to estimate residual stress in high restraint proximity regions of offshore jacket brace joints, which are welded with similar qualified welding processes [14-16]. However, in cases of proximity weld joint configurations, which are found commonly in life extension and replacement stages of in-service piping and pipelines, the ASME Sec IX code recommends [17, 18] separate qualification of welding procedures for which no study was found in open literature as per the authors' assessment [19]. Repair standards also lack clear guidelines in specifying the distance for repair weld placement in proximity to existing weld [19]. Repair welds are defined as the removal of unaccepted areas within a weld, and re-welding and reinstating original geometry during replacement is equally applicable for aging welded structures. The replacement procedures mentioned in API 1104 [20] and ASME Sec IX [17, 18] highlight the importance of using separate qualified welding procedures for repair welds [21, 22]; however, in practise, engineering judgement of non-overlapping heat-affected zones (HAZ) or maintaining some arbitrary distance is widely adopted.

The most determinantal effect due to repair welds is the development of harmful tensile residual stresses in pipe replacement procedures of girth welds[23]. Welding-induced residual stresses (WRS) has been identified as a major cause of stress corrosion cracking (SCC) in process and power piping's in repair welds due to stress triaxiality developed around weld toe regions [6]. Weld repairs during replacement procedures have been

identified as an integrity concern for aging pressure vessels and piping structures, which highlights the importance of correct estimation of residual stresses around weld toe regions [22] as their original state is influenced. Residual stress assessment in defect assessment procedures like API 579, BS 7910 and R6 [24-26] are practically non-existent for regions away from weld toes [27]. Due to the presence of high restraint in addition to existing restraint of girth welds in replacement procedures the development of high WRS is inevitable. The development of tensile residual stresses accelerates crack propagation [28], which can be considered one of the major contributing factors for the maximum failure rate of 30% due to fatigue and followed by 19% corrosion in piping's and tubes as per a recent survey of more than 1,000 cases in oil and gas and maritime by DNV [29].

These uncertainties in estimating residual stresses around weld toe regions in close proximity weld situations has led to major accidents in power and process piping [23] during repair welding. Qualification of new welding procedures for repair proximity welds needs to be established in contrast to pre-qualified procedures. WRS profiles estimation needs to be established for distance away from weld toe regions which are currently unavailable in defect assessment procedures by validating experimental with numerical results.

1.2 Research Gaps

1. **International fabrication codes and standards recommend limited or no guidelines for specifying criteria for maintaining a minimum distance between close proximity welds. This criterion is scattered across various fabrication codes for components like offshore structures, piping and pressure-containing equipment.**

Maintaining a minimum distance between welds is often debated among contractors, engineers and fabricators. Various international fabrication codes and standards provide ambiguous guidelines and demonstrate a

clear lack of consensus in their detailed assessment. Some codes recommend maintaining these distances based on engineering judgement, mutual agreement or detailed design checks. This causes high ambiguity among contractors and engineers during replacement procedures of in-service pipes for maintaining these distances due to compact layouts, restrained geometries, inaccessible welds and proximity to existing welds of branches, nozzles, valves, etc. Repair weld placement guidelines are not specified in these standards with the exception some limited guidance on avoiding overlapping of HAZ and maintaining some set arbitrary distance between welds [30]. There is a need to harmonise various fabrication codes as this criterion is scattered and no technical justification is provided. There is a clear need to identify key factors influencing these distances and investigate issues like the use of unqualified welding procedures, harmful residual stress profile development between proximity welds based on this large-scale experimental study.

2. **Fitness-for-service (FFS) codes and standards used in defect assessment procedures of weld centres and toe locations are found to be overly conservative for estimating residual stress profiles. Recommended profiles in FFS codes for WRS are practically non-existent for distances away from weld toe locations, which needs to be estimated for proximity welds.**

FFS codes like BS7910 and API-579 [25, 26] are found to be overly conservative [27, 31] for estimating WRS in girth welds due to the multi-physics nature of residual stress development. These FFS schemes are based on thickness or heat input of the welding process and are lacking in capturing key parameters for defining full field WRS profiles. Key parameters like thickness and heat input were identified as part of the Pressure Vessel Research Council (PVRC) Phase 1 [32] and key parameters like pipe geometry (radius to thickness ratio), heat input

(J/mm^2) and plastic zone-based shrinkage zones were identified as part of the PVRC Joint industry project (JIP) Phase 2 [33]. These parameters are vital for determining full field residual stress profiles at a distance away or at close proximity from existing weld toes, which is currently lacking in available FFS codes. Fast and effective numerical methods should be established for estimating WRS at weld toe locations. The global bending behaviour of compressive WRS on the outside and tensile on the pipe's inner surface are found to be deleterious for SCC cracking in piping's girth weld at a distance away from weld toe locations depending on the component geometry and heat input of welding process. Hence, there is a clear need to experimentally measure WRS around weld toe regions and validate with numerical models.

3. **Separate qualification of welding procedures is recommended by widely accepted welding codes like ASME Section IX for the repair of girth welds. However, in practise, these welding procedures are qualified without taking into account the change in mechanical and physical properties between proximity welds.**

"*Repair and re-repair welding may be performed using the same WPS as for the original weld, or a separately qualified procedure*" as stated in NORSOK M-101 [18] and ASME Sec IX [17], widely accepted codes in welding qualification. Maintaining sufficient distance between repair and existing welds is practically impossible in high restraint compact layouts of piping during pipe replacement procedures; hence, their qualification may be backed by a separate welding procedure qualification record (WPQR). Necessary mechanical testing (HAZ Charpy V-notch) needs to be performed to assess their integrity; however, change in mechanical properties needs to be verified as demonstrated by researchers for critical offshore jacket K-brace structures [14, 34, 35] where an influence of residual stress in fatigue loading was observed between the proximity regions of adjacent welds. Proximity regions are subjected to multiple cycles of heating and cooling and develops stress triaxiality hence, harmonised guidance based on

numerical and experimental validations are considered beneficial as per level 3 assessment of FFS codes [2].

1.3 Research Aim

The following topics were investigated:

- Gap assessment of international fabrication codes and standards recommending criteria for maintaining a minimum distance between close proximity welds.
- Identification of key parameters that are dominant in the development of residual stresses at distance away from weld toe locations.
- Establishing welding procedures' qualification records (WPQR) for close proximity repair weld configurations in accordance with EN and NORSOK welding codes
- Experimental investigation of residual stresses on close proximity welds by use of Neutron and X-ray diffraction (XRD) technique and its validation by the finite element method (FEM) based thermo-mechanical simulation in ABAQUS.

1.4 Research Limitations

This research work has the following limitations:

- Although a broad assessment of international codes and standards has been performed to highlight minimum distance criteria across various industries, the focus of this research has been limited to offshore structures, pipelines and the piping industry.
- Repair code guidelines for close proximity weld placement have been assessed for available codes and standards; however, in practise organizations have set their internal recommended

practises for critical weld joints, which are not available in public domain.

- This experimental study was performed on the most common structural steel grade, S355, used in the O&G industry and component geometry with a radius of thickness (r/t) ratio of 10. Repair proximity placement was maintained between 0.5 and 1.5 times the thickness of the joining member based on the industrial feedback and repair codes' guidelines.
- The numerical study performed in finite FEM is based on thermo-mechanical simulation without considering the effect of phase transformation and type-2 inter/intra-granular level stresses.

1.5 Thesis Outline

This thesis is broadly divided into two main sections. Part 1, Chapter 1 briefly presents the introduction of this research with a general overview followed by problem statements, the research aims and limitations. Chapter 2 presents the research methodology adopted for this research which summarises the results for all appended articles followed by a suitable conclusion and future research. Part 2 of this thesis is comprised of all appended conference and journal articles based on the research outcomes of this numerical and experimental study.

2. Research Methodology

2.1 General

Robert K Yin's classic definition of case study-based research was "*A case study is an empirical inquiry that investigates a contemporary phenomenon in depth and within its real-life context, especially when the boundaries between phenomenon and context are not clearly evident*" [36]. However, Robert E. Stake provided a different definition: "*A case study is the study of the particularity and complexity of a single case, coming to understand its activity within important circumstances*" [37]. Six types of case studies were defined by Baxter and Jack [38] as 1) Explanatory, 2) Exploratory, 3) Descriptive, 4) Muti-Case, 5) Intrinsic and 6) Instrumental. Every research method should be used at a fixed stage of an investigation, i.e., exploratory, descriptive, and explanatory. Case study-based methods have often been associated with providing explanations during the exploratory phase of a study whereas surveys are considered best in the descriptive phase of a study in contrast to experiments which are considered best in the explanatory phase.

Mixed research techniques of combining quantitative and qualitative methods into a single study are gaining attention nowadays. In general, every research method can be used in a holistic way by the inclusive combination of all methods, i.e., experiment, survey, archival analysis, history and case study [36]. To use these methods effectively in a holistic or embedded manner, researchers should know when to use each method by identifying its limitations [38]. To answer 'how' and 'why' research questions case study-type research is used in a contemporary set of events over which the investigator has little or no control in the explanatory phase of the study. Experiments are equally important in answering 'how' and 'why' research questions but require careful control of behavioural events and must focus on contemporary events.

2.2 Research Methodology

Multiple case studies are defined by Robert K. Yin [36] as "*A multiple case study enables the researcher to explore differences within and between cases. The goal is to replicate findings across cases. Because comparisons will be drawn, it is imperative that the cases are chosen carefully so that the researcher can predict similar results across cases, or predict contrasting results based on a theory*". Multiple case studies have been selected to create a compelling, stronger evidence-based expanded theory [39]. To design a multiple case study, we followed the steps of Baxter and Jack [38, 40]and Miles and Huberman [38, 40].

- **Propositions**: These are based on successful literature, personal/professional experience, generalizations, etc. In this current case study, broad empirical observations/propositions are proposed after feedback from industry experts, assessment of codes, etc., regarding placement of repair welds in close proximity to existing welds in pipe replacement procedures. Gap assessment of various codes and standards, feedback from industrial stakeholders and historical recorded failures were the main propositions in this study.

- **Application of a conceptual framework**: Identification of main propositions continue to develop during the progress of study with the development of a conceptual framework. Timely discussion with stakeholders is presented to avoid research becoming inductive or deductive and being too driven by the initial proposed framework.

- **Development of research questions:** After detailed literature investigations, research objectives were framed. Data collection from experimental results served as a potential tool to answer 'how' and 'why' research questions.

- **Linking data to propositions:** Data collection and analysis take place concurrently during the research period, although this largely depends on the type of the case study. Tools like use of multiple sources of evidence, establishing a chain of evidences and case study review by key informants were used to converge the data and reach a logical conclusion as proposed by Yin [36].

- **Interpreting findings:** Experimental tests were used in this case study to match findings with initial propositions. This criteria for judging the research design were able to answer the 'how' and 'why' research questions.

In this work, a mix of inductive and deductive reasoning (i.e., abductive approach) was adopted to determine the technical explanation for welds placed at proximity. An inductive approach was applied in the initial part of this research where specific observations for determining minimum proximity criteria were applied on various structures, pressure-containing equipment, etc. to derive broader generalisations. However, in the latter half of this thesis, experimental investigation was performed to determine a causal relationship as per the explanatory phase of this research. The current research study results from appended articles were established with steps of case study-based research as shown in Figure 2.

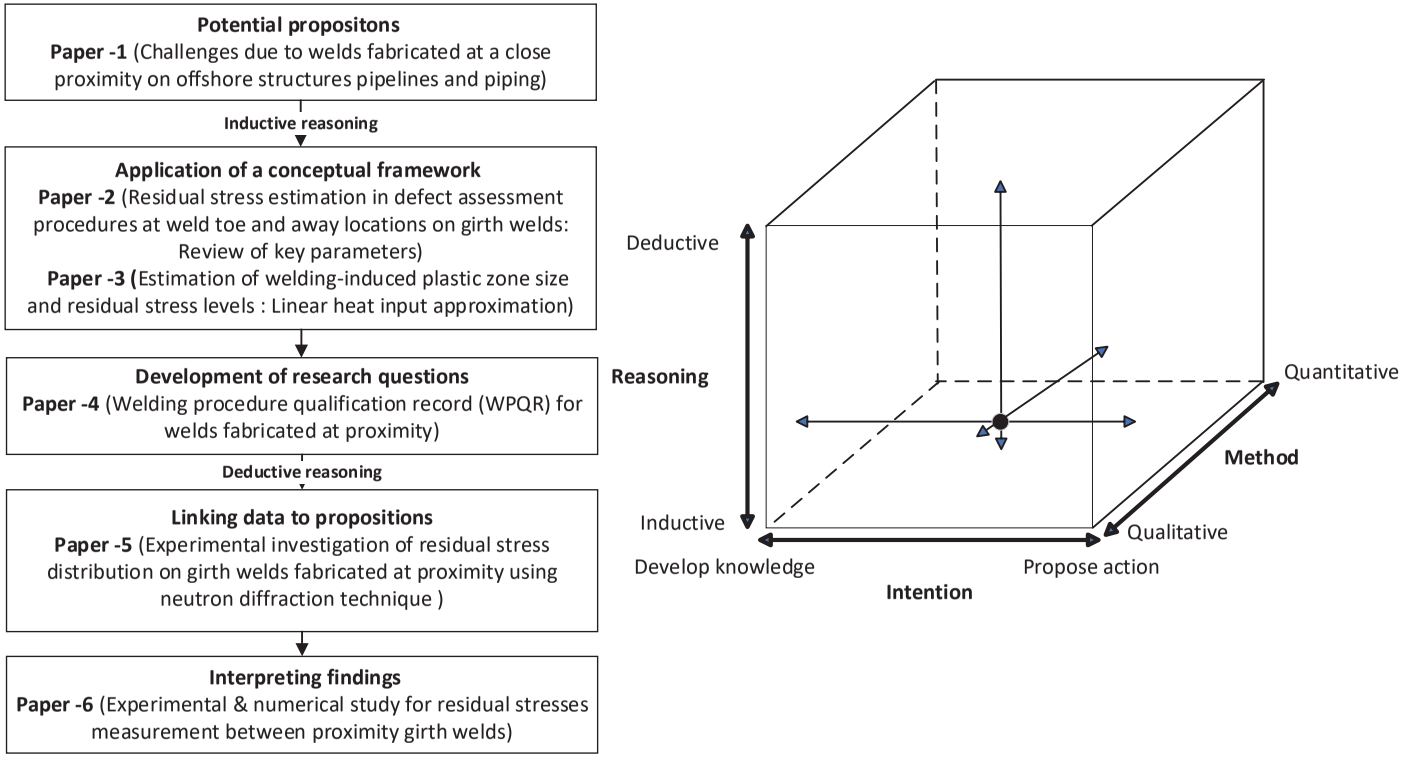

Figure 2 – Research Plan - Multiple case study-based approach

3. Discussion and Conclusion

3.1 General

Weld placement guidelines for newly fabricated steel structures are scattered all over standards and codes as criterion for maintaining a minimum distance between girth welds, which varies by a factor of 4–5 times the thickness for plates and 1–1.5 times the diameter for tubular structures. For example, the support structure code for wind turbines DNVGL-ST-0126 [41] recommends maintaining a distance of 300 mm between girth welds and states "*The minimum weld distances mentioned above have been derived based on practical experience. Shorter distances may be suitable but need to be proven both with respect to impact on stress concentration factor (SCFs) as well as residual stresses*". Similarly, the NORSOK M-601 code for welding and inspection of piping [42] recommends "*The distance between girth welds should be minimum one outside diameter of the pipe. If this for practical reasons is not possible the minimum distance between welds may be reduced to 2 times wall thickness or 50 mm (between the weld toes) whichever is the greatest, but not for standard pipe fittings*". Similarly, the DNVGL-ST-F101 Submarine pipeline systems code [30] recommends that "*Girth welds should be separated at least 1.5 pipe diameters or 500 mm, whichever is larger. Whenever possible girth welds shall be separated by the maximum possible distance".*

However, repair weld placement in highly restrained, compact pipe welded configurations needs to be investigated with due care as their criterion mentioned in repair codes are even more ambiguous. Weld placement guidelines for constrained geometry welds in the NORSOK M-601 code for welding and inspection of piping [42] recommends that "*If a flange is designed with a flange neck, the minimum distance between weld and flange rounding should be 0.5 times the plate thickness, but at least 5 mm*". Repairing Hazardous Liquid Pipelines, API 2200 [43] states that repair welds shall be installed less than 152 mm or

6 inches from an existing weld and the submarine pipeline systems code DNV-ST-F101 [30] recommend that "*It is acceptable to cut less than 25 mm providing it can be documented by macrograph that the entire HAZ has been removed".* These guidelines in pipe replacement procedures need to be standardised by providing a detailed technical explanation for maintaining these distances. Key parameters affecting the residual stress profiles of close proximity welds need to be investigated by use of non-destructive techniques (NDT) and the qualification of separate welding procedures. Hence, a detailed experimental and numerical investigation was planned for this research on proximity weld placement.

The criteria for maintaining minimum distances between close proximity welds are generally based on the factors thickness or diameter. A detailed gap assessment of all fabrication codes was performed across structural and pressure-containing equipment for fabrication and repair welds and presented in Paper 1. A detailed literature review of key parameters identified in defect assessment procedures of girth welds at a region away from weld toes are presented in Paper 2. Estimation of plastic zone size identified as the key parameter from PVRC JIP Phase 2 results in defining the WRS profile at a distance away from weld toe locations using FEM is presented in Paper 3. These recommendations are established for different component geometry and heat input of welding processes and can be helpful in defining WRS profiles for proximity welds. Welding guidelines for repair welds recommends qualification of separate welding procedure qualifications records as per the NORSOK [18, 42] and ASME [17] codes. Welding procedures are qualified for close proximity repair welds as per the EN and NORSOK codes and mechanical tests like Charpy, tensile and hardness etc, results are reported in Paper 4. Residual stresses are measured by the neutron diffraction technique at PSI, Switzerland and the results are reported in Paper 5. Finally, XRD-measured results are validated with FEM based numerical models and presented in Paper 6.

3.2 Overview of Appended Papers

This research thesis is comprised of six appended articles of which two articles are presented in internationally recognized conferences and the remaining four are published in peer-reviewed journals. This section briefly provides a summary of each appended article.

Paper I: Challenges due to welds fabricated at a close proximity on offshore structures, pipelines and piping: state of the art

In this article, the industrial challenge of specifying criteria for maintaining a minimum distance between close proximity welds was presented, which was found to be scattered across various international fabrication codes and standards. This assessment was performed across the most common fabrication codes used in offshore and general steel structures, pressure-containing equipment, pipelines and piping fabrication as shown in Table 1 [9-11, 18, 30, 44-48]. Repair guidelines [18, 30, 42, 43] for maintaining a close proximity was also assessed among the available repair codes of pipelines and piping's replacement procedures. A clear lack of consensus was assessed for defining this criterion which was found to be based on thickness or diameter. Terms like 'mutual agreement', 'if design allows' and 'avoid overlapping or removal of HAZ' were found, which motivated the authors to investigate the hypothesis further by identifying key degradation mechanisms that were prevalent due to weld proximity in high restraint critical welded joints.

Various challenges that can arise due to close proximity welds are discussed; for example, residual stress development, changes in microstructure on close proximity regions due to multiple cycles of heating and cooling, residual stress effect on fatigue life of welds and the effect of residual stresses on fracture/fitness for service of welds. This paper presents the main challenges due to proximities of welds in pipe

replacement procedures in ageing assets that need to be addressed during defect assessment procedures of repair welds.

Table 1 – Overview of international codes for defining criteria for the minimum distance between close proximity welds

S.no	International Standard Name	Category	Criteria for Minimum Distance between Welds	Remarks
1	ASME Sec VIII	Boiler & Pressure Vessel Code	5 x t	t-thickness of thicker plate, in cases of longitudinal welds
2	API 650	Welded Tanks for Oil Storage	5 x t	t-thickness of thicker plate, in cases of vertical welds
3	BS 2971:1991	Specification for Class II arc welding of carbon steel pipework for carrying fluids	Shall be agreed between the contracting parties	If design allows
4	ASME B31.3-2018	Process Piping	No defined criteria	Spacing between branch connection reinforcement welds mentioned
5	AWS D1.1	Structural Welding - Steel	a) 1 x d b) Staggered by 90 degrees	a) d-pipe diameter (b/w girth welds) b) Between longitudinal welds
6	ISO19902:2007	Petroleum and Natural Gas Industries Fixed Steel Offshore Structures	a) Not less than 50 mm b) 1 x d	a) Between braces b) Between circumferential welds
7	API RP 2A	Recommended Practice for Planning, Designing and Constructing Fixed Offshore Platforms	a) Clear distance of 2 inch b) Staggered by min 90 degrees	a) Between braces b) Between longitudinal welds
8	DNVGL-OS-C401	Fabrication and Testing of Offshore Structures	a) 1 x d b) Staggered by 50 mm	a) Between circumferential welds b) Between longitudinal welds
9	DNV-OS-F101	Submarine Pipeline Systems	a) 1.5 x d or 500 mm b) Staggered by 50 mm	a) Between circumferential welds b) Between longitudinal welds
10	NORSOK- N-004	Design of steel structures	a) Not less than 50 mm b) Minimum d/4 or 150 mm for overlap braces	a) Between braces b) Overlap joints, d = through brace dia

d = pipe diameter, t = thickness of thicker plate

Paper II: Residual stress estimation in defect assessment procedures at weld toe and away locations on girth welds: Review of key parameters

WRS estimation was identified as one of the important mechanisms that needs detailed investigation during defect assessment procedures of close proximity welds. A detailed review was performed in Paper II for WRS-recommended profiles in defect assessment procedures of the most common FFS codes like BS7910, API579 and R6 [24-26] for distances away from weld toe locations. Defect assessment procedures of BS 7910, level 2 for a distance away from weld toes recommend upper-bound WRS profiles to be constant for ±1.5W (±0.75 $\sqrt{rt}$ w.r.t. weld centre line) where W is the width of the weld whereas the R6 code recommends a liner reduction from an estimated yield boundary size. These recommendations were found to be overly conservative or non-existent in FFS codes for distances away from weld toe locations when compared with experimental results [27].

Parametric analysis of available residual stress experimental and numerical results from PVRC JIP Phase 1 and 2 studies [32, 33] was performed to highlight the key parameters influencing these profiles. Component geometry (e.g., r/t ratio), shrinkage zone controlled plastic zone and heat input per unit volume of weld area in J/mm^2 were identified as key parameters for defining full residual stress profiles at a distance away from weld toe locations. These parameters have been identified by researchers [49, 50] in the past for defining full field WRS estimation at weld toes and distant locations. A characteristic distance of $2.5\sqrt{rt}$ (radius times thickness) of joining members was identified as a distance where WRS completely vanishes. The recommended distance acts as a potential reference for defining optimum distance for repair weld placement in critical power or process piping application. A framework was also proposed for residual stress management of close proximity welds based on these findings and is presented in Appendix-1.

Paper-III: Estimation of welding-induced plastic zone size and residual stress levels: Linear heat input approximation.

As per PVRC JIP Phase 2 results and Paper II's review, the shrinkage zone-based plastic zone was identified as the key parameter in defining full field WRS profiles at a distance away from weld toe locations. Component geometry (r/t ratio) and heat input approximation in J/mm^2 were other key parameters. In Paper III, methods to determine plastic zone size, location and the length scale over which it is distributed was demonstrated and was validated by thermo-mechanical-based 'elastic perfectly plastic' numerical analysis in ABAQUS with the available experimental results. Methods to approximate linear heat input (J/mm^2) were demonstrated by use of analytical expressions [51] to avoid overheating problems in 2D thermal FEM-based models and Goldak's torch parameters [52], which were later employed in numerical a study on close proximity welds.

As shown in the weld schematic in Figure 3, total plastic zone width 'w_p' can be treated as one combined plastic and shrinkage zone due to the presence of highly localized thermal gradients at weld fusion toe locations where A_w is the weld pass area in mm^2 and d_p is defined as plastic size. Determining shrinkage zone size analytically and its use in FEM models shall be done carefully as temperature dependant mechanical properties are not always available for weld & parent metal.

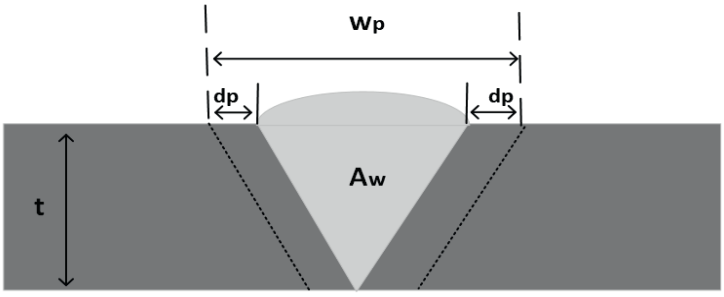

Figure 3: Weld deposition area A_w: w_p plastic zone width illustration

Paper IV: Welding procedure qualification record (WPQR) for welds fabricated at close proximity

The NORSOK M-601 [42] code for welding and inspection of piping states that "*For welds in SS type 6Mo, type 565, type 25Cr duplex and titanium base alloys only one attempt of repair is acceptable in the same area*". This demonstrates a clear need to establish welding procedures for repair welds in close proximity. Welding codes like NORSOK M-101 [18] and ASME Sec-IX codes [17] recommend qualification of separate qualification records for repair welds. In Paper IV, WPQR for welds fabricated at close proximity were qualified in accordance with the most widely-accepted welding codes, EN 15614-1 [53] and NORSOK M-101, prevalent in the North Sea and NCS, respectively. Experimental qualification was performed on a large-scale tubular structural steel pipe of S355 grade. Placement of existing and repair welds was maintained as per pre-defined weld proximity (WP) distances as shown in the schematic in Figure 4.

The findings reveal that the closest interaction of WP's leads to the development of high hardness and low Charpy energy values at close proximity locations between two adjacent welds. Optical microscopy and scanning electron microscopy results from macro and fracture specimens of welds, respectively, at proximity regions indicated interesting observations of brittle surface development. These regions have experienced temperature ranges between 725 and 915∘C for the formation of inter-critical HAZ zones, which are known for the development of martensite-austenite islands also known as local brittle zones [54]. These findings gave enough indications for identifying regions which are susceptible to deterioration under external and repeated loading. Due to varying heat input and shrinkage action of weld volume of existing and repair weld area, development of detrimental or beneficial residual stress profiles at different depths need to be investigated, which are summarized in Paper V.

Paper V Experimental investigation of residual stress distribution on girth welds fabricated at close proximity using the neutron diffraction technique

Shorter distances for proximity welds need to be proven for residual stress estimation as recommend in the DNVGL code for support structures for wind turbines [41]. In Paper V, a non-destructive technique of neutron diffraction (ND) was selected to be performed on large tubular structures using a POLDI neutron instrument at the Swiss spallation source SINQ in Switzerland to estimate WRS on proximity welds without changing their actual stress state. These measurements were performed at pre-defined points, starting from the centre of the existing ones to repair welds at three different depths of 2, 4 and 6 mm from the top of the weld cap into the thickness as shown in Figure 4.

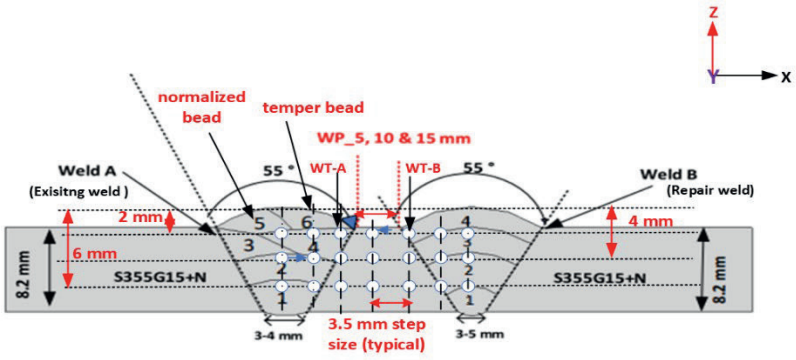

Figure 4: Neutron diffraction measurement points for proximity welds

The findings from these experimental results are shown in Figure 5 for different WPs and 6 mm depth in the hoop and axial direction. At 6 mm depth for 5 mm WP, harmful tensile WRS in the hoop and axial direction were found that are higher than the yield stress of the material. High tensile WRS in the hoop and axial direction develops perfect environment for SCC cracking at weld root locations for pipes flowing

with corrosive medium and pipe subjected to axial loading, respectively. However, at 2 mm depth compressive WRS's are observed for a minimum WP distance due to a tempering effect of adjacent weld toes and the sequence of the welding process with varying heat inputs. Development of yield magnitude stresses at proximity regions demonstrates how component geometry and heat input of welding process play a significant role in development of harmful tensile residual stresses. It further indicates that stress mitigation measures like heat treatment, shot penning, etc. for stress relaxation can be employed for proximity welds depending upon component geometry and end use.

a)

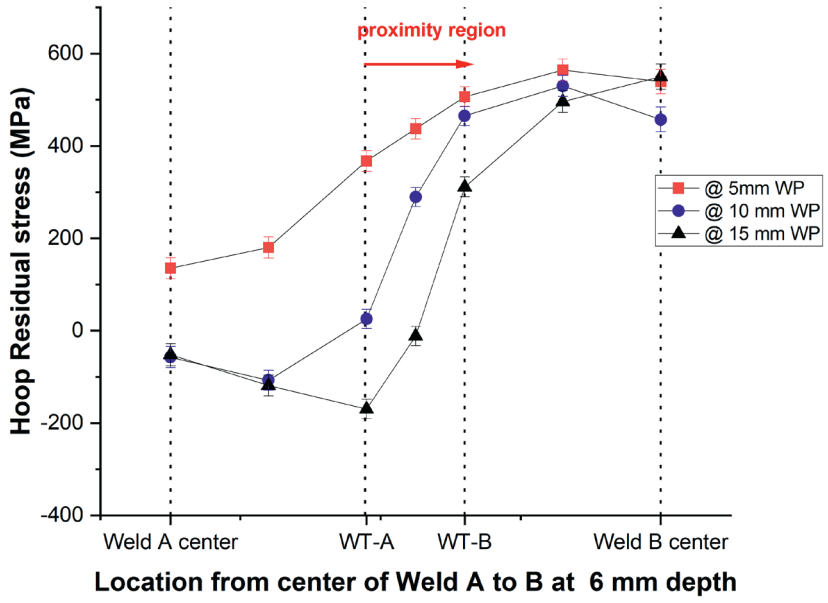

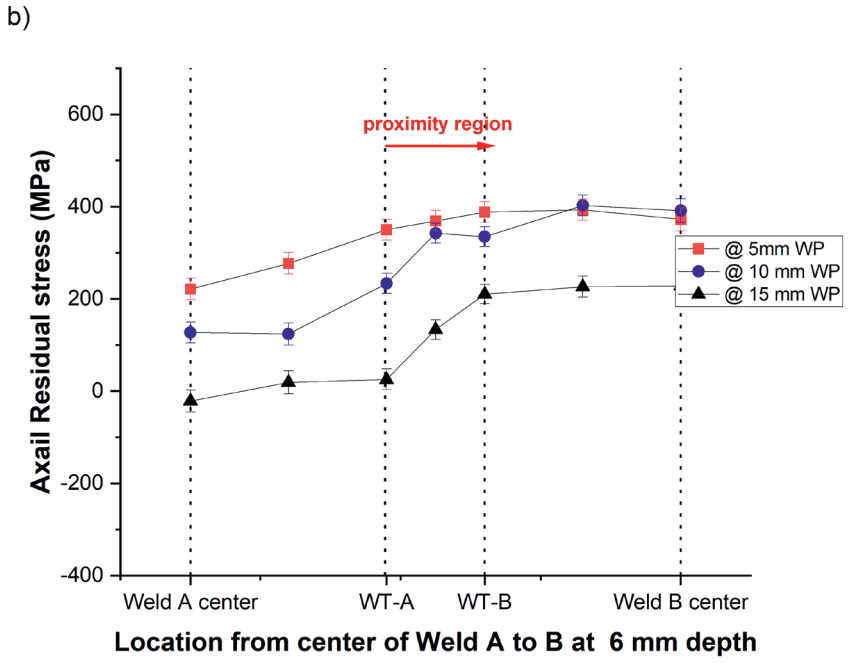

Figure 5: WRS distribution at 6mm depth for different WPs in the a) hoop & b) axial direction

Paper VI: Experimental and Numerical investigation of residual stresses in proximity girth welds

Maintaining minimum distance criteria for repair weld placement in compact layouts can lead to the development of detrimental tensile axial residual stress as observed by researchers in the past [4-6, 22]. Weld cap or root toe locations are considered important sites for investigating crack propagation behaviours under cyclic loadings [1]; hence, WRS distribution around these regions was investigated experimentally by surface level residual stress estimation techniques, for example XRD. In Paper VI, the NDT method of XRD was selected to measure residual stresses at surface level between proximity weld; cap and root level as shown in Figure 6. The thermo-mechanical-based numerical model is solved incrementally in a transient manner to estimate nodal temperature distributions and stresses and compared with experimental results.

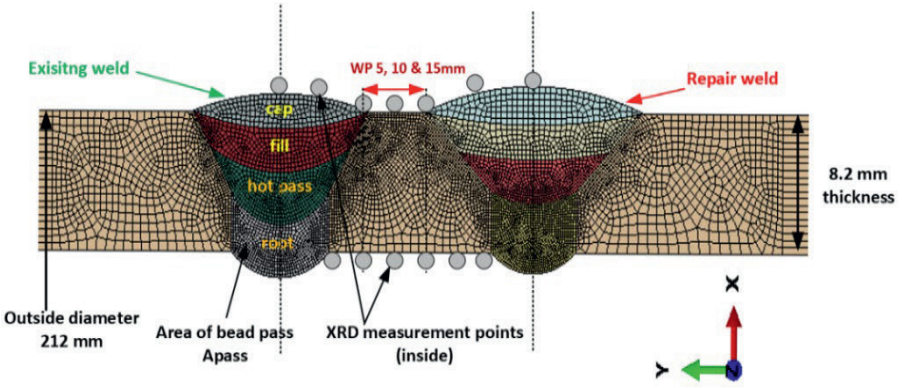

Figure 6: Axisymmetric FEM model of existing and repair welds reproduced from weld macrographs with XRD and ND measurement locations

The most realistic approach in defect assessment procedures requires the use of nonlinear finite element modelling results coupled with residual stress experimental measurements for defining residual stress profiles [27]. Two-dimensional linear heat approximation [51] and length scale-based stress decomposition theory [55] were used in numerical models

to estimate WRS at weld cap and root toe locations. Axial stress distribution in close proximity regions were found to be maximum for the closest proximity distance of 5mm at pipe inner surfaces as shown in Figure 7 a. Membrane component and through thickness distribution of WRS in the axial direction at existing weld toe locations was found to be maximum for 5mm WP at outside and inside surfaces as shown in Figure 7b. These parameters are considered important for determining the fracture driving force used in defect assessment procedures of structural integrity. These findings are helpful for conducting weld integrity assessments of critical geometries in cases of repair weld placement at close proximity. Recommending minimum distances between repairs and existing welds should be based on experimental results validation with FEM as key parameters like component geometry (radius to thickness ratio), heat input of the welding process and the sequence of welding with additional restraints plays an important role in defining WRS profile at a distance away from the weld toe.

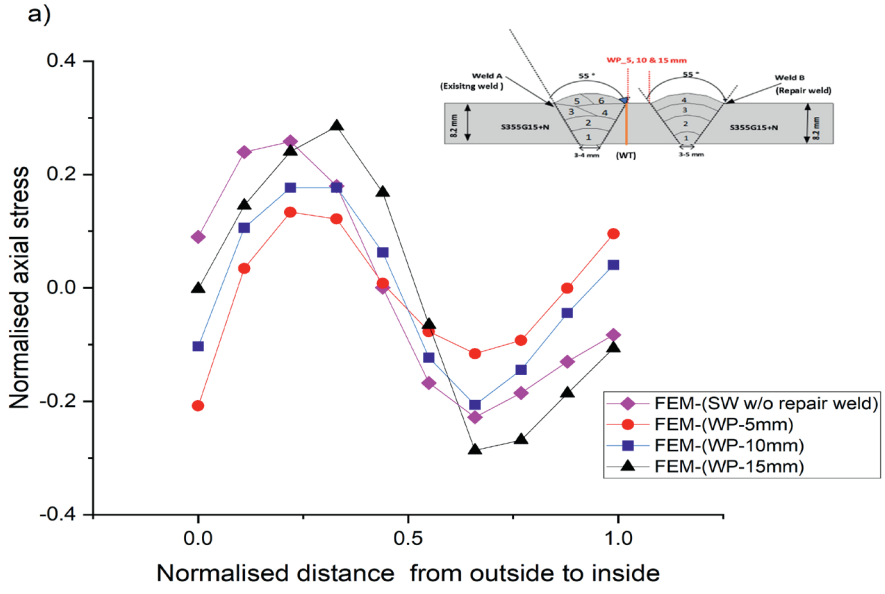

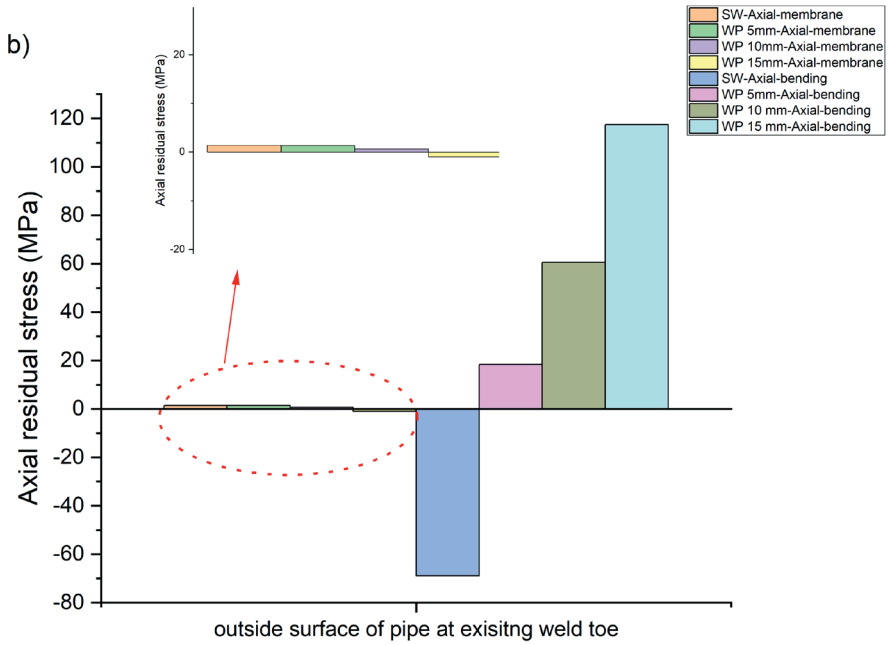

Figure 7: Axial residual stress distribution a), through thickness at the existing weld toe b) decomposed stress components at the existing weld toe

Research Contributions

This research aimed to identify key challenges due to the placement of repair welds in proximity to existing girth welds in S355 grade structural steels. In aging top sides of piping and related structures, maintaining distances between two adjacent welds becomes an industrial challenge for practitioners and engineers as codes and standards provide very vague recommendations. Criteria for deciding the minimum distance criteria for the placement of repair welds in pipe replacement procedures is practically non-existent for highly compact structures. To understand the changes in mechanical and material properties between adjacent welds, this large-scale experimental study was conducted. This case study-based research study provides an evidence-based technical explanation for practitioners by establishing welding procedure qualification records and recommending residual stress profiles based on experimental and numerical assessments. The main research highlights from the appended papers are as follows:

1. In Paper I, a detailed gap assessment of major structural, pressure-containing pipeline and piping codes were performed and criteria for maintaining a minimum distance between adjacent welds was presented. Lack of consensus or no prescribed recommendations for maintaining these distances were highlighted among major repair and fabrication codes. Key challenges like the estimation of residual stresses at locations away from weld toe locations were identified as the key factor to be considered in defect assessment procedures of structural integrity for proximity welds.
2. In Paper 2, a detailed literature review was carried out from PVRC JIP Phase 2, and the results identified key parameters affecting residual stress profiles at a distance away from weld toe locations. Component geometry (radius to thickness ratio), heat input (J/mm2) and a plastic zone-based shrinkage zone were identified as key parameters for defining full field residual stress profiles at a distance

away from weld toe locations that are currently under process to be included in the API RP 579-1/ASME FFS-1 code [25]. A conceptual roadmap was proposed for residual stress management of proximity welds as per Annexure-A.

3. In Paper 3, analytical method for linear heat input approximation and Goldak's welding torch parameters used in thermo-mechanical FEM-based numerical models was demonstrated to estimate residual stress at locations away from weld toe locations. This thermo-mechanical-based numerical-based FEM model can be conservatively used to estimate residual stresses.
4. In Paper 4, the welding qualification procedure record (WPQR) was developed and established for proximity repair welds at pre-defined proximity distances as per widely accepted welding code EN 15614-1. Key findings, for example high hardness and low energy values, were highlighted as major points of concern for maintaining distances between welds at half thickness in contrast to 1 or 1.5 times of the joining member.
5. In Paper 5, neutron diffraction findings established the development of yield magnitude, harmful tensile axial and hoop residual stresses at weld root locations for welds maintained at half thickness of the joining member. These findings enable practitioners to define optimised distances for proximity welds depending upon component geometry and heat input of welding process.
6. In Paper 6, FEM-based thermo-mechanical-based numerical models are validated with XRD measurements. Detrimental tensile axial residual stresses were found at pipe inner surfaces at repair and existing weld root toe locations in closest proximity. Distribution of tensile residual stresses away from weld toe locations are considered important in defect assessment procedures, hence repair weld placement criteria require careful assessment as per the level 3 approach of FFS codes by use of nonlinear finite element modelling coupled with residual stress experimental measurements.

Future Research

The focus of this research study was to investigate mechanical properties and estimated residual stress profiles for proximity welds based on case study based experimental study. However, it can be extended on the PVRC JIP Phase-2 recommendations. Detailed experimental and numerical parametric analyses can be performed on component geometry (radius to thickness ratio) r/t ranging from 10 to 100, heat input (J/mm^2) from 20 to 150 J/mm^2, weld geometry for single, double vee and narrow gap joints etc. However, this experimental study for establishing welding procedures and residual stress estimation was performed on the most common structural steel grade of S355, a tubular structure geometry with a r/t ratio of 10 and single vee weld configuration. This study can be expanded further on different steel grades like duplex stainless steel with a range of r/t ratios.

The neutron diffraction method was used to estimate residual stress at different depths using POLDI diffractometer at PSI, Switzerland where a coarser gauge volume was used. Narrow gauge volumes with finer resolutions can be effectively used in capturing full field residual stress profiles at different depths. In this research, various mitigation mechanisms and predictive modelling were proposed such as heat treatment, etc.; however, it can be expanded as future research.

This research was limited to the estimation of residual stress effects in weld integrity; however, its effect on fatigue life of proximity repair girth welds can be expanded further in developing SN plots for such joints. In practise, residual stress effects in fatigue testing of weld joints are considered by testing them at high R ratios, i.e., around 0.4–0.5 or estimating them to be equal to yield magnitude in linear fracture mechanics procedures.

Appendices-1

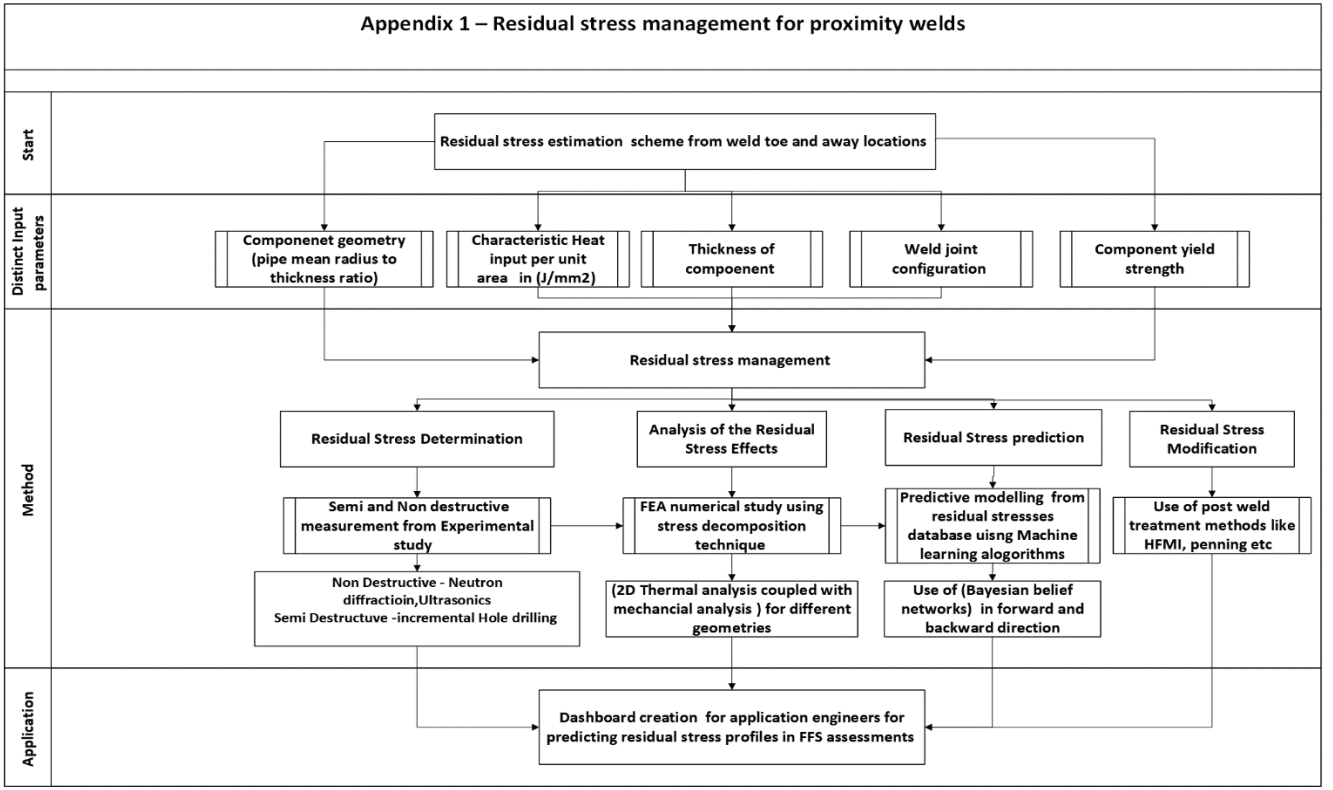

References

1. Lotsberg, I., *Fatigue Design of Marine Structures*. 2016, Cambridge: Cambridge University Press.
2. Mirzaee-Sisan, A. and G. Wu, *Residual stress in pipeline girth welds- A review of recent data and modelling.* International Journal of Pressure Vessels and Piping, 2019. **169**: p. 142-152.
3. Hobbacher, A.F., *Recommendations for Fatigue Design of Welded Joints and Components*. IIW Collection. 2016, Cham: Springer International Publishing, Cham.
4. Consonni, M. and F.W. Chen, *Repair rates in welded structures and components.* 2014. **66**: p. 61-68.
5. Gandy, D., S. Findlan, and R. Viswanathan, *Weld Repair of Steam Turbine Casings and Piping—An Industry Survey.* Journal of Pressure Vessel Technology-transactions of The Asme - J PRESSURE VESSEL TECHNOL, 2001. **123**.
6. Dong, P., *On repair weld residual stresses and significance to structural integrity.* Welding in the World, 2018. **62**(2): p. 351-362.
7. Ratnayake, R.M., *An algorithm to prioritize welding quality deterioration factors: A case study from a piping component fabrication process.* International Journal of Quality & Reliability Management, 2013. **30**.
8. Ratnayake, R.M., *A methodology for assessing most vulnerable welding procedure specifications and imperfection factors.* International Journal of Data Analysis Techniques and Strategies, 2014. **6**: p. 362-383.
9. Standardization, I.O.f., *ISO 19902:Petroleum and natural gas industries - Fixed steel offshore structures*. 2007.
10. Institute, A.P., *API RP 2A-WSD* in *Planning, Designing and Constructing Fixed Offshore Platforms - Working Stress Design*. 2014, API: USA.
11. ASME, *ASME B31.3-2018*, in *Process Piping*. 2018: USA.
12. Bhardwaj, S. and R.M.C. Ratnayake, *Welding procedure qualification record (WPQR) for welds fabricated at proximity.* The International Journal of Advanced Manufacturing Technology, 2022.

13. Ratnayake, R.M.C. and V.A. Brevik, *Experimental Investigation of Underwater Stud Friction Stir Welding Parameters.* Materials and Manufacturing Processes, 2014. **29**(10): p. 1219-1225.
14. Acevedo, C., J.-M. Drezet, and A. Nussbaumer, *Numerical modelling and experimental investigation on welding residual stresses in large-scale tubular K-joints.* Fatigue & Fracture of Engineering Materials & Structures, 2013. **36**: p. 177-185.
15. Larsson, M., et al., *Experimental Residual Stress Investigation of Weld Joints Fabricated at a Close Proximity in S420 Structural Steel*. 2021. p. 357-376.
16. Jacob, A., et al., *Residual stress measurements in offshore wind monopile weldments using neutron diffraction technique and contour method.* Theoretical and Applied Fracture Mechanics, 2018. **96**: p. 418-427.
17. ASME, *Boiler and Pressure Vessel Code, Section IX: Welding and Brazing Qualifications*. 2021.
18. NORSOK, *M-101 Structural steel fabrication*. 2011: Norway.
19. Bhardwaj, S. and R.M.C. Ratnayake. *Challenges due to Welds Fabricated at a Close Proximity on Offshore Structures, Pipelines, and Piping: State of the Art*. in *ASME 2020 39th International Conference on Ocean, Offshore and Arctic Engineering*. 2020.
20. Institute, A.P., *API STANDARD 1104 Welding of pipeline and related facilities*. 2021. p. p. 1–82. .
21. Hunter ANR, B.W., McDonald EJ, , *Specification, development, and optimisation of the welding and post-weld heat treatment procedures.* . Boiler Shell Weld Repair Sizewell A Nuclear Power Station,, 1999: p. 33–53.
22. Bouchard, P.J., et al., *Measurement of the residual stresses in a stainless steel pipe girth weld containing long and short repairs.* International Journal of Pressure Vessels and Piping, 2005. **82**(4): p. 299-310.
23. Song, S. and P. Dong, *Residual stresses at weld repairs and effects of repair geometry.* Science and Technology of Welding and Joining, 2017. **22**(4): p. 265-277.
24. Energy, E., *R6 revision 4, assessment of the integrity of structures containing defects. ;* . 2015: Gloucester,UK.

25. Institute, A.P., *API RP 579-1/ASME FFS-1. Houston, TX: American Petroleum Institute; August 2007.* 2007: USA.
26. Standard, B., *BS 7910 Guide to methods for assessing the acceptability of flaws in metallic structures*. 2019: UK.
27. Dong, P., et al., *On residual stress prescriptions for fitness for service assessment of pipe girth welds.* International Journal of Pressure Vessels and Piping, 2014. **123-124**: p. 19-29.
28. Withers, P.J. and H.K.D.H. Bhadeshia, *"Residual stress. Part 2 – Nature and origins".* Materials Science and Technology, 2001. **17**(4): p. 366-375.
29. DNV. *Tubes and piping are the most failure-prone components*. 2020; Available from: https://www.dnv.com/oilgas/laboratories-test-sites/article/tubes-and-piping-are-the-most-failure-prone-components.html.
30. DNVGL, *DNV-ST-F101*, in *Submarine Pipeline Systems*. 2021, DNV: Norway.
31. Bouchard, P.J., *Validated residual stress profiles for fracture assessments of stainless steel pipe girth welds.* International Journal of Pressure Vessels and Piping, 2007. **84**(4): p. 195-222.
32. P. Dong, Z.C., J.K. Hong, *Final PVRC Residual Stress and Local PWHT JIP Report on Investigation of Weld Residual Stresses and Local Post Weld Heat Treatment*. 2005, Welding Research Council, Inc.
33. Dong, P., S. Song, and X. Pei, *An IIW residual stress profile estimation scheme for girth welds in pressure vessel and piping components.* Welding in the World, 2016. **60**(2): p. 283-298.
34. Acevedo, C., *Influence of Residual Stresses on Fatigue Response of Welded Tubular K-Joints*. 2011, EPFL.
35. Acevedo, C. and A. Nussbaumer, *Effect of tensile residual stresses on fatigue crack growth and S-N curves in tubular joint in compression.* International Journal of Fatigue, 2013. **36**: p. 171-180.
36. Yin, R.K., *Case study research and applications : design and methods*. Sixth edition. ed, ed. R.K. Yin. 2018, Los Angeles, California: SAGE.
37. Stake, R.E., *The art of case study research*. 1995, Thousand Oaks, Calif: Sage.

38. Baxter, P. and S. Jack, *Qualitative Case Study Methodology: Study Design and Implementation for Novice Researchers.* Qualitative report, 2008. **13**(4): p. 544-559.
39. Ghosh, S. *Use of Qualitative Comparative Analysis on Multiple Case Studies to Analyze Conditions and Outcomes of Information Technology Project Selection in University*. 2018.
40. Miles, M.B. and A.M. Huberman, *Qualitative data analysis: An expanded sourcebook, 2nd ed*. Qualitative data analysis: An expanded sourcebook, 2nd ed. 1994, Thousand Oaks, CA, US: Sage Publications, Inc. xiv, 338-xiv, 338.
41. DNVGL, *DNVGL-ST-0126 Support structures for wind turbine*. 2018, DNVGL.
42. NORSOK, *M-601 Welding and inspection of piping*. 2016: Norway.
43. Institute, A.P., *API 2200 Repairing Hazardous Liquid Pipelines*. 2015, API: USA.
44. Institute, A.P., *API STD 650 Welded Tanks for Oil Storage*. 2020, American Petroleum Institute: USA.
45. Society, A.W., *AWS D1.1/D1.1M:2015 Structural Welding Code - Steel*. 2015: USA.
46. Standard, B., *BS 2633-1987Specification for Class I arc welding of ferritic steel pipework for carrying fluids*. 1987: UK.
47. Standard, B., *BS 4515-1:Specification for welding of steel pipelines on land and offshore. Carbon and carbon manganese steel pipelines*. 2009: UK.
48. Standards, B., *BS 2971:1991Specification for class II arc welding of carbon steel pipework for carrying fluids*. 1991: UK.
49. Song, S., P. Dong, and X. Pei, *A full-field residual stress estimation scheme for fitness-for-service assessment of pipe girth welds: Part I – Identification of key parameters.* International Journal of Pressure Vessels and Piping, 2015. **126-127**: p. 58-70.
50. Song, S., P. Dong, and X. Pei, *A full-field residual stress estimation scheme for fitness-for-service assessment of pipe girth welds: Part II – A shell theory based implementation.* International Journal of Pressure Vessels and Piping, 2015. **128**: p. 8-17.

51. Song, S., X. Pei, and P. Dong. *An Analytical Interpretation of Welding Linear Heat Input for 2D Residual Stress Models*. in *ASME 2015 Pressure Vessels and Piping Conference*. 2015.
52. Goldak, J.A. and M. Akhlaghi, *Computational Welding Mechanics.* Computational Welding Mechanics, 2005: p. 1-321.
53. 15614-1, E., *Specification and qualification of welding procedures for metallic materials — Welding procedure test.* 2017.
54. Lomozik, M., *Effect of the welding thermal cycles on the structural changes in the heat affected zone and on its properties in joints welded in low-alloy steels.* Welding International, 2000. **14**(11): p. 845-850.
55. Dong, P., *Length scale of secondary stresses in fracture and fatigue.* International Journal of Pressure Vessels and Piping, 2008. **85**: p. 128-143.

Part II: Papers

Proceedings of the ASME 2020 39th International Conference on Ocean, Offshore and Arctic Engineering
OMAE2020
August 3-7, 2020, Virtual, Online

OMAE2020-18586

CHALLENGES DUE TO WELDS FABRICATED AT A CLOSE PROXIMITY ON OFFSHORE STRUCTURES, PIPELINES, AND PIPING: STATE OF THE ART

Sachin Bhardwaj
Department of Mechanical and Structural Engineering and Material Science,
University of Stavanger, Norway

R.M. Chandima Ratnayake
Department of Mechanical and Structural Engineering and Material Science,
University of Stavanger, Norway

Theoretical and Applied Fracture Mechanics 111 (2021) 102848

Contents lists available at ScienceDirect

Theoretical and Applied Fracture Mechanics

journal homepage: www.elsevier.com/locate/tafmec

Residual stress estimation in defect assessment procedures at weld toe and away locations on girth welds: Review of key parameters

Sachin Bhardwaj *, R.M. Chandima Ratnayake

Department of Mechanical and Structural Engineering and Materials Science, University of Stavanger, N-4036 Stavanger, Norway

ARTICLE INFO

Keywords:
Residual stress
Girth welds
BS 7910
API 579
Structural integrity

ABSTRACT

The distribution of residual stresses in welded joints plays an important role within the fracture evaluation guidelines recommended in structural integrity assessment codes such as BS7910, API 579 RP-1/ASME FFS-1 and R6. The residual stress profile recommendations in these standards are based on extensive experimental results and finite element modelling (FEM) based parametric residual stress evaluations at the weld centerline and weld toe positions. The upper bound residual stresses' profiles based on these recommendations vary significantly from one type of welding process to another for a given weld configuration with identical welding conditions. These fitness-for-service codes (FFS) depict great variability in estimating residual stress profiles during defect assessment, as BS 7910 & R6 recommends a constant profile at a distance away from welds and API 579 provides a single curve for all locations in the axial direction. Thus, conservatism is widely associated with these recommended profiles in fracture potential evaluation and assessments, leading to suboptimal recommendations. In this manuscript, a detailed review is undertaken of residual stress estimation in various FFS codes, showing vast variability among them for locations away from the weld toe on girth welds. Key distinct parameter characteristics, pipe radius to thickness ratio and heat input are detailed and found to have a significant effect on residual stress profiles in structural integrity assessment, using a stress decomposition technique. These recommendations establish an overall analysis of the interrelationship between key parameters, considering a generalized broad range of applications. A framework is proposed, based on the current review, for conducting detailed investigation by employing thermomechanical numerical modelling, coupled with measurement results (nondestructive and semi-destructive) from an experimental study, as input to machine-learning algorithms for application guidance to engineers.

1. Introduction

1.1. Background

Welding and its application constitute one of the most varied and extensively used mechanical joining processes in the offshore structure and piping industry [1–4]. In an offshore and piping structure, weld joint fabrication in piping is carried out through different welding processes and welding procedure specifications (WPSs), comprising various essential and non-essential welding parameters [5]. Due to their compact layout and offshore jacket, primary (TKY) weld joints often face the challenge of maintaining a minimum distance between proximity welds [6]. Due to the lack of clarity in various fabrication codes regarding maintaining these distances, various challenges, such as the development of harmful tensile residual stresses, microstructural and strength changes in the heat affected zone (HAZ) as a result of varying cycles of heating and cooling etc., develop between proximity welds [6–8]. Varying cycles of heating and cooling can give rise to high residual stress between proximity welds, requiring the correct estimation of residual stresses in fitness-for-service codes at distances away from the weld [6,9]. In the failure assessment of such structures, residual stresses are found to have a deleterious effect on the structural integrity of welded joints, due to the presence of harmful tensile residual stress in weld toe or root locations, which helps in crack propagation, thus reducing the fatigue life of joints under cyclic loading [10].

High tensile stress at the root region helps to accelerate stress corrosion cracking in the case of corrosive fluid contact with weld root regions [11,12]. Residual stresses are internal self-equilibrating secondary stresses, which are inherent in structures because of the manufacturing process, welding process, restraint, etc. and are difficult to determine or calculate during defect assessment [13]. Hence, correct

* Corresponding author.
E-mail address: sachin.bhardwaj@uis.no (S. Bhardwaj).

https://doi.org/10.1016/j.tafmec.2020.102848
Received 3 August 2020; Received in revised form 20 October 2020; Accepted 25 November 2020
Available online 1 December 2020

Nomenclature

σ_m^r	membrane component of residual stress MPa	tn	weld pass layer thickness in mm
σ_b^r	bending component of residual stress MPa	$\dot{Q_1}$	heat content involved to deposit a molten weld pass at a specified melting temperature in J/mm
$\sigma_{s.e}^r$	self-equilibrating component of residual stress MPa	$\dot{Q_2}$	heat that is required to hold the melting temperature in J/mm
σ_y	yield strength in MPa	t_{hold}	hold time in sec
K	stress intensity factor	ρ	material density
t	thickness of pipe in mm	Cp	specific heat
x	distance from inside of pipe to outside of pipe in mm	$Apass$	averaged cross section weld pass area in mm^2
$\dot{Q}$	linear heat input in J/mm	k	thermal conductivity
I	welding current in Amp	α	thermal diffusivity
V	welding voltage in volts	$Lsurf$	weld pass surface contacted to the surroundings
u	welding travel speed in mm/sec	ΔT	temperature difference, temperature change from room temperature to the prescribed weld metal temperature
r	mean pipe radius in mm		
$\dot{Q}$	characteristic heat input in J/mm^2	ε	dimensionless factor

estimation in the structural integrity assessment of welded joints becomes a major part of fitness-for-service codes. Correct estimation of residual stresses is essential during defect assessment of weld joints in fitness-for-service codes (FFS) and standards like BS7910-2019, API 579 RP-1/ASME FFS-1 and R6 [14–18]. In these FFS codes, residual stress profile estimation is prescribed, based either on results from available experimentation measurements or finite element (FE) -based parametric residual stress solutions [19]. In FFS codes for welded joints, defect assessment generally follows three approaches, the first of which is the most conservative and the last the most realistic [20]:

(I) approximating tensile residual stress to be uniformly distributed which are equal in magnitude to the mean material yield strength,
(II) upper-bound profiles based on experimental and numerical residual stress results, recommended by various codes, and
(III) nonlinear finite element modelling results coupled with residual stress experimental measurements.

Upper bound profiles available in these FFS codes for residual stress estimation are generally available for location at weld centerline or weld toe in through-thickness transverse and hoop directions, as shown in Figs. 1 and 4.

1.2. Existing challenges in residual stress assessments of welded joints at a distance away from the weld

Residual stress through-thickness estimation at distances away from the weld is practically nonexistent in these FFS codes, which can result in overly conservative assessments when applying fracture mechanics-based structural integrity procedures [21]. During the defect assessment of regions in the proximity of welded joints [6] and residual stress-induced stress corrosion cracking in tube sheet welds [19,21,22], residual stress upper bound profiles at a distance away from the weld become important and information of which is not available in these FFS codes. Moreover, the available upper bound profiles in FFS codes [14–18] have been found to show drastic inconsistencies, considering different welding processes, weld geometries and weld joint configurations [23]. This is primarily due to the complex nature of welding, variability in various available finite element models and the different

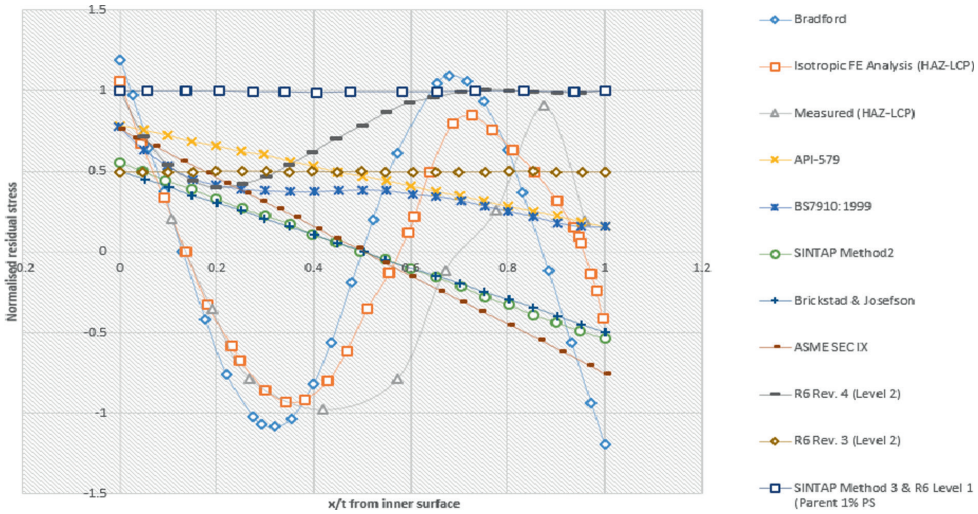

Fig. 1. Comparison, from current codes and recommended assessment procedures, of residual stress profiles in axial direction for a pipe girth weld; adapted from [23].

techniques available for residual stress measurement [24,25]. Fig. 1 illustrates variation in different residual stress distributions from various codes and recommended procedures for the same joint configuration and welding conditions [23].

Upper bound profiles prescribed in FFS codes, as shown in Figs. 1 and 4 for BS7910, are based on polynomial curve fits on selected welded components [14,16,18], supplemented with finite element results [26]. However, recent research has demonstrated that residual stress estimation profiles at a distance away from the weld can be significant, where component geometry pipe radius to thickness ratio (r/t) [27–29] and heat input [19,21,22] are identified as distinct parameters. Residual stress profiles in FFS codes are determined in terms of circumferential girth welds and longitudinal seam welds. For girth welds, the 2007 API RP 579 [30], provides a single curve-based upper bound profile for all distances away from the welds in the axial and hoop directions [21]. In longitudinal seam welds, guidance provided by FFS codes are limited in scope for residual stress profile estimation in defect assessment. In BS7910 [18] and R6 [16], the transverse residual stress profile remains the same over a circumferential distance of 1.5 W from the weld centerline, where W is the seam weld width, as shown in Fig. 5. BS 7910 [18] gives no guidance for locations beyond 1.5 W, and R6 [16] assumes a linear reduction to zero at a small distance.

FFS codes like BS 7910 [18] Annex Q consider the effect of heat input on girth welds by recommending three different profiles: 'high' (heat input $>$ 120 J/mm2), 'low' (heat input $\leq$ 50 J/mm2) and 'medium' (heat inputs between 50 and 120 J/mm2) [31]. BS7910 also follows the partitioning of polynomial distributions' [20] upper bound curve into decomposed components of membrane, bending and self-equilibrating from stress decomposition procedure [32], based on finite element parametric stress analysis results and validated experimentally on selected components by many researchers [23,32]. This decomposition technique helps in determining less conservative non-linear residual stress distribution in the pipe girth welds, decomposing them into global bending, local bending, and self-equilibrating components [20].

With this background, it is evident that residual stress profiles in these FFS codes contain practically no recommendations for locations far from the weld center, where fracture assessment can have a deleterious effect on structural integrity. Conservatism is widely associated with these FFS codes [22,26]; hence, distinct parameters like pipe r/t ratio and heat input role require detailed explanation in determining residual stress profiles for locations at weld center / weld toe and at a distance away from welds. Firstly, this manuscript briefly presents a comparison of residual stress profiles in various structural integrity codes at the weld center and at a distance away from the weld. Thereafter, it discusses in detail the role of distinct parameter characteristics such as pipe r/t ratio and heat input in the evaluation and assessment of piping girth weld residual stress profiles using the stress decomposition technique. Finally, it provides a brief review of a shell theory-based estimation scheme to be introduced in API/ASME Fitness-for-Service Joint Committee recommendations for determining consistent residual stress profiles. These recommendations establish an overall analysis of the interrelationship between key parameters, considering a generalized broad range of applications. Such analysis enables less conservative estimation criteria to be developed for the residual stress evaluation at a distance away from the weld and its assessment, to complement the current approaches suggested in structural integrity. Based on the current review, a framework, Appendix A, is proposed for conducting detailed investigation by employing thermo-mechanical numerical modelling, coupled with measurement results (nondestructive and semi-destructive) from an experimentation study as input to machine-learning algorithms for application guidance to engineers. Beneficial input parameter selection can be made by back propagation techniques, based on the accuracy of predicting residual stress from surrogate models in the front feed direction.

1.3. Stress decomposition technique

Residual stress distribution in welded joints typically consists of both high tensile and compressive stresses, as shown in Fig. 2. These stresses can have a magnitude equal or close to the yield strength of the component. However, their location, magnitude and distribution largely depend on weld joint geometry, the welding process, material characteristics and restraint condition. With this in mind, Dong and his co-workers [32,33] introduced a length scale-based characterization known as a stress decomposition technique. In this technique, residual stress through-thickness profiles are decomposed into stress components of membrane, bending and self-equilibrating stress, which are in decreasing length scale, as shown in Fig. 2 [32]. This stress decomposition is based on the following equations.

$$\sigma_m^r = \frac{1}{t}\int_0^t \sigma^r(x)dx \tag{1}$$

$$\sigma_b^r = \frac{6}{t^2}\int_0^t \sigma^r(x)\left(\frac{t}{2}-x\right)d \tag{2}$$

$$\sigma_{s.e}^r = \sigma^r(x) - \sigma_m^r - \sigma_b^r\left(1-\frac{2x}{t}\right) \tag{3}$$

An example of this technique on a T fillet weld transverse residual stress by finite element analysis is shown in Fig. 2, depicting the decreasing length scale [32], where x varies from the inside to the outside of the pipe of thickness t.

It is worth mentioning here that Eqs. (1)–(3) represent through thickness self-equilibrating stress distribution, highlighting the decreasing length scale of residual stress distributions in the form of membrane, bending, and self-equilibrating stress, with respect to the thickness t. This technique also separates the contribution of global (due to membrane and bending stresses) and local residual stress (due to self-equilibrating stress) components, which can help in estimating the stress intensity factor K, due to residual stresses [24]. The membrane component σ_m^r and the bending component σ_b^r play an important role in defect assessment procedures to estimate the fracture crack driving force and are well demonstrated in the work of Dong and his co-workers [19,34]. In addition, this technique also helps in visualizing clear and better patterns of residual stress distribution and in analyzing many residual stress cases, to identify the controlling parameters.

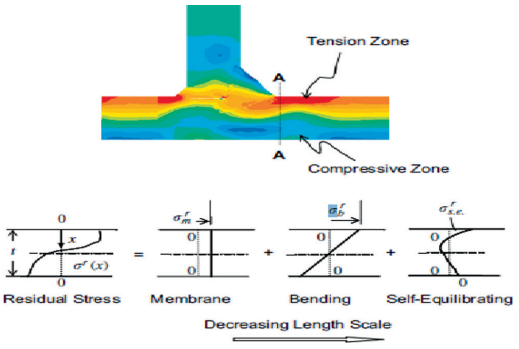

Fig. 2. Illustration of residual stress decomposition technique components with decreasing length scale [32] .

1.4. Scopes and objectives

- Carry out a brief review of the guidance on residual stress profiles for assessing flaws in as-welded joints recommended in Annex Q of BS 7910, API 579 and R6 for girth welds locations at the weld center/ weld toe and at distances away from welds.
- Review of important parameters that govern residual stress distribution, using a stress decomposition technique.
- Determination of the distance away from the weld center at which residual stress vanishes completely, based on component geometry by comparison of data from available literature.
- Comparison of several finite element analyses results from the open literature, covering a broad range of component geometries (r/t ratio), joint preparations (Single V, Double V), materials, and heat input.

2. Guidance on residual stress profiles for assessing flaws in FFS codes

2.1. Residual stress profiles in BS 7910:2019 & R6

BS 7910:2019 [35] is an FFS service code, serving as a "guide to methods for assessing the acceptability of flaws in metallic structures". In 2013, BS 7910 included substantial methods for incorporating welding residual stress into fracture assessment, originating mainly from BS 7910:2005 [18], R6 Revision 4 [16] and the European SINTAP/ FITNET procedures [14,17]. In the 2019 version of BS 7910 [35], no major changes took place in residual stress information, with the exception of the addition of a new Annex, V, on strain-based assessment and design [35]. BS 7910 Clause 7.1 8 states that residual stresses may be assumed to be uniform or non-uniform. Uniform (membrane) stress distributions are considered in this clause, which is more conservative, while non-uniform distributions are described in Annex Q. Annex Q provides guidance on residual stress profiles for assessing flaws in as-welded joints, i.e. joints which are not subjected to post weld heat treatment (PWHT), as shown in Fig. 3.

2.1.1. Transverse residual stress

In BS 7910 Annex Q [35], the transverse residual stress σ_t^r (perpendicular to the weld) has three types of through-thickness distributions, depending on the materials (ferritic versus austenitic) and welding heat input levels, as explained in the equations below.

$$\sigma_t^r(x) = \sigma_Y\left[1 - 6.80\left(\frac{x}{t}\right) + 24.30\left(\frac{x}{t}\right)^2 - 28.68\left(\frac{x}{t}\right)^3 + 11.18\left(\frac{x}{t}\right)^4\right] \quad \text{for } Q'/t \le 50 \text{ J/mm}^2 \tag{4}$$

$$\sigma_t^r(x) = \sigma_Y\left[1 - 4.43\left(\frac{x}{t}\right) + 13.53\left(\frac{x}{t}\right)^2 - 16.93\left(\frac{x}{t}\right)^3 + 7.03\left(\frac{x}{t}\right)^4\right] \quad \text{for } 50 < Q'/t \le 120 \text{ J/mm}^2 \tag{5}$$

$$\sigma_t^r(x) = \sigma_Y\left[1 - 0.22\left(\frac{x}{t}\right) + 3.06\left(\frac{x}{t}\right)^2 + 1.88\left(\frac{x}{t}\right)^3\right] \quad \text{for } Q'/t \ge 120 \text{ J/mm}^2 \tag{6}$$

where Q' represents the linear heat input of the welding electrode for the largest run of the weld. This linear heat input is related to the welding current (I), welding voltage (V) and welding travel speed (u), as per Eq. (7). The through-thickness longitudinal and transverse residual stress profiles given by Eqs. (4)–(6) are plotted in Fig. 4.

$$Q' = \frac{I.V}{u} \tag{7}$$

2.1.2. Residual stress profiles at a distance away from the weld in BS 7910

In the axial direction, BS 7910 specifies that through-thickness residual stress profiles are valid for a region within three times the weld width (3 W) w.r.t the weld centerline, as illustrated in Fig. 5 (a). R6 Sec. IV.4 [16] and FITNET [14] assume a linear distribution of longitudinal

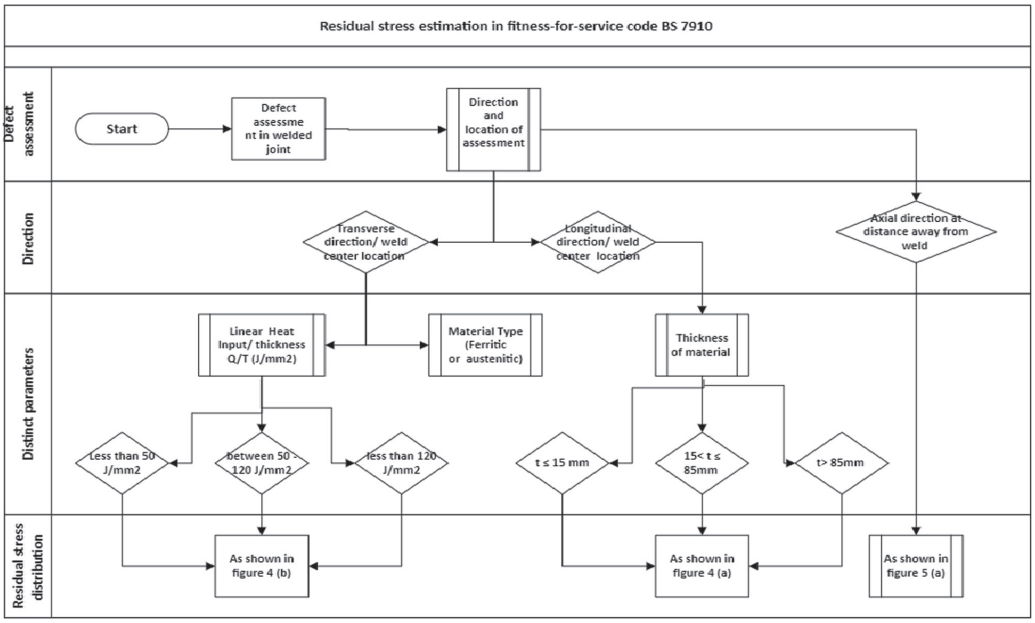

Fig. 3. Residual stress estimation in BS 7910 for welded joints.

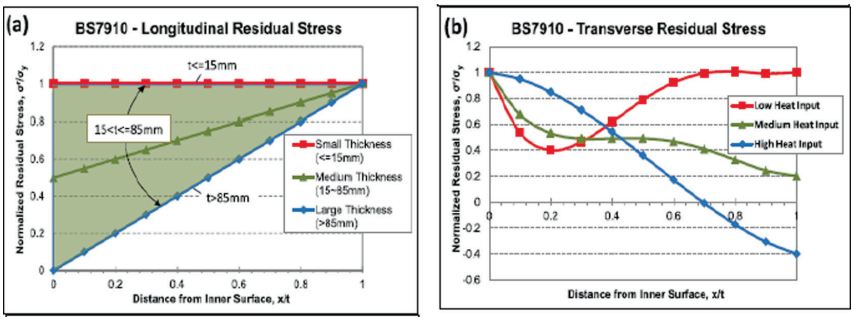

Fig. 4. Residual stress profiles prescribed in BS 7910 Appendix Q [35] and R6 Sec. IV [16]: (a) longitudinal, and (b) transverse directions, adapted from [21] .

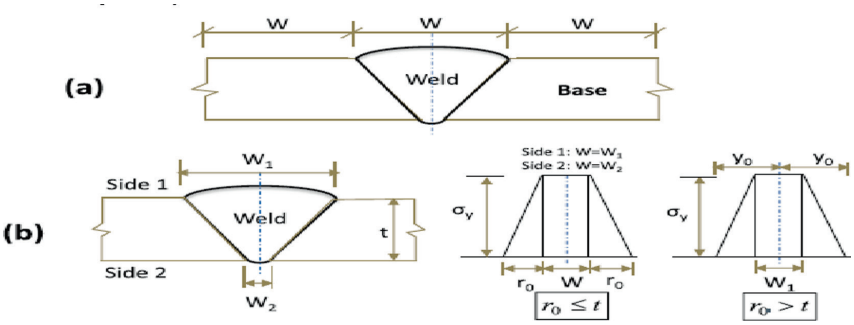

Fig. 5. Illustration of axial residual stress at a distance from weld of surface longitudinal residual stress component: (a) BS 7910 [35], (b) R6 [16], and FITNET [14].

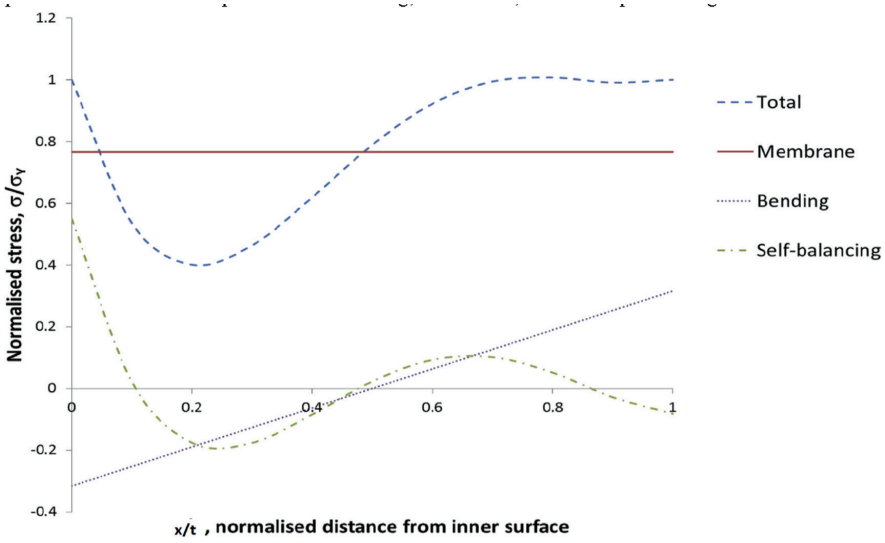

Fig. 6. Decomposed components of transverse stresses in ferritic pipe butt welds (with a low heat input) [31].

residual stress distribution, varying from material yield strength at the weld toe to zero at an estimated yield zone boundary, as illustrated in Fig. 5 (b). All residual stress profiles in BS 7910 are based on upper bound fits to experimental data and FE numerical results. These results are based on different weld geometries measured at weld locations, such as weld centerline and weld toe positions; this does not recognize the role of pipe geometry [36] and is proven to be overly conservative [34]. However, residual stress profiles at a distance away from the weld are not mentioned in FFS structural integrity assessment procedures [19] which can be used in the fracture assessment of proximity welds.

2.1.3. Stress decomposition in BS 7910

As shown in Fig. 6, a stress decomposition technique can be used for depicting a plot of decomposed components of transverse stresses in ferritic pipe butt welds made with a low heat input. The transverse stress $\sigma_t^r(x)$ was calculated from Eq. (4) for low heat input in ferritic pipe butt welds which is normalized to yield strength, σ_Y. This decomposition is shown in Fig. 6, where transverse residual stress normalized by yield strength is plotted against x/t where x is the distance from the inner surface through the wall thickness, t. Eqs. (1)–(3) have been used to calculate and decompose residual stress components into bending, membrane, and self-equilibrating stress.

2.2. API 579-1/ASME FFS-1: Residual stress profile at a distance away from welds

In the case of girth welds, API 2007 579 RP [30] recommends a common curve for axial and hoop residual stress profiles for distances away from the weld toe, based on an upper-bound residual stress profile. The residual stress through-thickness profile at a distance away from the weld is a quadratic variation over a circumferential distance in terms of $\sqrt{rt}$ in API 579 [15], based on a best fit of the upper bound of all finite element results over all r/t ratios and heat inputs. In API 579-1/ASME FFS-1 Annex 9D next update, residual stress profiles for various piping and pressure vessel configurations at distances away from the weld are based on various mechanics-based estimation schemes and the recent research results of Dong and his co-workers [19,34,36,37]. These estimation schemes provide analytically based descriptions of distances at which welding induced residual stress completely vanishes, affected by component geometry (e.g., r/t ratio), shrinkage zone (plastic zone size) controlled by joint preparation and heat input. The key enabler in this process can be attributed to the stress decomposition technique [32] and work done by Dong [19,22,34,38] and Song [21,24,36,37,39,40] in their work to establish a functional dependency of decomposed through-thickness membrane and bending stresses, based on pipe geometry and heat input-related parameters.

3. Review of key contributing parameters governing important residual stress distribution, using stress decomposition technique

To remove the inconsistency in recommended residual stress profiles in various FFS codes, the Pressure Vessel Research Council (PVRC) joint industry project (JIP), Phase 1 [41], was initiated in late 2000, highlighting important parameters affecting upper bound profiles in the 2007 issue of API 579 RP Appendix E [30]. To estimate consistent residual stress profiles, thicknesses of less than 50 mm (2″), mostly for single V joint preparation were used in the phase 1 JIP. Whereas in the phase 2, JIP of PVRC [40] a range of pipe thicknesses between 6.35 mm (1/4″) to 254 mm (10″) with joint preparations of Single V (SV), Double V (DV), and Narrow Groove (NG), were chosen for analysis, as illustrated in Fig. 7.

The outcome of the PVRC JIP, Phase 1 [41], recommended a large number of important governing parameters for estimating residual stress profiles, for example joint geometry, material chemistry, and welding process parameters. However, the role and characteristics of important parameters, such as pipe mean radius to thickness ratio (r/t) and linear heat input (Q), are underestimated in relation to FFS engineering assessment [34]. These distinct parameters affect changes in through-thickness residual stress distributions in the weld center region in the form of a localized distribution (e.g., of the self-equilibrating type). These distributions can be significant at distances away from the weld, which exhibits a "global bending" behavior in the axial residual stress direction [34], i.e. compression of the outer surface and tensile stress on the inside of the pipe geometry. This behavior depicts a decreasing length scale [32], as explained previously in relation to the decomposition technique illustrated in Fig. 2. This technique allows individual identification of residual stress decomposed components which are considered important in defect assessment procedures.

3.1. Component geometry, i.e. radius to thickness (r/t) ratio

Component geometry, such as radius to thickness ratio, serves as a significant distinct parameter having a considerable effect on through-thickness residual stress distribution in weld joints, as demonstrated by researchers like Yaghi [29], Dong [34] and his coworkers [40]. Pipe radial bending stiffness is approximately proportional to $\sqrt{rt}$ [33] , hence r / t ratio serves as an essential measurement criteria for measuring joint restraint conditions.

3.1.1. Demonstrating the effect of component geometry (r/t ratio) at the weld toe location

In this example, the work of Dong [33] and Song [40] sequentially coupled thermo-mechanical analysis based on a conventional heat flow solution for welding are referred [33], where temperature gradients serve as input to nonlinear thermo-mechanical analysis. This example shows the effect of the radius to thickness ratio (r/t) on the through-thickness residual stress profile at the weld center / weld toe region and at a distance away from the weld. The component selected for comparison is the 2.25CrMo-V type [24,29,34], which that is very commonly used in the piping industry. A large number of parametric analyses were performed by Dong [33] and Song [40] for thicknesses > 1″ (25 mm) for pipe to radius ratios (r/t) of 2 to 100; the results demonstrate the effect of the component geometry in estimating

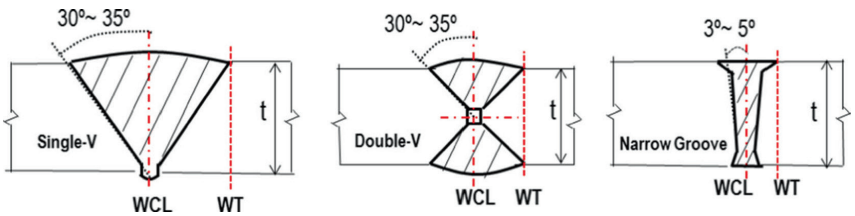

Fig. 7. Illustration of various weld joint configurations investigated in PVRC JIP Phase 2 [40]. Single V (SV), double V (DV), and narrow groove (NG), adapted from [34].

Fig. 8. Residual stress plots (x/t from inner surface) at weld toe locations for Single V & Double V girth welds with t = 1″: r/t ratio effects, adapted from [24].

residual stress profiles. Finite element (FE) results of research work [33] and [40] for single V and double V joint geometry components for thickness of 1″ (25 mm) are illustrated in Fig. 8 for axial and hoop components at the weld toe location. Observations from Fig. 8 are as follows:

- It is evident that axial residual stress for r/t ratio 2 varies from compression at the inner diameter (ID) to tension at the outer diameter (OD), i.e. through-thickness bending mode in the case of a single V joint configuration.
- A shift of compression to tension in the axial direction can be observed at the ID of the pipe, as shown in Fig. 8, as the r/t ratio increases from 2 to 100, starting from r/t = 20, i.e. settling to a self-equilibrating state at r/t = 100 [40]. These bending modes change for a small r/t ratio because the pipe is very stiff at these ratios, while, for a large r/t ratio (e.g. 100), they have increased pipe wall flexibility, i.e. attaining a self-equilibrating component [24].
- As the r/t ratio increases, the lines become flatter at the OD, implying a reduced bending component. Whereas at r/t ratio = 100, residual stress is tensile at ID and OD and a corresponding increased membrane component i.e. tensile at OD. A joint configuration change from single V to double V with an increasing r/t ratio also affects changes in the residual stress profiles, as shown in Fig. 8.

3.1.2. Demonstrating the effect of r/t ratio on residual stress profile at a distance away from weld at outer diameter (OD) and inner diameter (ID)

In Fig. 9, showing residual stress curves on the surface of a pipe along the (ID and OD) for single V girth welds with t = 1 in., reference is made

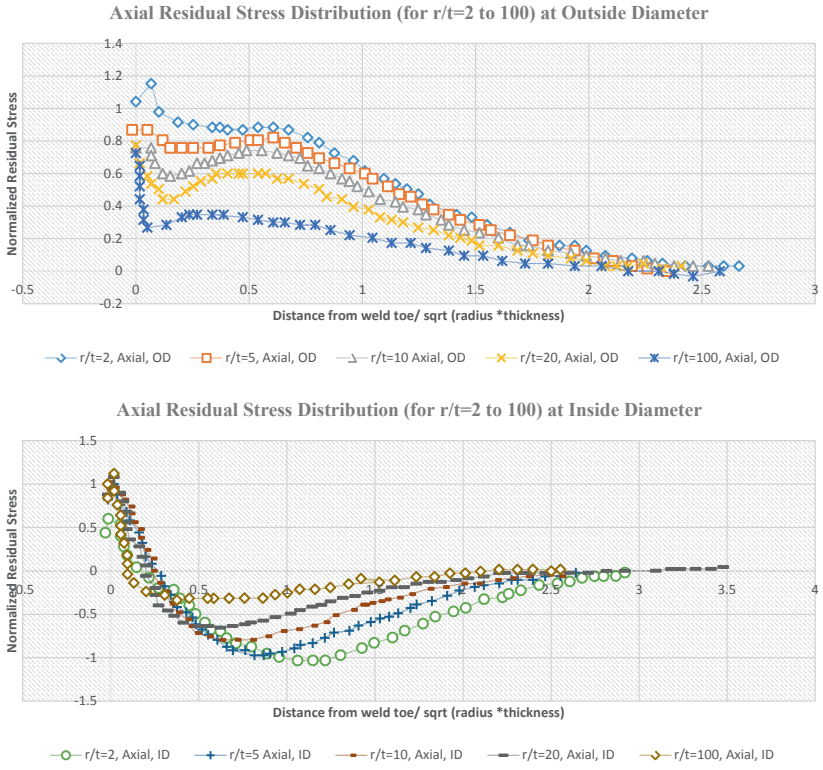

Fig. 9. Surface residual stress line plots along ID and OD for Single V girth welds with t = 1″: r/t ratio effects, adapted from [24].

to r/t ratio effects from the work of Dong[19] and Song [21]. In this comparison, the horizontal axis is a measure from the weld toe and is normalized by $\sqrt{rt}$, which is considered a characteristic parameter in residual stress distribution in the axial direction by PVRC JIP Phase 1 [41] and used in API 579–1/ASME FFS-1 [15]. It can be observed from Fig. 9 that axial residual stress at the OD decreases with increasing r/t ratio and eventually dies to zero at 2.5 times $\sqrt{rt}$. This distance can be considered an important parameter in fracture assessment for flaws away from weld and in proximity to exisitng welds.

3.1.3. Demonstrating the effect of r/t ratio on residual stress profile at a distance from weld in FFS codes

As previously explained, FFS codes [14–16,35] carry practically no recommendations for locations far from the weld center. BS 7910 does not provide any information on through-thickness residual stress profiles in transverse and longitudinal directions, except for the fact that, within the 3 W region, they remain constant (W being the width of the weld seam), as shown in Fig. 5. R6 [16] and FITNET [14], however, recommend a straight line of yield strength in the 0.5 W region (half width of the weld) with a constant residual stress profile, then decreasing it to zero in the longitudinal direction from the weld toe to a distance of r_0, as shown in Fig. 10 (b). In Fig. 10 (a), a comparison of transverse residual stress distributions and (b) longitudinal residual stress distributions along the outer surface (t = 4″, 101.6 mm) is depicted, to showcase the conservativeness associated with FFS codes from the work of Dong [19] and Song [21]. Some observations from Fig. 10 follow.

- It is evident from the results that both BS 7910 [35] and R6/FITNET [14,16] provide less conservative residual stress values within a region of 0.5 W from the weld centerline.
- As shown in Fig. 10, there is an overestimation of longitudinal residual stress at distances beyond 0.5 times the width of weld with prevalent residual stresses for different component geometries [33].
- Beyond the 0.5 W region in the longitudinal direction (Fig. 10 b) residual stress reverses its sign from compression to tension with r/t ratios greater than 2.
- Slope of RG/FITNET curve [14,16] is somewhat large when compared with FE results attained from work of Dong [19] and Song [21] for calculated distance r_o, in longitudinal direction as shown in Fig. 10 b.
- Similarly, for inner surface transverse (not illustrated) the residual stress is overestimated by BS 7910 profile. Longitudinal residual stress estimated by R6/FITNET, the slope is relatively large compared with the FE results.

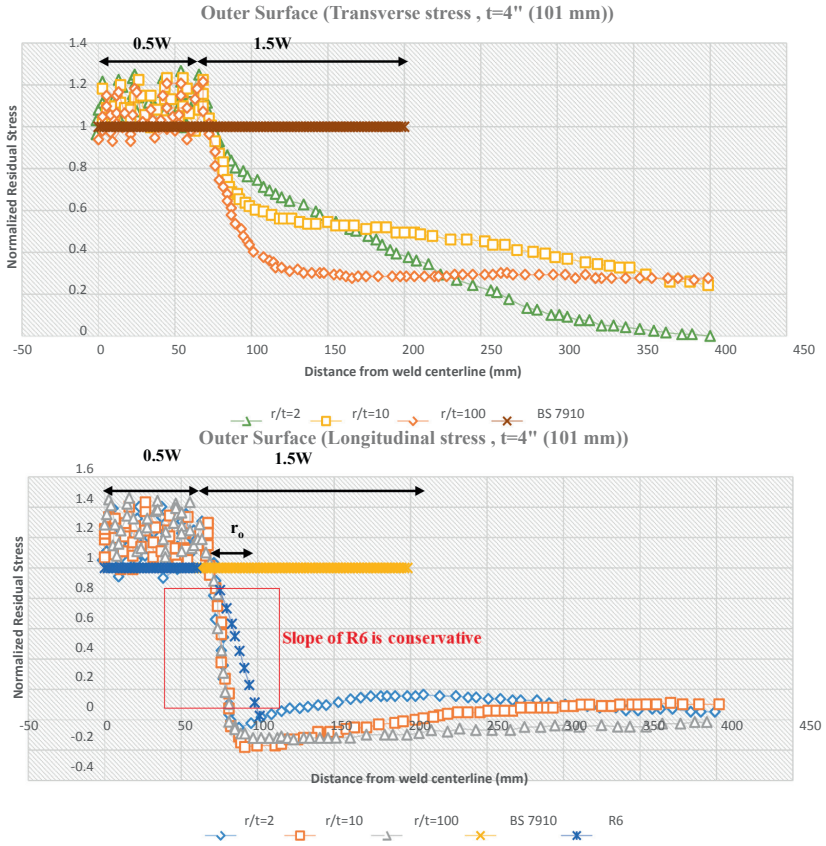

Fig. 10. Comparison of residual stress distributions along outer surface (a) transverse, and (b) longitudinal direction, adapted from [21].

3.1.4. Demonstrating the effect of r/t ratio on residual stress profile using stress decomposition technique

As previously explained, the stress decomposition technique [32] was used by Dong [19] and Song [21] in their work to quantitatively highlight the effect of decomposed components of stress for residual stress distributions. In Fig. 11, decomposed residual stress components at weld toe locations, as a function of r/t ratio for single vee (SV) and double vee (DV) girth welds, are shown, calculated from Eqs. (1)–(3). Observations from Fig. 11 follow.

- In Fig. 11, it can be observed that the decomposed bending component decreases linearly with increasing r/t ratio in the case of axial and hoop residual stresses. This implies a reduced radial restraint as r/t ratio increases, as it measures radial bending stiffness.
- The membrane component is usually negligible in the axial direction (not shown in Fig. 11), unless final assembly welds or severe restraints are present.
- The membrane component of hoop residual stresses increases linearly with increasing r/t ratio.
- This technique recognizes patterns of residual stress distributions at interesting locations (weld toe, weld center, etc.) for all thicknesses, joint configurations (SV, DV) regarding r/t ratio effects.
- The component geometry feature radius to thickness ratio (r/t) clearly highlights membrane and bending components of through-thickness residual stress distributions in the axial and hoop directions.

3.1.5. Demonstrating the effect of thickness on residual stress profile with increasing r/t ratio

In the Phase 1 report of PVRC JIP [41], thickness effect was characterized as an important criterion for residual stress distribution in different weld geometries, as mentioned in Fig. 7, for thicknesses up to 50 mm (2 in.). Phase 2 [40] of PVRC JIP focused on thicknesses from above 50 mm (2 in.) to 250 mm (10 in.) for different weld geometries. As illustrated in Table 1, the effect of thickness on axial residual stress distribution with increasing r/t ratio as mentioned in PVRC JIP Phase1 [41]. It shows that keeping the r/t ratio constant with increasing thickness leads to a global bending type behavior (i.e. compression on the outside and tension on the inner diameter), which changes to local

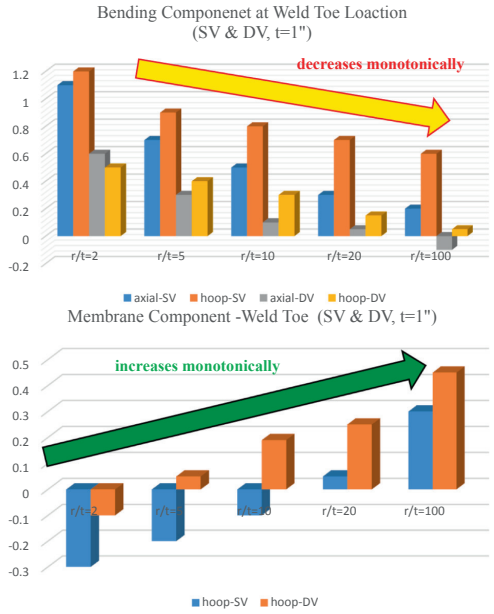

Fig. 11. Residual stress decomposed components at weld toe locations as a function of r/t ratio for Single V (SV) and Double V (DV) girth welds, adapted from [40].

bending (i.e. tension on the outside and compression on the inner diameter). As thickness increases or r/t increases, the bending component changes to a self-equilibrating type [24].

Thickness effects are better characterized in terms of decomposed stress components, as shown in Table 2. The effect of thickness on decomposed stress components with increasing thickness are shown for axial bending, hoop bending and hoop membrane at the weld toe location. The axial and bending hoop components increases between thickness 6.25–25.4 mm (1/4″-1″) and becomes constant for thickness 25.4–250.4 mm (1″–10″) for single and double V weld geometries, whereas, on the other hand, the hoop membrane component decreases with increasing thickness.

3.2. Heat input

As explained previously in Section 2.1.1 (Eq. (7)) and recommended by Phase 1 of the PVRC JIP [41], linear heat input is defined as a product of current, voltage and welding efficiency, divided by travelling speed, with units of J/mm. However, characteristic heat input per unit area (e.g., J/mm^2) or per unit volume (J/mm^3) has demonstrated better ability to highlight residual stress distribution patterns as defined in the PVRC JIP Phase 2 report [40]. Parameter $\dot{Q}$ referred to as characteristic heat input, is defined as follows in Eq. (8).

$$\dot{Q} = \frac{Q'}{A_{pass}} t_n \tag{8}$$

where A_{pass} is the average pass area and t_n represents weld pass layer thickness. Q' (linear heat input) is further defined in Eq. (9) as the sum of Q'$_1$ and Q'$_2$, taking account of additional 3D heat loss (η'= 1.35). In a 2D heat transfer model for welding [42], a less complicated approach is widely accepted among researchers [29 42], separating heat input into two parts, Q'$_1$ and Q'$_2$. Q'$_1$ represents heat content involved to deposit a molten weld pass at a specified melting temperature and Q'$_2$ is heat that is required to hold (t_{hold}) the melting temperature shown in Eq. (10) and Eq. (11).

$$\dot{Q'} = (\dot{Q_1'} + \dot{Q_2'}) \cdot \eta' \tag{9}$$

$$\dot{Q_1'} = \rho \cdot C_P \cdot \Delta T \cdot A_{pass} \tag{10}$$

Table 2
Thickness effect on decomposed stress components with increasing thickness [24].

Thickness effect on decomposed stress components with increasing thickness				
At weld toe	Weld Geometry	thickness		
		6.25 mm (1/4″)	25.4 mm (1″)	254 mm (10″)
Axial bending	Single V & Double V	Increases (1/4″-1″)		Constant (1-″10″)
Hoop bending		Increases (1/4″-1″)		Constant (1-″10″)
Hoop membrane		decreases		

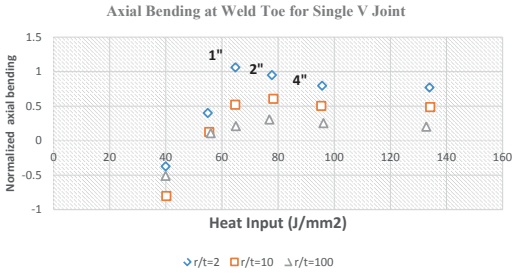

Fig. 12. Decomposed axial bending residual stress components at weld toe as a function of characteristic heat input for SV girth welds, adapted from [24].

Table 1
Thickness effect on axial residual stress distribution, adapted from [24].

Thickness effect on axial residual stress distribution with increasing r/t ratio							
r/t ratio		Thickness (mm)				Axial residual stress	Weld geometry
2		25	50	100	250	Changes global to local bending	Single Vee
10		Thickness increase while r/t constant				Local bending is gradually transitioned to self-equilibrating type	Single Vee
20							Single Vee
100		Thickness and r/t increases					Single Vee

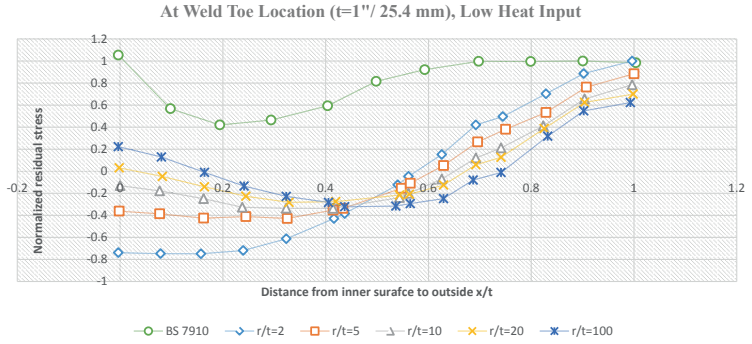

Fig. 13. Transverse residual stresses for low heat input cases t = 1″ (25.4 mm) at weld toe for different r/t ratios, adapted from [19].

$$\dot{Q_2} = 2k \cdot \Delta T \cdot \sqrt{\frac{t_{hold}}{\pi\alpha}} \cdot L_S \tag{11}$$

2D heat transfer models have a limitation of leaving heat loss in the third direction; hence, careful establishment must be applied between the heat input implied in the 2D cross-section models (e.g., axisymmetric or generalized plane strain models) and the linear heat input (Eq. (7)) used in practice [34]. The linear heat input parameter defined in Eq. (7), with units of J/mm, badly underestimates residual stress distributions in correlating different heat input conditions, as proven in investigations by Bouchard [23] and Dong [22]. In Phase 2 of the PVRC JIP, where a wide range of geometries and welding processes were investigated by Dong [22] and his co-workers [40], heat input $\dot{Q}$, mentioned in Eq. (8), was proposed as the characteristic heat input parameter for correlating through-thickness membrane and bending stress components.

3.2.1. Decomposed residual stress components in heat input

Characteristic heat input $\dot{Q}$, as defined in Eq. (8), is effective in correlating a large number of residual stress distributions related to r/t ratio and thickness effects, as proposed by Dong and his co-workers [39]. Decomposed residual stress components at the weld toe location are shown in Fig. 12, as a function of characteristic heat input$\dot{Q}$ for single V girth welds, as mentioned in the PVRC JIP Phase 2 report [40] for axial bending, hoop membrane and hoop bending components. In this example, $\dot{Q}$ (J/mm2), the heat input per unit of the weld layer cross-section area, was calculated from Eq. (8), in which Q' stands for linear heat input which can be calculated by using Eq. (10) and Eq. (11). Fig. 12 depicts decomposed normalized axial bending residual stress at the weld toe location for single-V girth welds as a function of characteristic heat input $\dot{Q}$ (J/mm^2). This demonstrates the ability to distinguish the effects of r/t ratio and thickness for the residual stress distribution of pipe girth welds. Similar results were also demonstrated for hoop membrane and bending components in the PVRC JIP Phase 2 report [40]. Characteristic heat input parameter$\dot{Q}$ (J/mm^2) can be directly related to weld shrinkage force in the hoop direction, as the maximum membrane hoop stress of yield magnitude exerts the maximum circumferential shrinkage force, causing the strongest axial bending stress, as demonstrated in the work of Song [39]. Thus, characteristic heat input parameter$\dot{Q}$ serves as an important driving force for highlighting the bending component of the axial residual stress.

3.2.2. Role of heat input in FFS codes (BS 7910) at weld toe location

As defined in Eqs. (4)–(6) and illustrated in Fig. 4, transverse residual stress in BS 7910 is divided into 'high' (heat input > 120 J/mm^2), 'low' (heat input ≤ 50 J/mm^2) and 'medium' (heat inputs between 50 and 120 J/mm^2). From the work of Dong [19], the results of parametric analysis are illustrated in Fig. 13 on 2¼ Cr-Mo-V steel for wall thickness 25.4 mm (1 in.) in low heat input at the weld toe location. BS 7910 provides an upper bound estimate of residual stress distributions as per Eq. (4). It can be clearly observed that, from Fig. 13, the BS 7910 profiles for low heat input become more conservative as the r/t ratio becomes smaller (r/t = 2) at the weld toe location. A noticeable effect is observed on the inside surface compared to the outer surface of the pipe.

In Figs. 14 and 15, transverse residual stress distributions for medium and high heat input for wall thicknesses of ¼ inches (6.35 mm) and 1 in. (25.4 mm), respectively, at the weld toe location are depicted from the work of Dong [19], to illustrate the conservatism associated with BS 7910. At the outer surfaces, with increasing r/t ratio, residual stresses are significantly lower. Transverse residual stress at the inside diameter of the pipe is close to yield strength, whereas the stress at the outer diameter is reduced to approximately 25% of yield strength for the case of medium heat input.

4. Complete residual stress profile estimation scheme at a distance away from weld

As reviewed and explained in earlier sections, pipe (r/t) ratio and characteristic heat input parameter$\dot{Q}$ serve as key parameters in estimating residual stress profiles applicable for wide weld geometries and welding conditions. In Eqs. (1)–(3), using stress decomposition technique clearly defines decomposed components of residual stress at girth weld locations in terms of bending, membrane and self-equilibrating, which can be further expressed as Eq. (12) and illustrated in Fig. 16.

$$\frac{\sigma_r(\varepsilon)}{\sigma_y} = \bar{\sigma_m} + \bar{\sigma_b}\varepsilon + \bar{\sigma_{se}}(\varepsilon) \tag{12}$$

where ε is a dimensionless factor, expressed as$\varepsilon = 2\left(\frac{x}{t}\right) - 1$, x measured

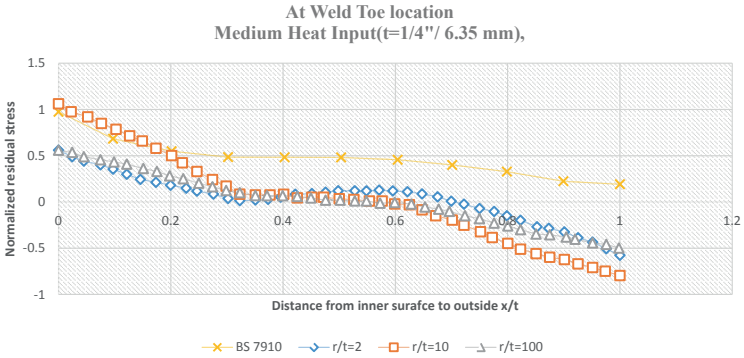

Fig. 14. Transverse residual stresses for medium heat input cases (t = 1/4″ (6.35 mm)) at weld toe for different r/t ratios, adapted from [19].

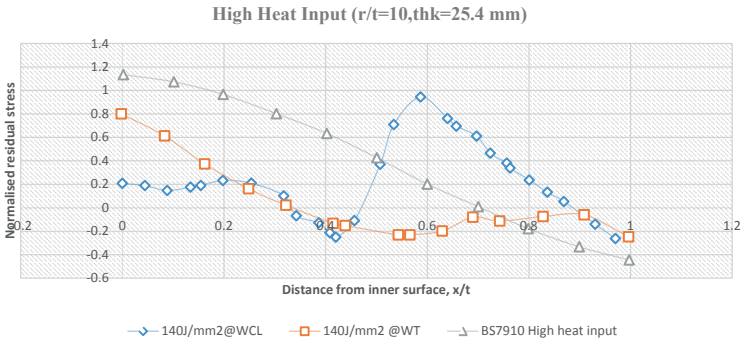

Fig. 15. Comparison of transverse residual stresses for high heat input cases (t = 1″, 25.4 mm), adapted from [19].

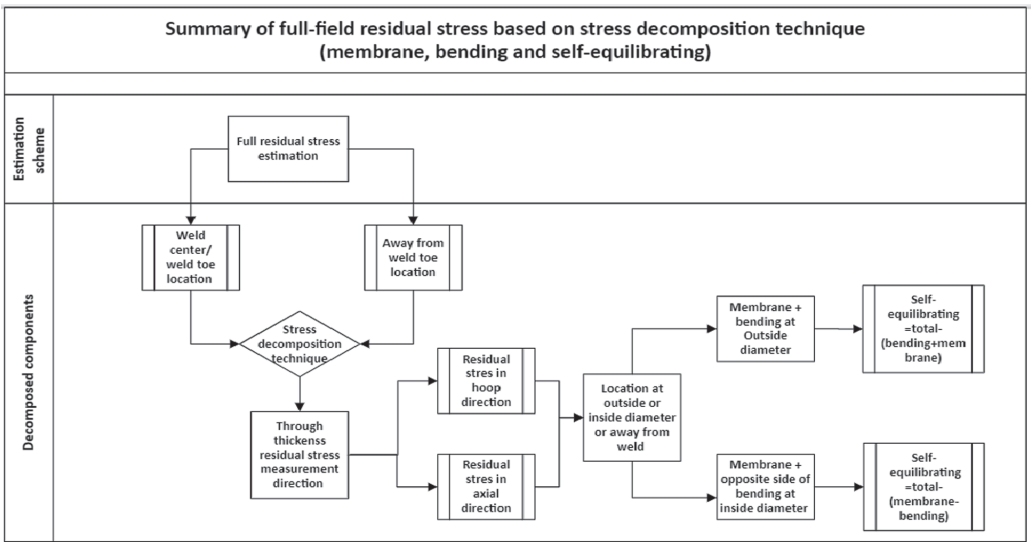

Fig. 16. Full residual stress estimation scheme, adapted from [24].

from the inside of the pipe to the outside, and $\sigma_y$is the yield strength of the material.

At a distance away from the weld, the residual stress estimation shell theory-based estimation scheme [43] proposed by Song and Dong [19,37] is referred. This theory was introduced by Song and Dong [19,37] to quantify the effect of restraint on residual stress estimation through thickness profiles for distances or positions along the axial direction of the pipe. Bending and membrane components of through-thickness residual stress profiles are known to contribute equally towards the crack driving force at distances away from the weld [19,32,38], in contrast to the self-equilibrating component. The role of component geometry like radius to thickness ratio, weld geometry configurations such as single or double Vee joints, heat input and material effects are well established in this scheme for estimating accurate residual stress distribution at distances away from the weld.

The use of the shell theory-based estimation scheme [43] has been found to produce conservative results [37] for thicknesses ranging from 6.25 to 100 mm and different weld joint configurations having varying r/t ratios between 10 and 100. This scheme has the advantage of estimating less conservative residual stress components at distances away from the weld, in terms of stress decomposition components, and highlighting the role of crack driving components, i.e. membrane and bending. Another advantage of using this scheme is the estimation of radial distortion in welded thick sections. This scheme can be used efficiently in the defect assessment of proximity girth welds.

5. Conclusion

In this manuscript, a detailed review is presented of residual stress estimation in fitness-for-service codes (FFS) like BS 7910, R6 & API 579 used in the defect assessment of welded components. Available profiles in these FFS codes are based on the results of the residual stress measurement technique coupled with finite element analysis results. Due to large variations in measurement techniques, modeling methods and the complex nature of welding, the residual stress profiles recommended in these FFS codes at the weld center or weld toe region are found to be overly conservative. Residual stress estimation schemes at a distance away from the weld recommended in these codes have been found to be practically nonexistent or overly conservative. BS 7910 has a constant transverse residual stress profile in 1.5 W region from the weld centerline, where W is weld width. Beyond this region, there are no prevalent recommendations in the BS 7910 code. R6 and FITNET assume a linear distribution of longitudinal residual stress distribution varying from material yield strength at the weld toe to zero at an estimated yield zone boundary. API 579, however, provides a single curve-based upper-bound estimate of axial and hoop residual stress profiles for locations away from the weld toe. This clearly highlights the overconservativeness brought by these codes while assessing residual stress at a distance away from the weld for application scenarios like proximity welds for the defect assessment of welded structural joints and piping joints, where the superposition of residual stresses can take place.

The stress decomposition technique, a length scale-based characterization, was introduced by Dong and his co-workers, decomposing residual stress components into membrane, bending and self-equilibrating stresses, corresponding to decreasing length scale. The introduction of this technique in the BS 7910 FFS code has been found useful in separating the contribution of global and local residual stress and visualizing better patterns of residual stress distribution and analyzing many residual stress cases to identify the controlling parameters. However, residual stress distribution at a distance away from welds exhibits a “global bending” behavior in the axial residual stress direction, i.e. compression of the outer surface and tensile stress on the inside of the pipe geometry, which provides valuable analysis in defect assessment procedures. For the development of consistent residual stress profiles prescribed in the FFS codes, the Phase 1 & 2 reports of the Pressure Vessel Research Council’s (PVRC) joint industry project (JIP) analyzed key contributing factors like material effects, thickness (t), weld pass, etc., of which the component geometry feature, pipe mean radius to thickness ratio (r/t), and the characteristic heat input, (per unit volume) ($\dot{Q}$), has shown a functional dependency of decomposed through-thickness membrane and bending stresses. Key important features like component geometry (e.g., r/t ratio), shrinkage zone (plastic zone size), controlled by joint preparation and heat input, highlight the important residual stress profiles for various piping and pressure vessel configurations. The research findings of Dong and his co-workers are under consideration to be adopted as part of the API 579 FFS codes’ revisions for residual stresses, comprising various mechanics-based estimation schemes for distances away from the weld.

While determining full residual stress profiles at the weld center and toe regions by use of the stress decomposition technique, membrane and bending components have been shown to contribute significantly towards the determination of the crack driving force, in contrast to the low contribution of the self-equilibrating component. However, at a distance away from the weld, shell theory recommended from the research results of Song and Dong provides consistent through-wall residual stress distributions in terms of bending and membrane components. The role of component geometry, such as radius to thickness ratio and heat input, is well established in this scheme for estimating accurate residual stress distribution at distances away from the weld. The use of machine learning algorithms based on input data from the results of FE analysis, coupled with experiments on selected components with varying geometries and welding processes, can help in developing application guidance tools for predicting accurate residual stress profiles on welded joints at distances away from the weld.

CRediT authorship contribution statement

Sachin Bhardwaj: Conceptualization, Investigation, Methodology, Visualization, Writing - original draft, Writing - review & editing. **R.M. Chandima Ratnayake:** . **:** Conceptualization, Formal analysis, Funding acquisition, Project administration, Supervision.

Declaration of Competing Interest

The authors declare that they have no known competing financial interests or personal relationships that could have appeared to influence the work reported in this paper.

Acknowledgment

This work has been carried out as part of a PhD research project, performed at the University of Stavanger, Norway. The research is fully funded by the Norwegian Ministry of Education.

Appendix A. Proposal for estimating residual stress profile at weld toe and away locations on girth welds

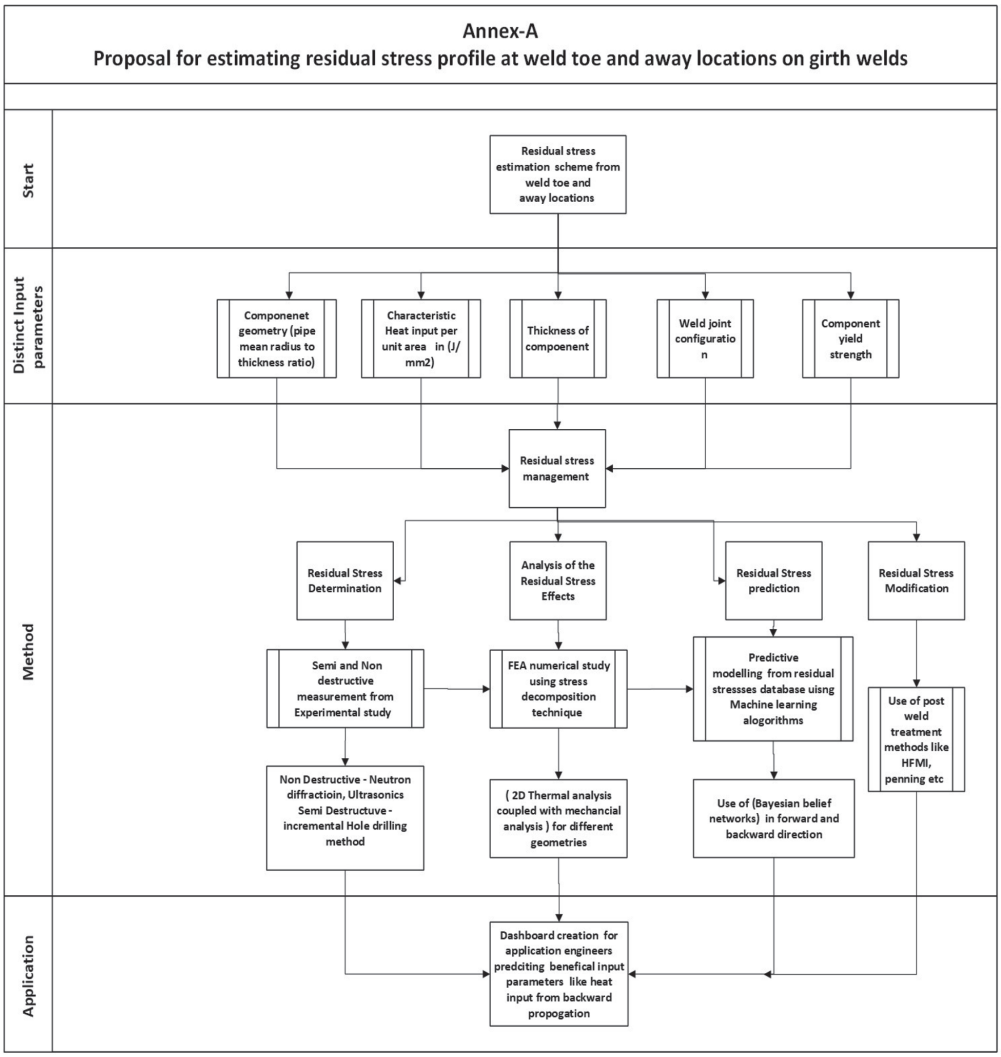

References

[1] R.M.C. Ratnayake, V.A. Brevik, Experimental investigation of underwater stud friction stir welding parameters, Mater. Manuf. Processes 29 (10) (2014) 1219–1225.

[2] R.M. Ratnayake, et al., Underwater friction stud welding optimal parameter estimation: engineering robust design based approach, J. Offshore Mech. Arct. Eng. 137 (2015).

[3] R.M. Ratnayake, D. Dyakov, Optimal arc welding process parameter combination design and metallographic examination for SDSS Butt Welds, J. Offshore Mech. Arct. Eng. 139 (2017).

[4] R.M. Ratnayake, An algorithm to prioritize welding quality deterioration factors: A case study from a piping component fabrication process, Int. J. Qual. Reliab. Manage. 30 (2013).

[5] R.M. Ratnayake, A methodology for assessing most vulnerable welding procedure specifications and imperfection factors, Int. J. Data Anal. Tech. Strategies 6 (2014) 362–383.

[6] S. Bhardwaj, R.M.C. Ratnayake, Challenges due to welds fabricated at a close proximity on offshore structures, Pipelines, And Piping: State Of The Art, in: OMAE2020, ASME, Editor, 2020, ASME: OMAE2019-18586.

[7] Larsson Magnus, L. Mattias, R.M.C. Ratnayake. Investigation of fatigue strength behaviour in dual weld S420 steel joints fabricated at a close proximity, in: Proceedings of 1st International Conference on Structural Damage Modelling and Assessment. Lecture Notes in Civil Engineering, vol. 110, 2020.

[8] Larsson Magnus, L. Mattias, R.M.C. Ratnayake, Experimental investigation of weld joints manufactured at close proximity in S420 structural steel, in: Proceedings of 1st International Conference on Structural Damage Modelling and Assessment. Lecture Notes in Civil Engineering. Vol 110, 2020.

[9] Larsson Magnus, L. Mattias, X. Ficquet, R.M.C. Ratnayake, Experimental Residual Stress Investigation of Weld Joints Fabricated at a Close proximity in S420 Structural Steel. Proceedings of 1st International Conference on Structural Damage Modelling and Assessment. Lecture Notes in Civil Engineering. Vol 110, 2020.

[10] S.K. Bate, et al., A review of residual stress distributions in welded joints for the defect assessment of offshore structures. Offshore technology report. Vol. OTH 482, 1998, Sudbury: HSE Books.
[11] B. Brickstad, B.L. Josefson, A parametric study of residual stresses in multi-pass butt-welded stainless steel pipes, Int. J. Press. Vessels Pip. 75 (1) (1998) 11–25.
[12] M. Law, et al., Residual stress measurements in coil, linepipe and girth welded pipe, Mater. Sci. Eng., A 437 (1) (2006) 60–63.
[13] M.N. James, et al., 10 - Assessing residual stresses in predicting the service life of welded structures, in: K.A. Macdonald (Ed.), Fracture and Fatigue of Welded Joints and Structures, Woodhead Publishing, 2011, pp. 276–296.
[14] FITNET, European Fitness-for-service Network, 2006.
[15] American Petroleum Institute, API 579-1/ASME FFS-1.Appendix E, Houston, TX: American Petroleum Institute: USA, 2016.
[16] British Energy Generation Ltd, Procedure R6 revision 4, assessment of the integrity of structures containing defects, UK, 2013.
[17] SINTAP, Structural Integrity Assessment Procedures for European Industry, BriteEuRam Project Final Report, 1999.
[18] British Standard, BS 7910:2005: Guide to methods for assessing the acceptability of flaws in metallic structures, 2005,: UK. p. 535.
[19] P. Dong, et al., On residual stress prescriptions for fitness for service assessment of pipe girth welds, Int. J. Press. Vessels Pip. 123–124 (2014) 19–29.
[20] A. Mirzaee-Sisan, G. Wu, Residual stress in pipeline girth welds- A review of recent data and modelling, Int. J. Press. Vessels Pip. 169 (2019) 142–152.
[21] S. Song, P. Dong, J. Zhang, A full-field residual stress profile estimation scheme for pipe girth welds, vol. 9, 2012.
[22] P. Dong, J.K. Hong, On the residual stress profiles in new API 579/ASME FFS-1 Appendix E, Welding in the World 51 (5) (2007) 119–127.
[23] P.J. Bouchard, Validated residual stress profiles for fracture assessments of stainless steel pipe girth welds, Int. J. Press. Vessels Pip. 84 (4) (2007) 195–222.
[24] S. Song, Analysis and characterization of residual stresses in pipe and vessel welds, in: Naval Architecture and Marine Engineering, University of New Orleans New Orleans, USA, 2012.
[25] Ali Mirzaee-Sisan, P.J.B., Foroogh Hosseinzadeh, Standardisation on Measurement and Interpretation of Residual Stress Data, in OMAE2019, ASME, Editor, ASME: OMAE2019-96615, 2019.
[26] P.J. Bouchard, Code characterisation of weld residual stress levels and the problem of innate scatter, Int. J. Press. Vessels Pip. 85 (3) (2008) 152–165.
[27] A. Yaghi, et al., A comparison between measured and modeled residual stresses in a circumferentially butt-welded P91 steel pipe, J. Pressure Vessel Technol. 132 (2010).
[28] A. Yaghi, et al., Residual stress simulation in thin and thick-walled stainless steel pipe welds including pipe diameter effects, Int. J. Press. Vessels Pip. 83 (11) (2006) 864–874.
[29] A.H. Yaghi, et al., Residual stress simulation in welded sections of P91 pipes, J. Mater. Process. Technol. 167 (2) (2005) 480–487.
[30] American Petroleum Institute, API RP 579, Houston, TX: American Petroleum Institute; August 2007, USA, 2007.
[31] J. Sharples, I. Hadley, Treatment of residual stress in fracture assessment: background to the advice given in BS 7910:2013, Int. J. Press. Vessels Pip. 168 (2018).
[32] P. Dong, Length scale of secondary stresses in fracture and fatigue, Int. J. Press. Vessels Pip. 85 (3) (2008) 128–143.
[33] P. Dong, Recommendations for determining residual stresses in fitness-for-service applications, Welding Res. Council Bull. (2002) 1–61.
[34] P. Dong, S. Song, X. Pei, An IIW residual stress profile estimation scheme for girth welds in pressure vessel and piping components, Welding World 60 (2) (2016) 283–298.
[35] British Standard, BS 7910:2019: Guide to methods for assessing the acceptability of flaws in metallic structures, 2019, UK. p. 535.
[36] S. Song, P. Dong, A framework for estimating residual stress profile in seam welded pipe and vessel components Part II: Outside of weld region, Int. J. Press. Vessels Pip. 146 (2016) 65–73.
[37] S. Song, P. Dong, X. Pei, A full-field residual stress estimation scheme for fitness-for-service assessment of pipe girth welds: Part II – A shell theory based implementation, Int. J. Press. Vessels Pip. 128 (2015).
[38] P. Dong, F. Brust, Welding residual stresses and effects on fracture in pressure vessel and piping components: a millennium review and beyond, J. Pressure Vessel Technol.-Trans. ASME – J. Pressure Vessel Technol. 122 (2000).
[39] S. Song, P. Dong, A framework for estimating residual stress profile in seam-welded pipe and vessel components part I: Weld region, Int. J. Press. Vessels Pip. 146 (2016) 74–86.
[40] S. Song, P. Dong, X. Pei, A full-field residual stress estimation scheme for fitness-for-service assessment of pipe girth welds: Part I - Identification of key parameters, Int. J. Press. Vessels Pip. 126–127 (2015) 58–70.
[41] P. Dong, Z. Cao, J.K. Hong, Final PVRC Residual Stress and Local PWHT JIP Report on Investigation of Weld Residual Stresses and Local Post Weld Heat Treatment, Phase I, 2005.
[42] S. Song, X. Pei, P. Dong, An analytical interpretation of welding linear heat input for 2D residual stress models, in: ASME 2015 Pressure Vessels and Piping Conference, 2015.
[43] S. Timoshenko, Theory of Plates and Shells, McGraw-Hill Inc., 1959.

Proceedings of the ASME 2021 40th International Conference on Ocean, Offshore and Arctic Engineering
OMAE2021
June 21-30, 2021, Virtual, Online

OMAE2021-62843

ESTIMATION OF WELDING-INDUCED PLASTIC ZONE SIZE AND RESIDUAL STRESS LEVELS: LINEAR HEAT INPUT APPROXIMATION

Sachin Bhardwaj [1], R.M. Chandima Ratnayake
Department of Mechanical and Structural Engineering and Material Science,
University of Stavanger, Norway

The International Journal of Advanced Manufacturing Technology
https://doi.org/10.1007/s00170-022-09022-5

ORIGINAL ARTICLE

Welding procedure qualification record (WPQR) for welds fabricated at proximity

Sachin Bhardwaj[1] · **R. M. Chandima Ratnayake**[1]

Received: 26 October 2021 / Accepted: 5 March 2022

Abstract
Maintaining the minimum allowable distance between proximity welds has always been considered a subject of debate among design engineers, welding engineers/inspectors and fabricators/engineering contractors. The scattered nature of guidelines available in welding codes and standards for maintaining the minimum allowable distance poses a significant challenge in the welding procedure and inspection criteria development process. This is especially critical for complex welded joints on submerged sections of offshore structures, in compact layouts/branched connections of topside piping components, and on topside structural joints (depending on the complexity). This manuscript presents the findings of an experimental study that was performed by fabricating two girth welds at proximity on an S355 steel tubular section with diameter of 219.1 mm and thickness of 8.18 mm. Proximity girth welds were fabricated on S355 tubular sections at three different distances between their weld toes, 5, 10, and 15 mm, respectively, using two different welding procedures. Welding procedure qualification record (WPQR) was performed, and all prescribed mechanical tests were recorded as per NORSOK M-101, a structural steel fabrication code. Although all results from the mechanical test met the minimum specified values as defined in the NORSOK code, the research findings revealed a noticeable difference in Charpy and hardness values for proximity region between adjacent welds. Considerable changes in final microstructure morphology were observed between proximity welds due to varying thermal cycles. These observations can form the basis for the future welding procedure qualification of critical welded joints, especially for proximity welds on critical welded joints of offshore structures and welds fabricated during replacement/repair procedures in compact piping layouts.

Keywords Proximity welds · Welding procedure qualification record · NORSOK M-101

1 Introduction

Welding is the most widely accepted method for the joining of two structural members with or without the use of filler wire when it comes to the fabrication of steel and various advanced engineering alloys, ranging from offshore jackets, floating structures, piping and pipelines to bridges, and aircrafts [1–6]. In the past, many accidents and delays have been related to weld failures; however, this issue persists, despite the improvement in welding techniques and inspection procedures [7]. For instance, the Alexander L. Kielland offshore accommodation rig failure in the restrained geometry of its brace hydrophone support was reported to be due to insufficient fillet weld size and high residual stress, leading to an overload of welds and catastrophic fatigue cracking [8]. The recent delay of Equinor's Johan Castberg floating production, storage and offloading (FPSO) hull for Barents Sea has been credited to faulty welds [9]. The popularity of both fixed and floating types of wind turbines cannot be ignored, as accidents due to cracks in welds are gaining attention, in contrast to the usually reported cracks in the bolts of turbines [10]. Such incidents in large structures cannot be overlooked, as the consequences due to failure leading to loss of life, climate, and property, are very high and irrevocable.

The fabrication of large structures like offshore jacket structures, onshore and offshore wind monopiles and tubular truss bridge structures often brings forward the challenge of welds coming within proximity of each other, as shown in Fig. 1. This challenge of maintaining a minimum distance between welds is often debated among designers, inspectors,

✉ R. M. Chandima Ratnayake
chandima.ratnayake@uis.no

[1] Department of Mechanical and Structural Engineering and Material Science, University of Stavanger, Stavanger, Norway

Published online: 16 March 2022

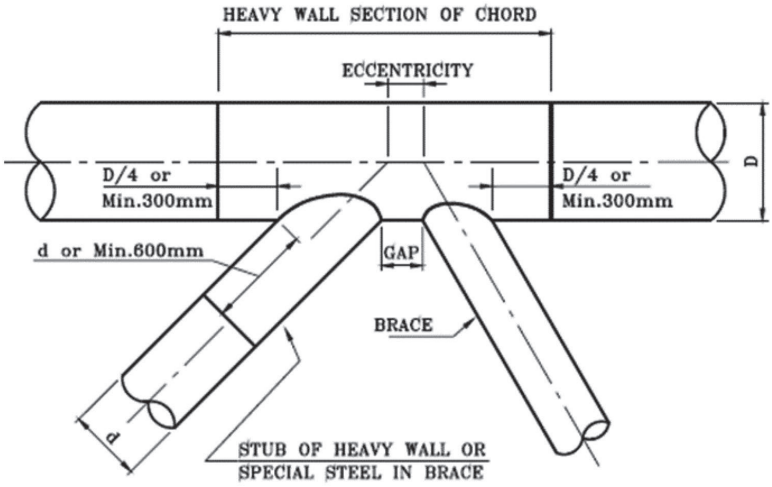

Fig. 1 Detail of offshore joints [13]

and contractors who often rely on international codes and standards for recommendations [11]. A detailed assessment of these codes and practices for maintaining minimum distance criteria between welds has been performed previously by the authors in [12] where a clear lack of consensus has been found regarding maintaining a final distance that is often based on a factor of 4 or 5 times the thickness or 1 or 1.5 times the diameter. In procedures for replacing compact layouts of piping racks, unavoidable situations of placing a new weld close to an existing weld of branched connections, nozzles, etc., are often encountered, as is the case in offshore jacket critical joints, e.g., non-overlapping braces. In the case of repair or replacement procedures, international codes and standards offer no guidance on defining, either the minimum distance between welds or welding procedures for proximity welds, and such decisions are often left to stakeholders' engineering judgment.

DNVGL-ST-0126 code on support structures for wind turbines [14] recommends maintaining a distance between consecutive girth welds of not less than 300 mm for an outer diameter of less than 300 mm and states that *" The minimum weld distances mentioned above have been derived based on practical experience. Shorter distances may be suitable but need to be proven both with respect to impact on stress concentration factor (SCFs) as well as residual stresses*". This indicates a need to further investigate areas between proximity welds with an unqualified welding procedure qualification record (WPQR) which have experienced multiple cycles of heating and cooling and unprescribed residual stress profiles used during defect assessment procedures, as per fitness for service (FFS) codes [15, 16]. The importance of potential factors that degrade welding quality in terms of defects requires an assessment of the most vulnerable welding procedure specifications (WPSs) and imperfection factors that contribute to the majority of defective welds [17]. Pressure Vessel Research Council (PVRC) Phase 2 [18, 19] highlights the conservativeness in residual stress profiles at a distance away from welds, as per FFS codes such as BS7910, API 579 RP-1/ASME FFS-1, etc.

With this background, the aim of the current study is to qualify WPQRs for two different girth welds, placed at proximity with a minimum distance between their weld toes of 5 mm, 10 mm, and 15 mm, respectively. All necessary mechanical testing was performed in accordance with NORSOK M-101 [20], the code for structural steel fabrication, to understand changes in hardness and Charpy values at the proximity region. Lastly, detailed microstructure characterization was performed to understand the grain morphology at the proximity region due to the varying thermal cycles of two different welds. The remainder of the paper is structured as follows: Sect. 2 presents the experimental details. Thereafter, in Sect. 3, the results are presented and discussed. Subsequently, in Sect. 4, a conclusion is drawn.

2 Experimental set-up

A schematic diagram of the experimental set-up is shown in Fig. 2, pictorially displaying the fabrication steps from 'a' to 'c'. Structural steel grade S355G14 + N seamless pipes were selected for this experiment, with an outside diameter of 219.1 mm and a thickness of 8.18 mm. As shown in Fig. 2a–c, vee joint geometry was machine cut for welds A and B in accordance with prequalified WPS adopted from reputable industrial partners. As shown in Fig. 2b, initially, weld A was fabricated as a single weld on a pipe section

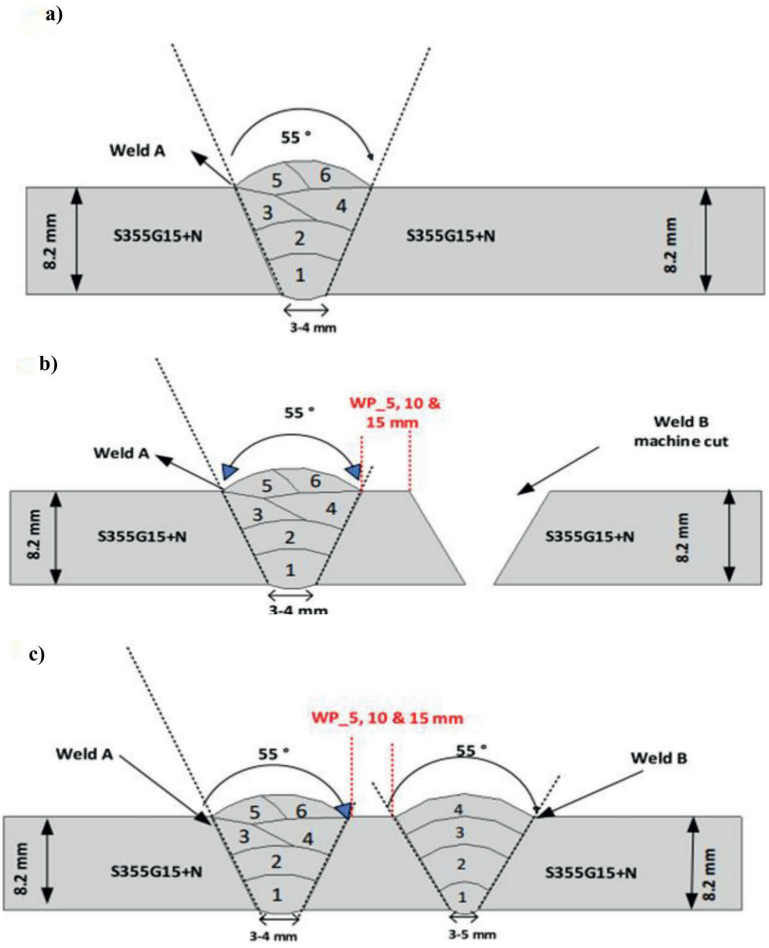

Fig. 2 Schematic diagram of experimental set up from (**a**) to (**c**)

and, subsequently, the vee groove for weld B was machine cut. Lastly, weld B was welded after weld A was completed, maintaining proximity distances between their weld toes of 5,mm, 10 mm, and 15 mm, respectively, as shown in Fig. 2c and summarized in Table 1.

In this study, welding parameters were maintained as per pre-qualified WPS for welds A and B, and digital weld log data was maintained during the experiments, as mentioned in Table 2. The mechanical and material composition of the tubular pipe and filler wire is also presented in

Table 1 Summary of fabrication procedure for each weld proximity case

Weld type	Proximity distance (mm)			Welding process	EN classification	Weld groove	Shielding gas	Welding position
A	5	10	15	Tungsten inert gas (TIG)	141	Vee Joint	Argon	PA/1G/Flat
B				Metal Active Gas(MAG)-metal cored + Flux cored Arc welding (FCAW)	138 + 136	Vee Joint	20% carbon dioxide (CO_2) in pure argon (Ar)	PA/1G/Flat

Table 2 Welding parameters for Weld A, TIG welding process (141) and welding parameters for Weld B, MAG + FCAW welding process (138 + 136)

Pass	Weld	Filler (mm)	Welding process	Current (A)	Voltage (V)	Polarity	Travel speed (mm/min)	Gas flow (l/min)	Heat input (kJ/mm)
1	A	2.4	141	100–135	10–20	DC −	39–40	15–20	1.5–2.49
2	A	2.4	141	140–180	10–14	DC −	75–80	15–20	1.05–2.02
Fill	A	2.4	141	160–230	11–15	DC −	85–120	15–20	0.88–2.44
Cap	A	2.4	141	160–230	11–15	DC −	85–120	15–20	0.88–2.44
1	B	1.2	138	90–125	14–16	DC +	65–85	16–20	0.89–1.85
2	B	1.2	136	160–220	22–29	DC +	180–400	16–20	0.53–2.13
Fill	B	1.2	136	180–250	22–29	DC +	180–400	16–20	0.59–2.42
Cap	B	1.2	136	180–250	22–29	DC +	180–400	16–20	0.59–2.42

Tables 3 and 4, respectively. In this study, to simulate the practical situation of weld proximity encountered during repair and replacement procedures, weld B was welded with a different welding procedure, i.e., MAG-metal core (138) semi-automatic method for root pass, as it employs a short-circuiting technique for better root penetration and FCAW (136) semi-automatic method for the remaining passes for faster production. In weld A, all passes were completely fabricated with TIG (141), a semi-automatic welding process. This demonstrates the practical situation of critical welded joints fabricated under shop conditions, by using a controlled procedure like TIG, and during on-site repair or replacement situations, welded with a faster and more mobile procedure like MAG + FCAW.

NORSOK M-101 [20] code was used for qualification of WPQR and adopted in this project catering for the Norwegian continental shelf (NCS) and offshore-welded tubular structures used in oil exploration and the processing industry. NORSOK M-101 code for WPQR is strictly valid within the limitations specified in ISO 15614–1 [21], the widely accepted code for welding qualification around the world. Welding was performed under controlled conditions after optimizing the welding parameters as mentioned in Tables 2 and 3 in line with pre-qualified WPS. Three samples from each proximity distance were finally fabricated and were subjected to mechanical tests as per NORSOK M-101 and ISO 15614–1 as detailed in Table 5.

All necessary and recommended destructive and non-destructive testing (NDT) was performed, and the general procedure and acceptance criteria for each method are summarized in Table 6, as per ISO EN15614-1 [21]. Charpy specification as per EN ISO 9016–2012 was performed; however, in the case of WPQR for proximity welds, Charpy locations shown in Fig. 3 were selected. The notch for Charpy specimens was made at locations shown in Fig. 3.

- Notch in center of weld
- Notch in fusion line (FL)
- Notch in heat affected zone (HAZ), 2 mm from fusion line
- Notch in HAZ, 5 mm from fusion line

Hence, in the case of a weld proximity distance of 5 mm, six samples and four sets of Charpy locations were extracted, as the fusion line (FL + 5 mm) was not possible due to the 5 mm proximity distance. In the proximity case of 10 and 15 mm case, a total of eight samples and four sets were extracted due to there being sufficient proximity distance.

3 Results and discussion

3.1 Visual and radiographic examination

As shown in Table 6, all mechanical destructive and NDT was performed in accordance with relevant EN standards. Visual and NDT testing of radiography was performed to 100% extent on each proximity distance sample. Due to

Table 3 Physical and material properties of tubular pipe grade S355 G14 + N

Yield point (min 355) Mpa			Tensile point (460–620) Mpa			Elongation min 22%			Impact test (5–25 J) @-40 °C		Hardness HRB max 99		
444			553			28			102		84		
C	Mn	Si	P	S	Cu	Ni	Cr	N	Mo	V	Ti	Nb	B
0.14	1.19	0.337	0.016	0.003	0.07	0.02	0.06	0.0091	0.005	0.059	0.001	0.003	0.0005

Table 4 Physical and material properties of **a)** Filler wire ESAB Tigrod 13.26 used in 141 welding process **b)** Filler wire SF-3AM used in 138 welding process **c)** Filler wire SF-47A used in 136 welding process

	Yield point (460 min) Mpa			Tensile point (530–680) Mpa			Elongation (20 min) %		Impact test (J) (47 J min) @ − 40 °C		
a)	480			580			30		60		
	C	Mn	Si	P	S	Cu	Ni	Cr	MO		
	0.11	1.41	0.89	0.018	0.015	0.52	0.85	0.04	0.001		
b)	518			585			27		163		
	C	Mn	Si	P	S	Cu	Ni	Cr	MO	V	Nb
	0.05	1.13	0.27	0.01	0.004	0.28	1.03	0.02	0.01	0.01	0.01
c)	509			597			28		118		
	C	Mn	Si	P	S	Cu	Ni	Cr	MO	V	Nb
	0.06	1.24	0.59	0.008	0.008	0.26	0.93	0.02	0.01	0.01	0.01

spray mode in MAG + FCAW welding process Weld B, a wider and irregular cap weld bead was observed in contrast to a smooth weld cap bead of weld A [22], which was welded with TIG process as shown in Fig. 4. As per the acceptance criteria of ISO 10675–2016, both joints were accepted after performing radiography testing on proximity.

3.2 Hardness testing

Vickers hardness testing on each case of weld-proximity distances of 5, 10, and 15 mm was performed according to NS-EN ISO 9015–1:2011. As per indentation marks shown in Fig. 5, there was a recommended distance of 1 mm between indentations and, in HAZ ≤ 0.5 mm, between the center point of the indentation and the fusion line. The indentation marks shown in Fig. 5 can be seen clearly in macro graphs of each weld proximity case in Fig. 9a–c. As the proximity distance was the area of concern, hardness measurement points between adjacent weld toes at 'weld cap and root level' for 5, 10, and 15 mm proximity distances are shown in Fig. 6a, b, respectively. High hardness values were observed at the proximity distance (PD-A&B) between two weld metals (WM-A&B) and their respective adjacent HAZ-A&B, in constrast to the parent metal (PM). This proximity distance, or area known as 'alien metal', has experienced microstructural changes due to high restraint and successive thermal cycles of multipass welds, as noticed in [23] for proximity-welded joints K-brace joints of offshore jacket structures.

A maximum value of 210 HV was observed close to a HAZ value of 225 HV on either side for 5 mm proximity distance welds at cap level, as shown in Fig. 6a. Cold cracking chances increase if hardness values are between 350 and 400 HV. This region may be prone to cracking, as it has accumulated high stresses and chances of martensitic formation have been sustained due to successive thermal cycles of heating and cooling [23]. Similar hardness points' profiles for weld proximity distances of 10 and 15 mm are shown in Fig. 6a, b for fair comparison. As the proximity distance is increasing, a drop in hardness values can be seen and is comparable to PM in the 10 and 15-mm cases. In case of 10-mm proximity distance, the highest value of 186 HV was observed at the proximity region and of 167 HV in the case of 15-mm distance, which is almost equivalent to parent metal value at weld cap level. It is also worth mentioning that hardness values at weld cap level in the 5-mm case are maximum in the HAZ area, in comparison to 10 and 15-mm cases.

3.3 Charpy testing

Charpy testing was performed in accordance with KV8, NS-EN ISO 148–1:2016 and ISO 9016:2012 at −20 °C. As discussed previously and shown in Fig. 3, due to the limited space for FL + 5 mm samples, only six specimens were available for 5-mm proximity distance whereas FL + 5 mm was possible for 10- and 15-mm proximity distances. Sample size was kept at 5 × 10 × 55 mm size, as the pipe thickness was 8.2 mm; hence, a conversion factor of 2/3 was

Table 5 Examination of the test weld for WPQR as per NORSOK M-101

Joint configuration	Joint thickness (mm)	Mechanical testing			
		Tensile test	Bend test	Charpy V notch	Hardness and macro
Butt welds (Tubular)	t ≤ 50 mm	2	4	4 sets	1

Table 6 Examination and testing of the test pieces

Activity description	Specification/procedure	Acceptance criteria
Visual testing	ISO 17637:2016	EN ISO 5817:2014 B/C
Radiographic testing	ISO 17636–2:2013	ISO 10675–1:2016
Macro examination	NS-EN 17,639:2013	EN ISO 5817:2014 B/C
Transverse tensile test	ISO 4136:2012, ISO 6892–1:2016 Method A1	NS-EN 15,614–1: 2017, NS-EN 10,225:2009
Charpy V Impact test	NS-EN ISO 148–1:2016, ISO 9016:2012	NS-EN 15,614–1: 2017, NS-EN 10,225:2009
Vickers Hardness test	NS-EN ISO 9015:2011	NS-EN 15,614–1: 2017

applied, when calculating energy values as per code EN 15,614–2017.

Figures 7 and 8, respectively, illustrate scanning electron microscope (SEM) micrographs of fracture surface at FL + 2 mm and the Charpy energy values chart. A region compromised of a mainly dimple-like ductile fracture zone is observed, as shown in SEM micrographs in Fig. 7a, for 5-mm WP distances. However, some cleavage river-like patterns, along with dimples, are observed in Fig. 7a, indicating some regions of brittle fracture, in contrast to Fig. 7b, where dominant dimples like a ductile fracture surface are observed for the 15-mm weld proximity case. Features like the area of the ductile fracture zone of HAZ and the shear lip of HAZ can also help in determining the dominant fracture mode in HAZ [24].

As shown in Fig. 8, low energy values are noted for 5 mm weld proximity (WP). It can be observed from Fig. 8 that the least energy values of 55 J at the proximity region, i.e., weld A-FL + 2 mm, were observed for the 5-mm proximity distance, in contrast to the 10 and 15-mm cases. To draw fair comparison, FL + 2 mm Charpy values are highlighted in Fig. 8, with values of 62 J and 66 J being observed, i.e., between welds A–B for the 10 and 15-mm cases. Due to high hardness and high restraint in the 5-mm proximity case, a drop in energy values can be observed. This drop can be attributed to the high hardness values observed, as explained in Sect. 3.2, and the mixed pattern of cleavage river and dimples, leading to brittle and ductile fracture surfaces, respectively. However, microstructure graphs shown later in Sect. 3.4 also substantiates the high hardness values at proximity regions for changed morphology of grain size in the proximity region.

3.4 Macro testing

Macro examination was performed in accordance with NS-EN 17,639–2013 and was accepted as per the criteria of NS-EN ISO 5817:2014, with imperfection inside quality level B, as shown in Fig. 9a–c. In the proximity case of 5-mm between its weld toes, overlapping of the heat-affected zone cannot be observed, as shown in Fig. 9a; however, no visual changes in the proximity region (metal subjected to successive cycles of heating and cooling) were observed between proximity welds.

3.4.1 Microstructure characterization

Due to the high values in hardness and the drop in Charpy values for the 5-mm weld proximity case, there was a need to further perform microstructure characterization. Optical microstructures across the weld interface, starting from the parent metal to HAZ of weld A, then to proximity region to HAZ of weld B, were analyzed on macro specimen samples of 5-mm weld proximity, as shown in Fig. 10a–d. The

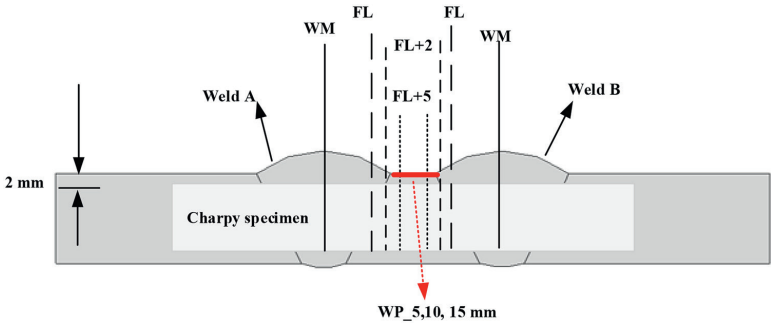

Fig. 3 Schematic of location for Charpy test locations

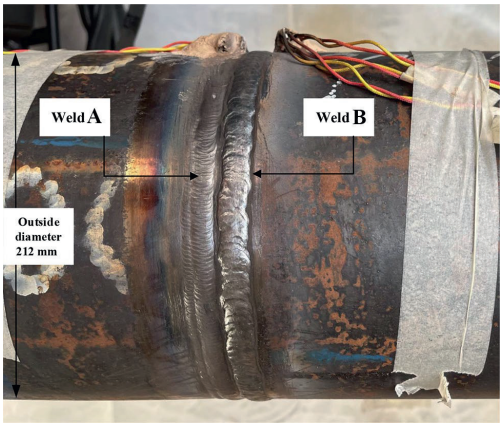

Fig. 4 Visual image of welds A and B

microstructures at HAZ showed acceptable weld interface without any defects; however, different orientation of grains was observed in the region identified as the proximity region/alien metal i.e., between two welds, as shown in Fig. 10d.

Microhardness results at the designated location of HAZ and the proximity area between welds (PA) correspond to values of 225 HV and 210 HV, respectively, as shown in Fig. 6a, for the 5-mm proximity case. Based on this information, the microstructure in HAZ regions can be mainly composed of ferrite (50 to 80%), bainite (0 to 30%), pearlite (0 to 20%), and martensite (0 to 20%) corresponding to Vickers hardness values for steel S355 [23]; refer to Table 7 [25].

The optical images seem to confirm regions of perlite (P) and ferrite (F) in the parent metal, as shown in Fig. 10 a. Acicular ferrite (AF-large light areas) with grain boundary ferrites (GBF) can be observed in weld metal A and B. Depending on the final temperature range attained, HAZ is divided into coarse-grained HAZ (CGHAZ), fine-grained HAZ (FGHAZ), and the inter-critical HAZ (ICHAZ) [12]. In HAZ, the structure is formed upon temperature attained between Ac1 and Ac3, i.e., upper, and lower critical temperatures as shown in Fig. 10 b and d. As the proximity area/alien metal corresponds to a fine-grained structure in contrast to CGHAZ and FGHAZ, it can be identified as a region close to ICHAZ that is subjected to successive cycles of heating and cooling between Ac1 and Ac3 temperatures, i.e., 725–915 °C, with finer grain, as confirmed from thermocouple data.

It is difficult to identify the presence and quantify the fraction of martensite; however, sufficient evidence of martensite-austenite (M-A) islands has been identified in the inter-critically reheated coarse-grained heat affected zone (ICCGHAZ) undergoing partial austenization and forming austenitic-martensitic (M-A) phases, which are brittle and known as local brittle zones (LBZ) [26]. However, their presence needs further investigation by performing scanning electron microscopy (SEM) analysis which will be presented in future research.

3.5 Tensile and bend tests

Tensile tests were performed for all three weld proximity cases (5-, 10-, and 15-mm), in accordance with ISO 6892–1:2016. Table 8 summarizes the values of all tensile test data along with its fracture location. It was interesting to note that values of tensile strength for the 5-mm weld proximity case were found to be somewhat lower than in the 10- and 15-mm cases. Fracture location could not provide any conclusion, as it changed from outside of weld A or B, i.e., sufficiently far from HAZ and the proximity region. It would have been interesting if failure had occurred between welds for the 5-mm case. However, in the case of 15-mm proximity, fracture occurred between welds in one case. It can be inferred that the 15-mm distance is sufficiently far, and the fracture location can be considered close to the parent metal.

Fig. 5 Hardness measurement point locations at cap and root level

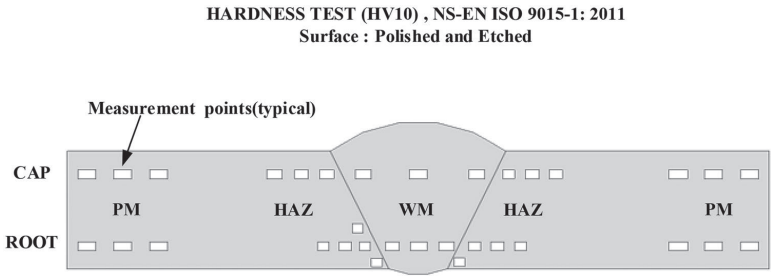

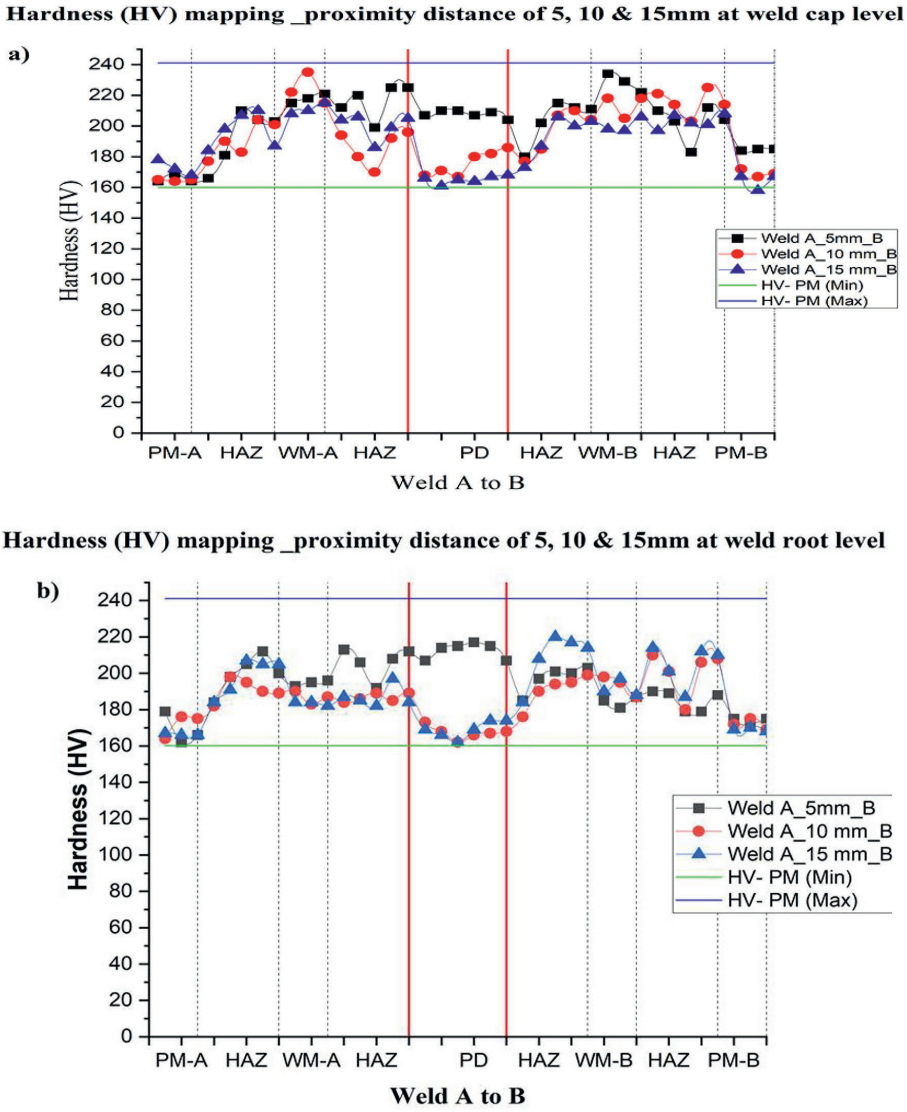

Fig. 6 Vickers hardness profile from left side PM of weld A to right side PM of weld B at **a**) cap **b**) root level for proximity distance of 5, 10, and 15 mm, respectively

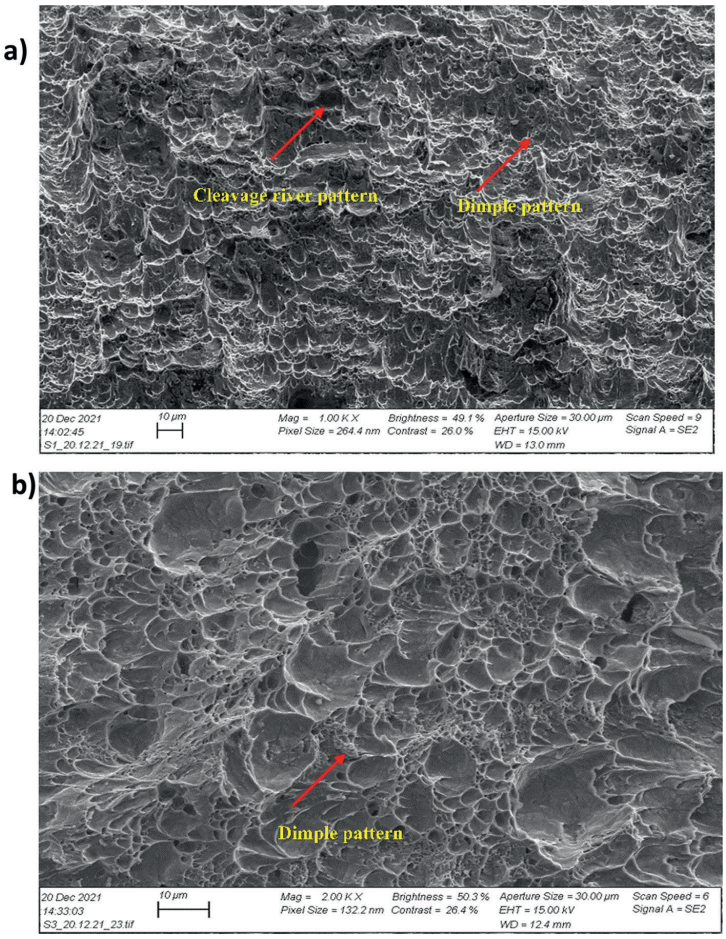

Fig. 7 SEM micrographs of FL + 2 mm fracture surface for proximity distances of **a**) 5, and **b**) 15 mm

Tensile results sufficiently meet the required strength of 460–620 MPa; however, all values were found to be less than the pipe measured value of 553 MPa, as referred to in the material test certificate mentioned in Table 3. Elongation values in all cases were found to be less than 22%, indicating the high restraint and residual stresses caused by welds placed at proximity.

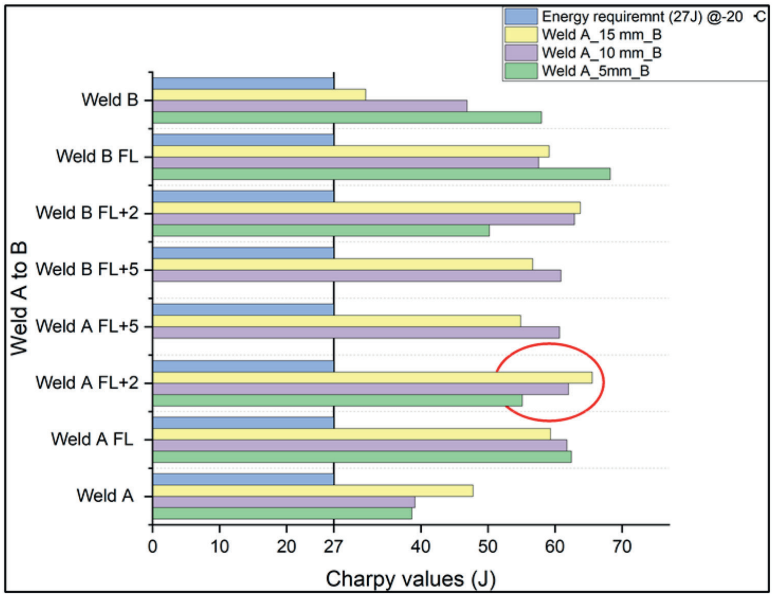

Fig. 8 Charpy testing values for all proximity distances of 5, 10, and 15 mm

Bend tests were also performed as per EN ISO-5173:2010 at the designated location of root and face, as mentioned in NORSOK M-101 and EN 15,614–2017. For thickness of less than 12-mm, two samples each for face and root bend were tested. For all weld proximity samples of 5, 10, and 15-mm, testing did not reveal any one single flaw greater than 3-mm in any direction. Flaws appearing at corners of test specimen were ignored, as mentioned in EN 15,614–2017.

a)

b)

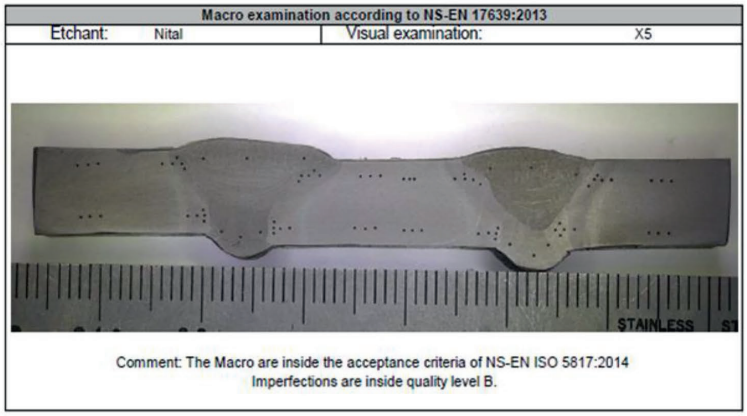

c)

Fig. 9 **a–c** Macro examination and hardness points location for **a** 5-mm, **b** 10-mm, and **c** 15-mm weld proximity joints

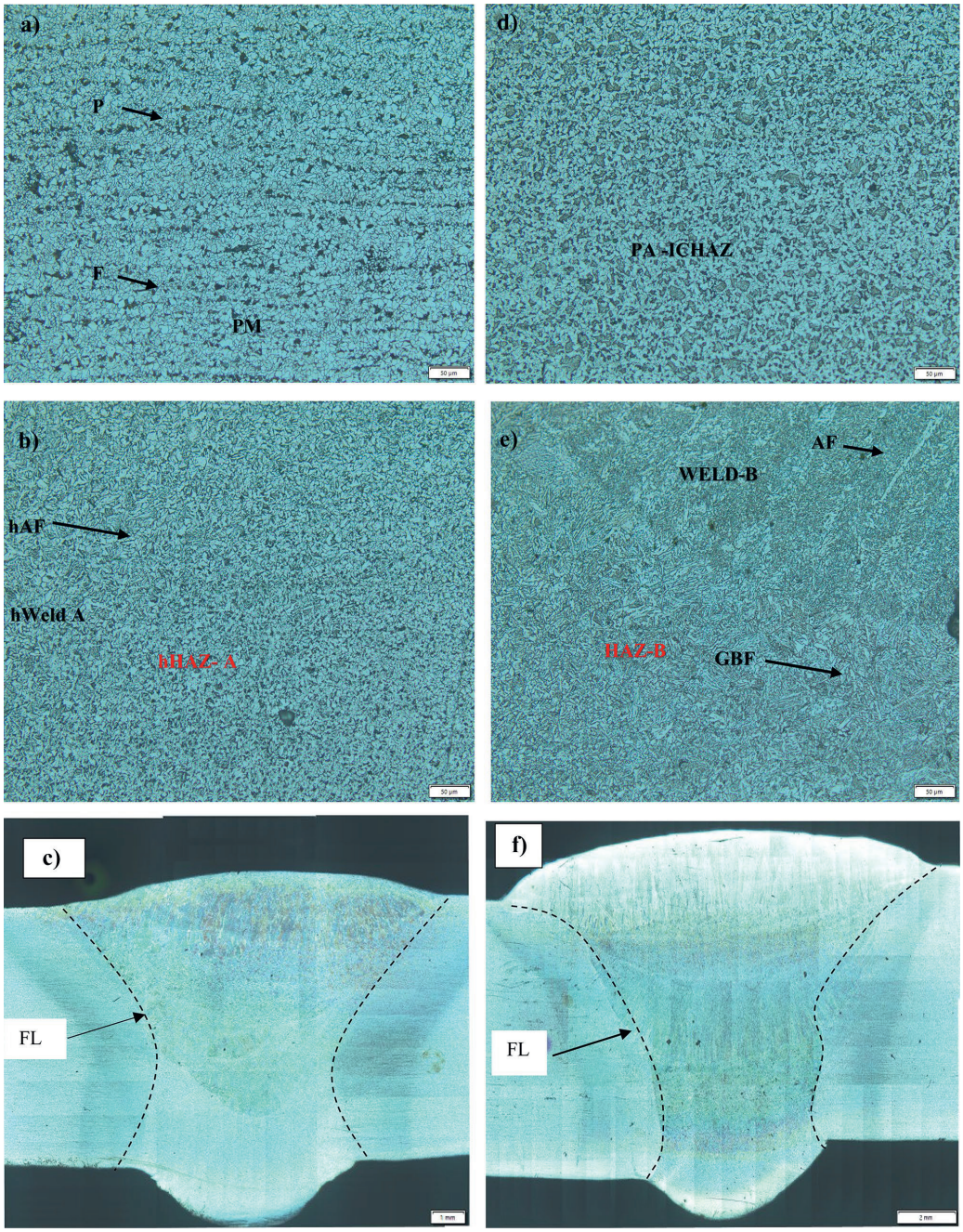

Fig. 10 Optical microstructures for 5-mm weld proximity case **a)** Parent metal (PM), **b)** HAZ of weld A, **c)** Weld A with fusion line (FL), **d)** Proximity area /alien metal between welds (PA), **e)** HAZ of weld B, **f)** Weld B with fusion line (FL)

Table 7 Microstructures and the corresponding Vickers hardness ranges of a low-alloyed steel [25]

Microstructures	Average Vickers hardness (approximately)
Ferrite	84
Austenite	263
Perlite (granular)	211
Perlite (lamellar)	316
Cementite	632–684
Martensite	421–948

Table 8 Examination and tensile testing data for all weld proximity cases

Weld proximity (mm)	No of samples	Test indent	Thickness (mm)	Width (mm)	Area (mm^2)	Tensile (Mpa)	Elongation %	Fracture location
5	2	Cross weld 1	8.61	24.93	214.6473	480	14.71	Basemetal B side
		Cross weld 2	8.16	24.91	203.2656	489	12.93	Basemetal A side
10	2	Cross weld 1	8.41	24.91	209.4931	493	16.31	Basemetal A side
		Cross weld 2	8.12	25.04	203.3248	516	17.36	Basemetal A side
15	2	Cross weld 1	8.2	25.09	205.738	487	12.10	Basemetal between welds
		Cross weld 2	8.58	24.92	213.8136	498	15.59	Basemetal A side

4 Conclusion

Welding procedure qualification record (WPQR) was performed on grade S355 tubular pipes' girth welds with a proximity distance between their weld toes of 5, 10, and 15 mm. Welds were fabricated with two different welding processes, in accordance with the pre-qualified welding procedure specification (WPS). WPQR was performed in accordance with NORSOK M-101, which follows EN 15,614–2017 standard, and all relevant mechanical tests were performed. Based on detailed mechanical evaluation, an increase in Vickers hardness values and a drop in Charpy values for the 5-mm weld proximity case were observed. It is also pertinent to mention here that the drop in elongation values observed in tensile test data in all cases can be attributed to the high restraint and residual stresses caused by welds placed at proximity. It was also inferred from the microstructure characterization that there was the formation of an inter-critically reheated coarse-grained heat affected zone (ICCGHAZ), as verified from thermocouple data, which is prone to cracking due to the presence of austenitic-martensitic (M-A) phases which are brittle and known as local brittle zones (LBZ).

After performing welding qualification on proximity welds, mechanical results justify the need to avoid such situations, especially when the proximity distance is less than half the thickness of the joining member between adjacent weld toes i.e., 5 mm in this current study. One times the thickness and two times the thickness of the joining member, i.e., 10 mm and 15 mm also used in this current study, did not show any harmful effect, as verified by mechanical test results. The codes and standards also do not provide any recommendation for maintaining minimum proximity distances for repair and replacement welds [12]. The region identified as 'proximity region or alien metal' between adjacent welds requires careful defect assessment and inspection procedures in relation to the compact welded joints found in offshore jacket structures and high restraint situations developed during pipe replacement procedures in compact layouts. Detailed assessment and record keeping of previous welding process parameters and mechanical tests can help in the future qualification of new welding procedures for repair welds placed at proximity. In the future, the authors plan to measure residual stress profiles and fatigue life between proximity welds, for their detailed assessment and to provide practical recommendations to industrial partners for maintaining the minimum distance between proximity welds.

Acknowledgements We would like to acknowledge the support of M/s Rosenberg Worley, Stavanger, Q-lab Forsand, and Jan-Tore Jakobsen, Wakshum Mekonnen, lab engineer at University of Stavanger, Norway for their support in the fabrication and testing of samples. We would also like to thank all reviewers involved in the publication process, for providing their valuable suggestions.

Author contribution **Sachin Bhardwaj**: Conceptualization, Experimentation, Investigation, Methodology, Visualization, Writing—original draft, Writing—review and editing. **R.M.Chandima Ratnayake**: Conceptualization, Formal analysis, Funding acquisition, Project administration, Supervision.

Funding Open access funding provided by University Of Stavanger. The research is fully funded by the Norwegian Ministry of Education (Internal PhD project No. IN-12168). This work has been carried out as part of a PhD research project, performed at the University of Stavanger, Norway.

Availability of data and material All data generated and analyzed during this research are included in this published article.

Declarations

Ethics approval and consent to participate Not applicable.

Consent for publication Not applicable.

Conflict of interest The authors declare no competing interests.

References

1. Norrish J (2006) 1 - An introduction to welding processes, in Advanced Welding Processes, J. Norrish, Editor, Woodhead Publishing. p 1–15
2. Ratnayake RMC, Brevik VA (2014) Experimental investigation of underwater stud friction stir welding parameters. Mater Manuf Processes 29(10):1219–1225. https://doi.org/10.1080/10426914.2014.930891
3. Oliveira JP et al (2019) Microstructure and mechanical properties of gas tungsten arc welded Cu-Al-Mn shape memory alloy rods. J Mater Process Technol 271:93–100. https://doi.org/10.1016/j.jmatprotec.2019.03.020
4. Oliveira JP et al (2021) Laser welding of H-phase strengthened Ni-rich NiTi-20Zr high temperature shape memory alloy. Mater Des 202:109533. https://doi.org/10.1016/j.matdes.2021.109533
5. Oliveira JP et al (2022) Dissimilar laser welding of a CoCrFeMnNi high entropy alloy to 316 stainless steel. Scripta Mater 206:114219. https://doi.org/10.1016/j.scriptamat.2021.114219
6. Shamsolhodaei A et al (2020) Controlling intermetallic compounds formation during laser welding of NiTi to 316L stainless steel. Intermetallics 116:106656. https://doi.org/10.1016/j.intermet.2019.106656
7. Ratnayake RM (2013) An algorithm to prioritize welding quality deterioration factors: a case study from a piping component fabrication process. Int J Qual Reliab Manag. https://doi.org/10.1108/02656711311325584
8. Lotsberg I (2016) Fatigue design of marine structures. Cambridge University Press, Cambridge
9. Link M (2021) Equinor: Several Factors Behind Faulty Welds on Johan Castberg FPSO Hull. Available from: https://www.marinelink.com/news/equinor-several-factors-behind-faulty-486965#.YH4FKi90m_8.linkedin. [Cited 2021 29/09/2021]
10. Talkshop TS (2014) 100m Turbine collapse: not bolts this time – weld failure in the main tower. Available from: https://tallbloke.wordpress.com/2014/12/17/100m-turbine-collapse-not-bolts-this-time-weld-failure-in-the-main-tower/. [Cited 2021 29/10/2021]
11. Larsson M, Larsson M, Ratnayake RM (2021) Investigation of Fatigue Strength Behaviour in Dual Weld S420 Steel Joints Fabricated at a Close Proximity. https://doi.org/10.1007/978-981-15-9121-1_27
12. Bhardwaj S, Ratnayake RMC (2020) Challenges due to welds fabricated at a close proximity on offshore structures, pipelines, and piping: State of the Art. In ASME 2020 39th International Conference on Ocean, Offshore and Arctic Engineering. https://doi.org/10.1115/omae2020-18586
13. NORSOK N-004 Standard (2021), Design of steel structures, Norway
14. DNVGL-ST-0126 Standard (2018), Support structures for wind turbine, DNVGL
15. Larsson M, Larsson M Ratnayake RM (2021) Experimental Investigation of Weld Joints Manufactured at Close Proximity in S420 Structural Steel. https://doi.org/10.1007/978-981-15-9121-1_25
16. Larsson M et al (2021) Experimental Residual Stress Investigation of Weld Joints Fabricated at a Close Proximity in S420 Structural Steel. https://doi.org/10.1007/978-981-15-9121-1_26
17. Ratnayake RM (2014) A methodology for assessing most vulnerable welding procedure specifications and imperfection factors. Int J Data Anal Tech Strateg 6:362–383. https://doi.org/10.1504/IJDATS.2014.066606
18. Bhardwaj S, Chandima Ratnayake RM (2020) Residual stress estimation in defect assessment procedures at weld toe and away locations on girth welds: Review of key parameters. Theor Appl Fract Mech. https://doi.org/10.1016/j.tafmec.2020.102848
19. Dong P et al (2014) On residual stress prescriptions for fitness for service assessment of pipe girth welds. Int J Press Vessels Pip 123–124:19–29. https://doi.org/10.1016/j.ijpvp.2014.07.006
20. NORSOK M-101 Standard (2011) Structural steel fabrication: Norway
21. BS EN 15614–1 Standard (2017) Specification and qualification of welding procedures for metallic materials — welding procedure test
22. Oliveira JP et al (2020) Gas tungsten arc welding of as-rolled CrMnFeCoNi high entropy alloy. Mater Des 189:108505. https://doi.org/10.1016/j.matdes.2020.108505
23. Acevedo C (2011) Influence of residual stresses on fatigue response of welded tubular K-joints. EPFL
24. Xiong Z et al (2015) The contribution of intragranular acicular ferrite microstructural constituent on impact toughness and impeding

crack initiation and propagation in the heat-affected zone (HAZ) of low-carbon steels. Mater Sci Eng A. https://doi.org/10.1016/j.msea.2015.03.090
25. ISF Welding and Joining Institute (2004) Chapter 4-Classification of Steels, Welding of Mild Steels
26. Lomozik M (2000) Effect of the welding thermal cycles on the structural changes in the heat affected zone and on its properties in joints welded in low-alloy steels. Weld Int 14(11):845–850. https://doi.org/10.1080/09507110009549281

The International Journal of Advanced Manufacturing Technology
https://doi.org/10.1007/s00170-022-09574-6

ORIGINAL ARTICLE

Experimental investigation of residual stress distribution on girth welds fabricated at proximity using neutron diffraction technique

Sachin Bhardwaj[1] · R. M. Chandima Ratnayake[1] · Efthymios Polatidis[2] · Jan Capek[2]

Received: 7 April 2022 / Accepted: 17 June 2022

Abstract
Maintaining minimum distance between repair and existing welds often becomes impractical due to the presence of compact layouts, original welds of branches, nozzles, etc. on offshore structural elements, pipelines, and piping. Although some international codes and standards provide criteria for maintaining a minimum distance between proximity welds, most of them lack technical justification in relation to their effect on the structural integrity of welded components. The development of residual stresses has a significant effect (i.e., a negative effect on tensile stresses and a positive effect on compressive stresses) on the integrity of the welds fabricated at proximity. Hence, it is important to investigate the residual stress distribution on welds fabricated at proximity, especially at a distance away from the weld toe. This study presents findings on the characterization of residual stresses by neutron diffraction at the proximity region between two girth welds. The two welds were fabricated at proximity, using two different welding procedure specifications and at three different distances, on a structural steel pipe, grade S355. The three different welding distances between weld toes were maintained at 5, 10, and 15 mm respectively. The neutron diffraction-based residual stress distributions were investigated at the POLDI neutron instrument at the Swiss spallation source SINQ in Switzerland. The axial, hoop, and radial components of the residual stresses were experimentally investigated between proximity welds. The findings revealed that residual axial stresses at a 5-mm proximity distance were increased beyond the yield strength of the structural steel, grade S355. The findings of this study enable practitioners to take remedial actions to minimize the residual stresses developed in girth welds fabricated at proximity. Also, the findings enable us to derive technical justification for maintaining a minimum distance and developing welding procedure for welds fabricated at proximity.

Keywords Residual stress · Neutron diffraction · Proximity welds · Repair welds

1 Introduction

Welds placed at proximity have always been found to be a subject of debate among fabricators, inspectors, and contractors. International fabrication codes and standards often fail to provide technical justification for maintaining a minimum distance between proximity welds [1, 2]. During the replacement/repair fabrication procedures of tubular structures, the standards provide no guidelines regarding maintaining minimum distances between original and repair welds [3]. Proximity welds' placement should be based on practical experience, and shorter distances may need to be proven with respect to both impact on stress concentration factors (SCFs) and welding residual stresses' (WRS) estimation, as mentioned in code [4], which is used for offshore wind turbines' assessment. Detailed evaluation of this criteria has been performed in the past by the authors [3] for proximity weld configurations found in various structural fabrication and repair codes [3]. The challenges of welding repair joints on or at proximity to existing welds, leading to the development of harmful tensile WRS development, have been well documented by [5–7]. These can cause failures due to stress corrosion cracking at a distance away from weld in welded austenitic steel piping. Imperfections in welds, coupled with high tensile WRS under high cyclic loading conditions, are well known for causing major weld failures in high restraint

✉ R. M. Chandima Ratnayake
chandima.ratnayake@uis.no

[1] Department of Mechanical and Structural Engineering and Materials Science, University of Stavanger, N-4036 Stavanger, Norway

[2] Laboratory for Neutron Scattering and Imaging, Paul Scherrer Institute, CH-5232 Villigen PSI, Switzerland

Published online: 24 June 2022

proximity welds of tubular braces and offshore jackets [8], floating production storage and offloading (FPSOs) [9], and tubular bridge structures' truss welds [10]. Hence, it is important to estimate the WRS distribution around the weld toe and proximity regions.

WRS characterization around the weld toe region has always been considered a subject of interest for designers, manufacturers, and integrity engineers, as harmful tensile residual stresses have been found to accelerate crack propagation, in contrast to beneficial compressive stresses in welded joints [11]. Accurate estimation of stress intensity factors due to residual stresses can further help in better predicting the remaining fatigue life of welded joints, while using fracture mechanics procedures for welded joints [12]. In the various defect assessment procedures of fitness for service codes (FFS) like BS 7910 [13], API-579 [14], and R6 [15], WRS profiles for distances away from the weld toe (WT) [16], and welds placed at close proximity, like critical offshore brace joints, piping welds etc., are not available [1], often leading to conservative assessments in FFS procedures. In addition to the formation of deleterious tensile residual stresses between proximity welds, heat input, weld sequence, and restraint conditions in the employed welding process play a vital role in developing yield level residual stress at the weld center and proximity regions.

The estimation of tensile residual stresses between proximity welds, fabricated with similar welding processes on a butt-welded plate, have previously been reported by [17], by the use of techniques like X-ray diffraction and incremental center-hole drilling. Similar findings, developed at proximity regions between proximity K-welded tubular joints, by the use of neutron diffraction and X-ray diffraction (XRD) techniques, have been reported by [18]. However, in both the cases, through thickness level, residual stresses were not measured at proximity region developed between adjacent weld toes, due to depth measurement limitation of XRD technique and use of neutron diffraction technique at weld toe location only. Changes in mechanical properties of proximity welds like fatigue life, hardness, tensile, and impact tests on butt-welded plate and partial penetration K-welded joints of tubular offshore joints, respectively, have been reported by authors [2, 19] and [20] in the past. Mechanical test results and welding qualification for repair proximity welds, fabricated on a pipe, have previously been presented by authors [21], indicating the development of high hardness and low energy values at proximity regions. However, in repair/replacement welds, fabrication with two different welding processes at different proximity distances, leading to the development of harmful or beneficial WRS profiles, needs to be investigated, for which no reported experimental study was found in open literature.

Therefore, the aim of the current study is to investigate the effect of proximity welds on WRS profiles developed between adjacent weld toes, fabricated with two different welding processes on a structural steel pipe of grade S355. The neutron diffraction (ND) technique was employed for characterizing the residual stresses between proximity welds on a large tubular welded mockup, with the use of the time of flight neutron diffractometer (POLDI, SINQ) at the Paul Scherrer Institute (PSI), in Switzerland. The remainder of the paper is structured as follows: Sect. 2 describes the experimental methodology, followed by the results and discussion. Subsequently, in Sect. 4, a conclusion is drawn.

2 Experimental procedure

2.1 Large, welded mockup samples

Proximity multi-pass girth welds were fabricated on structural steel-grade EN 10,225–09 S355G14 + N seamless pipe, generally used in the fabrication of offshore structural members [8], with dimensions of 219.1 mm outside diameter and 8.18 mm thickness. Initially, weld A was fabricated as a single weld on a pipe Sect. 700 mm long, welded with tungsten inert gas (TIG), a semi-automatic welding process, and, subsequently, a vee groove for weld B was machine cut. Lastly, weld B was welded with metal active gas (MAG), a semi-automatic method for root pass, and Flux cored arc welding (FCAW), a semi-automatic method for the remaining passes after the completion of weld A. Weld proximity (WP) distances of 5 mm, 10 mm, and 15 mm were maintained between adjacent weld toes, as shown in Fig. 1 schematic.

As discussed previously, to simulate the practical situation of repair or replacement procedures, weld B was welded with different and faster welding processes like MAG and FCAW, in contrast to weld A, which was welded with TIG, which is a more factory-controlled welding process. Complete details about the material properties, fabrication process, welding procedure qualification record (WPQR), filler wire, digital weld log data, and mechanical testing results can be found in the authors' previous work [21]. All necessary NDTs, e.g., radiography & destructive testing (DT), e.g., tensile, Charpy, hardness, and bend tests to qualify WPQR for proximity welds were performed on all samples, as per the criteria mentioned in ISO EN15614-1 [22].

ISO EN15614-1 [22] code was used for the qualification of WPQR and adopted in this project catering for the Norwegian continental shelf (NCS) and offshore welded tubular structures used in oil exploration and the processing industry. ISO EN15614-1 is a widely accepted code for welding qualification around the world. Welding was performed under controlled conditions after optimizing the welding parameters found in [21] as per pre-qualified welding procedure specification (WPS) adopted from reputable industrial partners. Three samples from each proximity distance of 5,

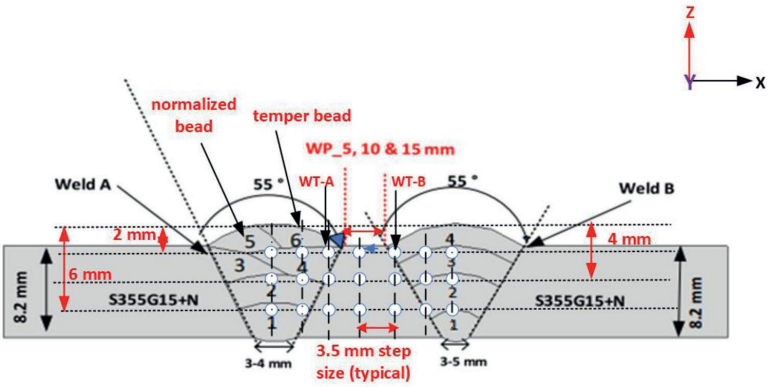

Fig. 1 Schematic of proximity welds at 5, 10, and 15 mm distances and neutron diffraction measurement points

10, and 15 mm were finally fabricated and characterized by neutron diffraction, as explained in following section.

2.2 Neutron diffraction measurements

Neutron diffraction is a nondestructive technique (NDT) that is capable of measuring residual strains in the bulk of multi-pass welds and most polycrystalline metal and alloys [23]. Neutron diffraction measurements were performed at the pulse overlap diffractometer (POLDI), located at the Swiss Spallation Source, SINQ, at the Paul Scherrer Institute in Switzerland [24] as shown in Fig. 2 schematic. POLDI is a time-of-flight (ToF) thermal neutron diffractometer, well suited to measuring spatially resolved residual stresses in engineering components. A ToF instrument like POLDI has the advantage of capturing several diffraction peaks, which is essential for the analysis of stress in strongly textured materials. The obtained data were fitted using open source software Mantid [25]

Strain can be calculated by measuring a change in the atomic lattice spacing $d_{hkl} \sim d$, acting under stress when compared with stress-free spacing d_o, as per Eq. (1). Miller indices (hkl) are parallel to the crystallographic planes of the material, and its lattice spacing d can be found by Bragg's law, as mentioned in Eq. (2).

$$\varepsilon = \frac{d - d_o}{d_o} \tag{1}$$

$$n\lambda = 2d\sin\theta \tag{2}$$

The axial (perpendicular to weld), hoop (parallel to weld), and radial (through thickness) strain components were measured using the 211 diffraction peak for the body-centered

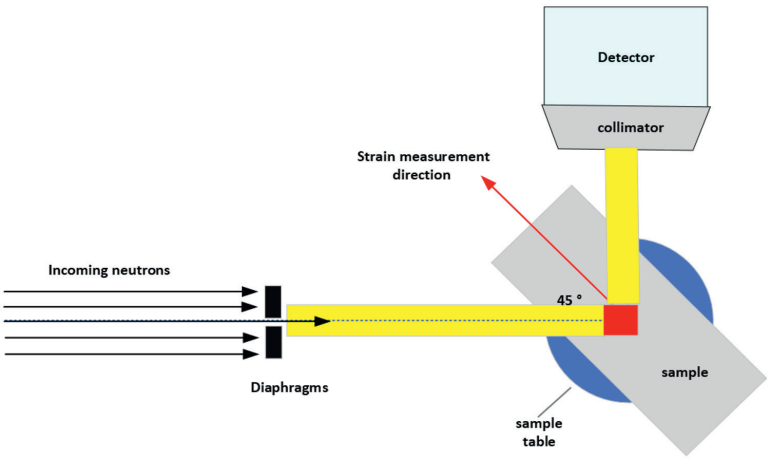

Fig. 2 Schematic of POLDI at PSI, Switzerland, adapted from [24]

cubic (BCC) crystal structure of the S355 alloy, as recommended in ISO21432:2019 standard [26]. Residual stresses can be calculated using generalized Hooke's law [26], as per Eqs. (3), (4), and (5) using the plane-specific elastic constants $E_{211} = 220000MPa$ and Poisson's ratio $v_{211} = 0.28$ [10]

$$\sigma_x = \frac{E}{(1+\mu))(1-2\mu)}\left[(1-\mu)\varepsilon_x + \mu(\varepsilon_y + \varepsilon_z)\right] \tag{3}$$

$$\sigma_y = \frac{E}{(1+\mu))(1-2\mu)}\left[(1-\mu)\varepsilon_y + \mu(\varepsilon_x + \varepsilon_z)\right] \tag{4}$$

$$\sigma_z = \frac{E}{(1+\mu))(1-2\mu)}\left[(1-\mu)\varepsilon_z + \mu(\varepsilon_y + \varepsilon_x)\right] \tag{5}$$

where x, y, z are 3 principal orthogonal directions corresponding to either axial, or hoop or radial directions in the sample coordinate system.

Measurement points started as a line scan from the center of weld A, along the case-specific proximity distance, moving towards the center of weld B, with a step size of 3.5 mm and a gauge volume of $3.8 \times 3.8 \times 3.8$ mm^3, as illustrated in Fig. 1. The line scan area was selected away from the weld start and stop positions and was performed in three different depths, i.e., 2, 4, and 6 mm from the top of the weld cap into the thickness, as shown in Fig. 1. As shown in Fig. 3, neutron beam exit paths through window cuts are illustrated for hoop and axial measurements. The beam is incident at 45° to the measurement location and exits at an angle of 90°. Appropriately sized window cuts were machined with a size of 200×50 mm at 90° to the line scan area, i.e., the proximity region from the center of weld A to B, during hoop stress measurements. A similar size window cut was also made at 180° to the line scan area, 150 mm away from the pipe center, for the beam exit during axial stress measurements. This was done to avoid the neutron attenuation by the beam

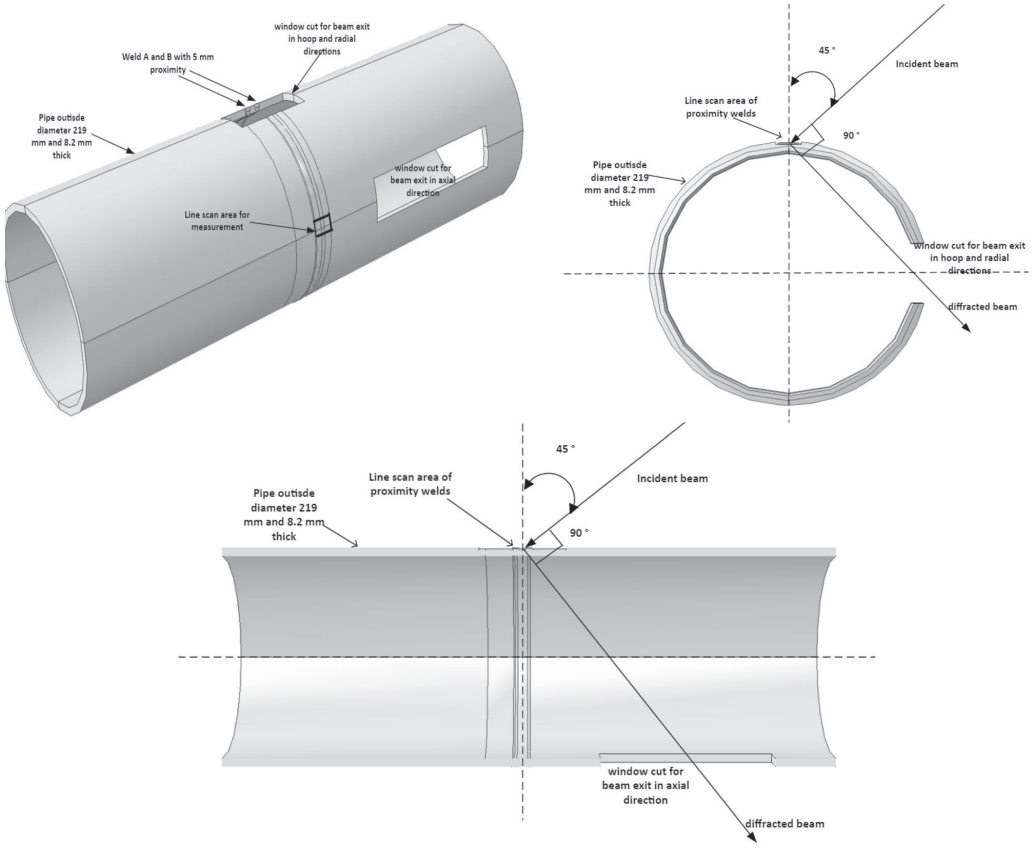

Fig. 3 Neutron beam exit path schematic in hoop and axial directions

passing through the tube wall for the second time in either the incident or diffracted direction.

2.3 Stress-free reference samples for "d0" measurements

A stress-free location for d_0 measurements was chosen, starting from center of weld A towards B, to take account of any chemical variation taking place due to the use of different welding processes, as shown in Fig. 4. The d_o samples were cut by electrical discharge machining (EDM), as thin slices of 1 mm thickness, to achieve a stress-free state, as previously reported by [18, 27] for tubular welded structures. The reference d_o measurement was undertaken at mid-thickness of d_o samples, i.e., at 4 mm depth from the top, starting from the center of weld A towards B, at five different locations, i.e., the center of weld A, weld toe A (WT-A), proximity area, weld toe B (WT-B), and center of weld B, as shown in Fig. 4. It was also decided to anneal d_o samples for 2 h at 1066 °C, a common stress-relieving procedure [28], and perform measurements at the same locations as the EDM cuts for various proximity distances. This was done to take account of any uncertainty observed when taking measurements with two different techniques. It was observed that there is very small variation (i.e., below variation resulting in 100 με uncertainty) within the line scan of the d_0 samples, and therefore a single d_0 value was used throughout the analysis, i.e., a value of 1.1738 Å.

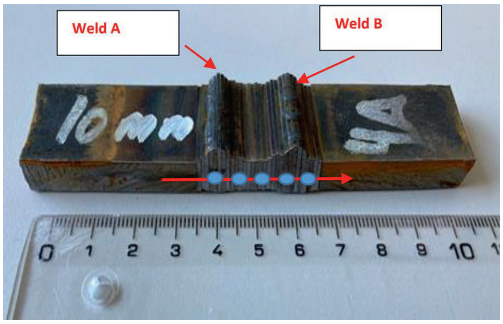

Fig. 4 Stress-free reference samples for d_o measurement at specified locations

3 Results and discussion

The diffraction spectrum, representing the intensity versus the scattering angle for all diffraction peaks are shown in Fig. 5. As explained in Sect. 2.2, the (211) peak intensity used for strain calculation is also highlighted for measured samples. The results of line scan are presented in Figs. 6, 7, and 8, in axial (perpendicular to the weld direction), hoop (parallel to the weld direction), and radial (into the thickness) principal directions, respectively, when measured at

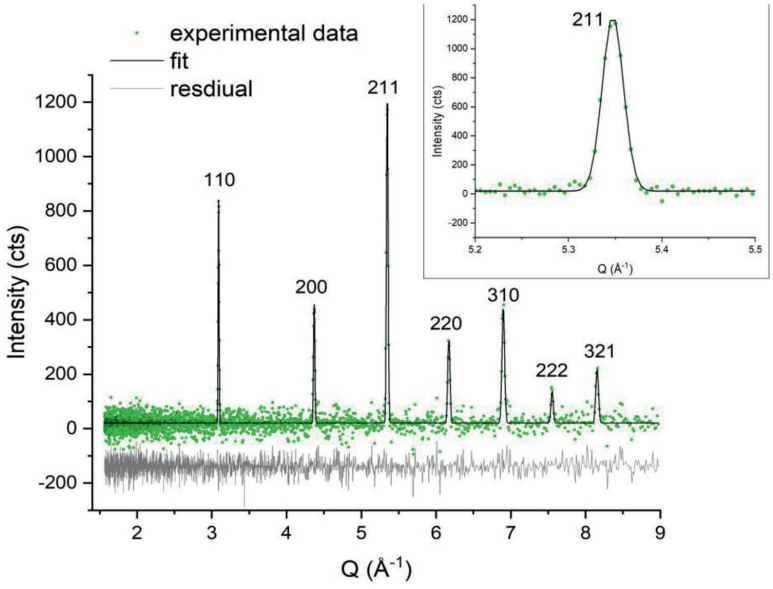

Fig. 5 Representative neutron diffraction pattern: experimental data (green circles), the fit profile (solid black line), and the residuals (solid grey line). The inset represents a zoom of the 211 diffraction peak

2, 4, and 6 mm depths from top of the weld cap into the thickness, by neutron diffraction technique.

3.1 Axial residual stress: transverse to weld direction

Axial residual stresses (perpendicular to weld direction–transverse) become more important in girth welds' assessment of piping, pipelines, and tubular structures, due to the dominant axial loading conditions [29]. As shown in Fig. 6, axial residual stress for WP 5, 10, and 15 mm distances are presented when measured at different depths (2, 4, and 6 mm) from the top of the weld cap to the bottom, starting from the center of weld A towards B.

3.1.1 Stress at proximity regions

At 2 mm depth from the top of the weld cap into the thickness, due to the closest interaction between the adjacent weld cap toes, i.e., 5 mm, and maximum tempering effect due to the adjacent placement of weld B, axial residual stresses observed at the proximity region are low in magnitude, with a value of compressive 86 ± 18 MPa, as shown in Fig. 6a. At 2 mm depths from the top of the weld cap into the thickness

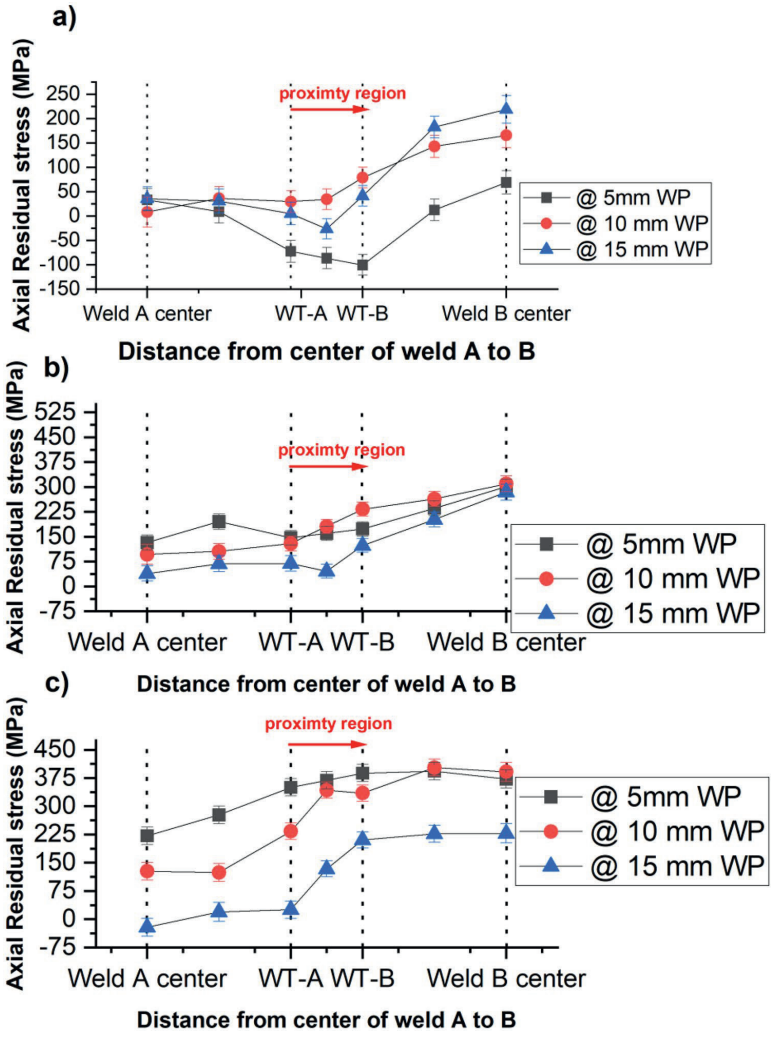

Fig. 6 Axial residual stress for WP_5mm, WP_10mm, WP_15mm proximity distances at **a**) 2 mm (cap) **b**) 4 mm (mid thickness) **c**) 6 mm depth (root), level respectively

for 10 and 15 mm weld proximity distances, the axial stress values are seen to become tensile, in contrast to the 5 mm proximity distance, due to the decreasing effect of tempering, present between adjacent weld caps.

At the closest WP distance, i.e., at 5 mm, the effect on axial residual stress can be seen to be most dominant at 4 and 6 mm depths, when compared with 10 and 15 mm proximity distances, as shown in Fig. 6b and c. This can be attributed to the following reasons: maximum restraint effect caused by adjacent weld B, higher rate of cooling of weld B (FCAW – low heat input process), and welding sequence, as weld B was fabricated after the completion of weld A. The closest proximity distance of 5 mm leads to an increase in the magnitude of axial tensile residual stresses from 160 ± 18 MPa to 368 ± 18 MPa, when compared at 4 and 6 mm depths, respectively. The highest value of tensile axial stress of 368 ± 18 MPa, measured for 5 mm proximity distance at 6 mm depth from the top, is found to be higher than the yield strength of the parent material S355 used in this study, i.e., 355 MPa, which can be detrimental for the weld integrity, when superimposed with axial cyclic loadings, as observed by [18] from the neutron diffraction results of K-tubular proximity welds. Stresses, measured at the proximity region of 10 mm distance, at 4 and 6 mm depths, show values increasing from 181 MPa to 342 ± 18 MPa, respectively, in contrast to the 15 mm proximity distance, where values increase from 46 ± 18 MPa to 133 ± 18 MPa, respectively. As 15 mm is the maximum proximity distance used in this current study, the stress values observed between welds are found to be lower when compared with 5 and 10 mm proximity cases.

As reported by [30, 31], repair welds tend to produce high tensile residual stress, due to the local effect developed at the proximity regions or around the weld toes, causing high restraint and stress zones. The current study of fabricating repair weld B adjacent to original weld A also creates the situation of high restraint and stresses at proximity regions. These regions are important, from the aspect of structural integrity, as, residual stress through thickness component of membrane stress has a dominant effect in estimating the stress intensity factor for a growing crack in the high tensile residual stress region, as investigated by [30], by the use of the stress decomposition technique [16]. Significant elevation in residual stress decomposed components of bending and membrane stress has been observed by [31] in repair welds.

3.1.2 Stress at weld center

Stresses measured at 2 mm depths in the center of weld A for all proximity distances were found to be generally less in magnitude when compared with the center of weld B, due to the weld pass sequence effect and the high heat input of the TIG welding process (lower rate of cooling), as observed by [32] for plate butt welds. At the center of weld A, for 15 mm WP at 4 and 6 mm depths, a decrease in axial residual stress from 38 ± 18 MPa to compressive 21 ± 18 MPa was observed, in contrast to the 5 mm proximity distance, where an increase in axial tensile residual stress value from 132 ± 18 to 221 ± 18 MPa was found, as shown in Fig. 6b and c, respectively. For the 10 mm proximity distance, an increase in values from 96 ± 18 to 126 ± 18 MPa was found, when measured at 4 and 6 mm depths at the center of weld A.

In the 15 mm WP case, the minimum interaction is present between proximity welds; hence, the axial residual stresses observed at the center of weld B at 2 mm depth from the top are found to be higher than the 5 and 10 mm proximities. However, the axial tensile residual stress magnitudes for 5 and 10 mm proximities were found to be higher at 4 and 6 mm depths, in contrast to 15 mm WP. The most dominant effect is seen for 5 mm WP, where stresses increased from 69 ± 18 to 371 ± 18 MPa for 2 and 6 mm depths, respectively. Stresses measured at the center of weld B, at 6 mm from the top, were found to be give an average value of more than 355 MPa, which is higher than the yield strength of the parent metal for 5 and 10 mm proximity distances, in contrast to 15 mm WP. This behavior can be attributed to the complex interaction between the rate of cooling per unit weld pass volume of weld B and the high restraint present between 5 and 10 mm proximity welds.

3.2 Hoop residual stress: longitudinal to weld direction

The maximum tensile residual stresses measured in the hoop direction, i.e., longitudinal, or parallel to the weld, are generally found to be higher in magnitude when compared with axial stresses, as reported by other authors [32, 33]. As shown in Fig. 7, hoop residual stresses for 5, 10, and 15 mm WP are presented when measured at different depths (i.e., 2, 4, and 6 mm) from the top of the weld cap into the thickness, starting from the center of weld A towards B.

3.2.1 Stress at proximity regions

The values of hoop stresses measured at 2, 4, and 6 mm depths were found to be highest for the 5-mm proximity distance, when compared with the 10 and 15 mm proximity distances. At 2 mm depth from the weld cap into the thickness, a tensile hoop stress value of 177 ± 18 MPa was found for the 5 mm proximity distance, when compared with the 10 and 15 mm proximity distances, where values of 141 ± 18 MPa and compressive 102 ± 18 MPa, respectively, were measured, as shown in Fig. 7a. The values measured at 2 mm depths close to WT for all proximity cases were less

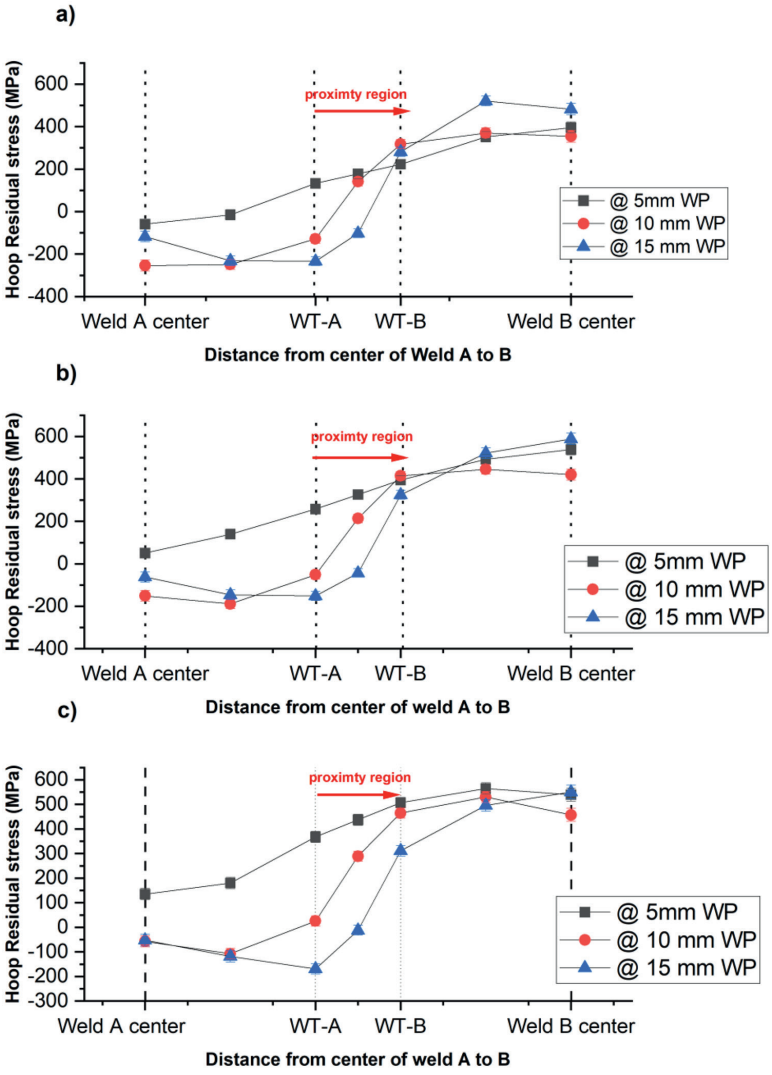

Fig. 7 Hoop residual stress for WP_5 mm, WP_10 mm, WP_15 mm proximity distances at **a**) 2 mm (cap) **b**) 4 mm (mid thickness) **c**) 6 mm depth (root), level respectively

tensile in magnitude than for the 4 and 6 mm depths, due to the maximum interaction and tempering effect present between adjacent welds. The highest hoop stress values of 326 ± 18 MPa and 437 ± 18 MPa were found at 4 and 6 mm depths, respectively, for 5 mm proximity distance between adjacent welds, as shown in Fig. 7b and c, respectively. In the case of 10 and 15 mm WPs, due to the increasing distance between tapered weld grooves along the thickness, hoop stresses' values were found to be low in magnitude in contrast to the 5 mm WP.

At 10 mm proximity distance, stress values measured at the proximity region were less tensile in nature, with magnitudes of 213 ± 18 MPa and 290 ± 18 MPa at 4 and 6 mm depths, respectively; however, these were still lower than the 5 mm proximity distance, due to the lesser restraining effect of adjacent weld B. As 15 mm is the maximum distance used as proximity in this study, the values found between adjacent weld toes were found to be compressive in nature. This corroborates the fact that residual stresses are self-balanced internal stresses, where tensile stresses found at the weld

center are balanced by compressive stresses [28] found generally in the heat-affected zone (HAZ) of girth welds. This trend was also noted in axial residual stress at the proximity region, as high tensile stresses at weld B's center are balanced by less tensile or converging towards compressive stresses for the 15-mm proximity case, at all depths.

3.2.2 Stress at weld center

Hoop stresses measured at the center of weld A were found to be considerably lower in magnitude than those measured at the center of weld B at all depths and WP distances. However, at the center of weld B, hoop stresses are more tensile in nature, with high magnitude. Stresses found at the center of weld B were found to be in the range of minimum 355 ± 18 MPa and maximum 590 ± 18 MPa in magnitude, for all proximity distances, which was found to be more than the yield strength values of parent metal S355, used in this current study. With increasing depths, the magnitudes of hoop stresses at weld B center were found to be higher, due to through thickness stress gradient, without being affected by additional restraint caused by weld A, for all proximity distances. It was interesting to note that the stress value found at 6 mm depth of weld B center was higher than 590 MPa, as shown in Fig. 7c, which can be attributed to the following reasons: (a) tensile strength of the filler wire used for fabricating weld B, was found to be in the range of 530–680 MPa as reported in [21]; (b) not using proper diffraction elastic constants which might be varying along the weld and the depth of the weld due to crystallographic texture and also slight chemical heterogeneities; (c) the chemical composition of the filler wire is slightly different although the cut samples did not show significant variations in the lattice parameter, some chemical segregation might locally affect the measured lattice parameter; (d) possible porosity in the weld which would result in measurement pseudo-strains.

Hoop residual stresses measured at weld B's center for 5 mm WP were found to be increasing with increasing depths, due to the complex interaction between naturally developed hoop direction restraint and additional restraint caused by the minimum proximity distance for girth welds. Hoop stresses observed for the 5 mm proximity region in the center of weld B at 4 and 6 mm depths were found to be higher than axial residual stresses at the same locations, in agreement with the general trend, as reported by [32, 33] for plates and [34] for tubular girth welds. However, hoop residual stresses at the center of weld A, were found to be lower in magnitude than the corresponding axial stress components. This can be attributed to the complex interaction developed at weld A, due to different welding sequences and maximum restraint caused using two different heat inputs.

3.3 Radial residual stress: into the weld thickness

As shown in Fig. 8, radial residual stresses for 5, 10, and 15 mm WP are presented when measured at different depths (i.e., 2, 4, and 6 mm) from the top of the weld cap into the thickness, starting from the center of weld A towards B.\

3.3.1 Stress at proximity regions

The values of radial stresses measured at 2, 4, and 6 mm depths were found to be generally lower in magnitude in contrast to axial and hoop components for all proximity distances. At 2 mm depth from the weld cap into the thickness, a tensile radial stress value of 65.3 ± 18 MPa was found for the 5 mm proximity distance, when compared with the 10 and 15 mm proximity distances, where values of 48 ± 18 MPa and compressive 8.75 ± 18 MPa, respectively, were measured, as shown in Fig. 8a. The values measured at 2 mm depths close to WT for all proximity cases were less tensile in magnitude than for the 4 and 6 mm depths, due to the maximum interaction and tempering effect present between adjacent welds. The highest radial stress values of 84 ± 18 MPa were found at 4 and 6 mm depths, respectively, for 5-mm proximity distance between adjacent welds, as shown in Fig. 8b and c, respectively. In the case of 15 mm WPs, due to the increasing distance between tapered weld grooves along the thickness, radial stresses' values were found to be low in magnitude in contrast to the 5 mm WP. At 10 mm proximity distance, stress values measured at the proximity region were less tensile in nature, with magnitudes of 65 ± 18 MPa and 117 ± 18 MPa at 4 and 6 mm depths, respectively; however, these were less than the 5 mm proximity for 4 mm depth and higher at 6 mm depth that can be attributed to complex restraining effect of adjacent weld B. As 15 mm is the maximum distance used as proximity in this study, the values found between adjacent weld toes were found to be compressive in nature. It should be noted that radial stresses become less important for estimating crack propagation direction in tubular restrained joints in contrast to its axial component [20].

3.3.2 Stress at weld center

Radial stresses measured at the center of weld A were found to be considerably lower in magnitude than those measured at the center of weld B at all depths and WP distances. However, at the center of weld B, radial stresses are more tensile in nature, with high magnitude but less than its respective axial and hoop components. Stresses found at the center of weld B were found to be in the range of minimum 56 ± 18 MPa and maximum 233 ± 18 MPa in magnitude, for all proximity distances, which was found

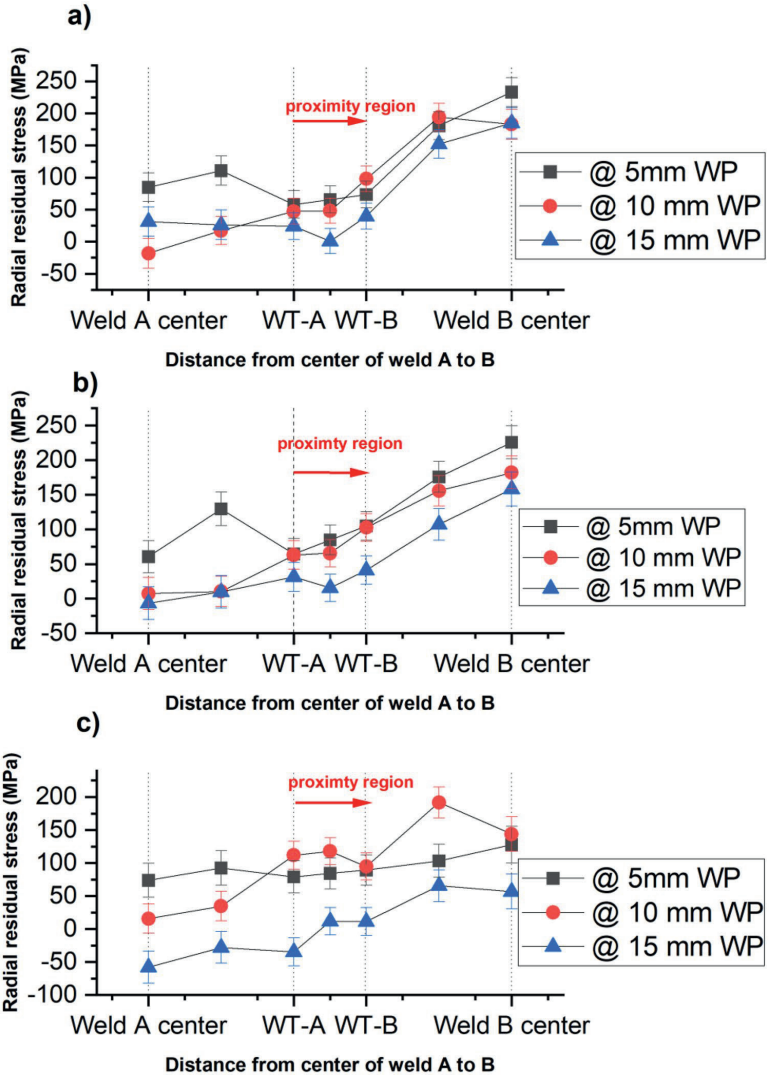

Fig. 8 Radial residual stress for WP_5 mm, WP_10 mm, WP_15 mm proximity distances at **a**) 2 mm (cap) **b**) 4 mm (mid thickness) **c**) 6 mm depth (root), level respectively

to be less than the yield strength values of parent metal S355, used in this current study.

3.4 Through thickness axial and hoop residual stress at proximity region

Residual stresses measured in the through thickness direction displayed an increasing trend when measured from the outside to the inside of the pipe at the proximity region for different depths, as shown in Fig. 9. When measured at the proximity region for 5 mm WP, residual stresses were found to have values equal to and higher than the yield strength of the parent material in the axial and hoop directions, respectively, at 6 mm depth. This region is important for maintaining the structural integrity of proximity girth welds. Residual stresses at the proximity region in through thickness were found to be maximum for 5 mm WP, in contrast to the 10 and 15 mm cases, due to the presence of maximum restraint and complex interaction between the high rate of cooling at 6 mm depths. Beyond mid-thickness, i.e., 4 mm, the stress gradient effect is more pronounced when compared with 2 mm depths, having

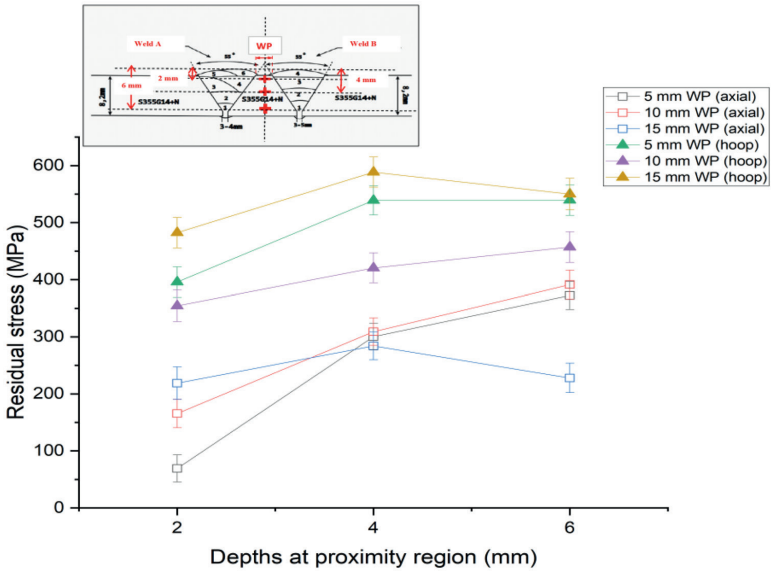

Fig. 9 Through thickness axial and hoop residual stress at proximity region of WP_5 mm, WP_10 mm, WP_15 mm proximity distances at 2, 4, and 6 mm depths

compression on the outside and tension on the inside of the pipe, as discussed by [29, 35], for weld toe regions of thin girth welds. In principle, the general trend of hoop stresses being higher than axial stresses was found relevant at the proximity regions used in this study.

4 Conclusion

In this work, welding-induced residual stresses were measured experimentally at the proximity region of tubular girth welded samples of S355 steel, with 5, 10, and 15 mm minimum distances maintained between their weld toes, by the use of the neutron diffraction technique on the POLDI time-of-flight diffractometer at the Paul Scherrer Institute. The welds placed at proximity were welded with two different welding processes, simulating the practical situation of a repair weld (weld B) being welded adjacent to an existing weld (weld A), generally fabricated during repair/replacement procedures on piping, pipelines, and the high restraint weld geometry of offshore jacket structures. The neutron diffraction method is a powerful technique for measuring welding-induced residual stresses in the bulk of the material. The findings of this study enable practitioners to take remedial actions to minimize the residual stresses developed in girth welds fabricated at proximity. Also, the findings enable us to derive technical justification for maintaining a minimum distance and developing welding procedure for welds fabricated at proximity. The key findings of this experimental study are as follows:

- Axial residual stresses were found to be maximum at the proximity region of 5 mm WP, when measured at 6 mm depth from the top for line scan measurements, displaying global bending behavior, i.e., compression on the outside and tension on the inside surface of the pipe.
- Tensile axial residual stresses for 5 mm WP at 6 mm depth, when measured at the proximity region, were found to be more than the yield strength of the parent material used in this study. This is important while performing weld integrity assessments on the girth welds of tubular structures, due to the dominant axial loading conditions present in tubular welded structures.
- Hoop residual stresses for 5 mm WP, when measured at the proximity region, were found to increase with deeper depths of measurement and exceeding the value of the yield strength of the parent material used in this study at 6 mm depth from the top of the weld cap into the thickness.
- Hoop residual stresses measured at the center of weld B were found to be the highest in magnitude at 6 mm depth, exceeding the value of the yield strength of the material for all proximity distances, due to the complex interaction developed between the natural hoop direction restraint present in girth welds and the restraint developed due to minimum proximity distance between adjacent welds.
- Stresses measured (both axial and hoop) at the center of weld A were mainly low in magnitude (less tensile), due to the high heat input of TIG welding, generating lower cooling rates, followed by the welding sequence

of weld B (FCAW – low heat input process), which was welded after the completion of weld A. The maximum effect of tempering was seen at 2 mm depth from the top of the center of the weld for all WPs.
- The most deleterious effect was observed at the proximity region location for the 5 mm proximity distance at the inner diameter of the pipe, as the maximum stress values of hoop and axial tensions were recorded.
- Radial stresses observed for all proximity distances were low in magnitude in contrast to hoop and axial components.
- The maximum proximity distance of 15 mm used in this study did not seem to indicate any deleterious effect between adjacent welds and followed the general residual stresses principle of high tension being balanced by compression at the weld center and HAZ or proximity region.

Hence, stress relaxation procedures like heat treatment can be introduced with the utmost care, as an important part of welding qualification procedures for proximity welds, when the minimum distance between adjacent weld toes is less than one thickness of the joining structural member. In future, the authors plan to measure residual stress distribution through other NDT techniques like XRD etc. and compare them with numerical thermo-mechanical numerical models in finite element for various distances on proximity welds.

Abbreviations λ : Wavelength; n: An integer; d : Spacing between planes of atomic lattice under strain; hkl: Miller indices defining lattice plane; d_o: Spacing between planes of atomic lattice in strain-free state; θ : Angle between incident and scattering beams; ε : Strain; σ_x : Residual stress in axial direction; σ_y : Residual stress in hoop direction; σ_z : Residual stress in radial direction; ε_x : Residual strain in axial direction; ε_y : Residual strain in hoop direction; ε_z : Residual strain in radial direction; E: Young's modulus; μ: Poisson's ratio

Acknowledgements We would like to acknowledge the support of M/s Rosenberg Worley, Stavanger, Norway, and Jan-Tore Jakobsen, lab engineer at University of Stavanger, Norway, for their support in the fabrication of samples. We would also like to acknowledge the support of the Norwegian McNeutron program, under which three days' beam time was allotted at PSI, Switzerland, and the University of Stavanger, Norway UiSScatt program, for providing financial assistance for this study. The research is fully funded by the Norwegian Ministry of Education (Internal PhD project No. IN-12168). This work has been carried out as part of a PhD research project, performed at the University of Stavanger, Norway. Jan Capek gratefully acknowledges financial support from the Strategic Focus Area Advanced Manufacturing (SFA-AM) initiative of the ETH Board.

Author contribution Sachin Bhardwaj: conceptualization, experimentation, investigation, methodology, visualization, writing – original draft, writing – review and editing, data analysis; R.M. Chandima Ratnayake: conceptualization, formal analysis, review and editing, funding acquisition, project administration, supervision; Efthymios Polatidis: experimentation, data analysis; Jan Capek: experimentation, data analysis.

Funding Open access funding provided by University Of Stavanger. The research is fully funded by the Norwegian Ministry of Education (Internal PhD project No. IN-12168). This work has been carried out as part of a PhD research project, performed at the University of Stavanger, Norway.

Data availability All data generated and analyzed during this research are included in this published article.

Code availability Not applicable.

Declarations

Ethics approval Not applicable.

Consent to participate Not applicable.

Consent for publication Not applicable.

Conflict of interest The authors declare no competing interests.

References

1. Bhardwaj S, Ratnayake RC (2020) Residual stress estimation in defect assessment procedures at weld toe and away locations on girth welds: review of key parameters. Theoretical and Applied Fracture Mechanics: p. 102848. https://doi.org/10.1016/j.tafmec.2020.102848
2. Larsson M, Larsson M, Ratnayake RM (2021) Experimental Investigation of weld joints manufactured at close proximity in S420 structural steel. in Proceedings of 1st International Conference on Structural Damage Modelling and Assessment. Singapore: Springer Singapore. https://doi.org/10.1007/978-981-15-9121-1_25
3. Bhardwaj S, Ratnayake RC (2020) Challenges due to welds fabricated at a close proximity on offshore structures, pipelines, and piping: state of the art. in ASME 2020 39th International Conference on Ocean, Offshore and Arctic Engineering. https://doi.org/10.1115/OMAE2020-18586
4. DNVGL-ST-0126 Standard (2018) Support structures for wind turbines. DNVGL
5. Bouchard PJ et al (2005) Measurement of the residual stresses in a stainless steel pipe girth weld containing long and short repairs. Int J Press Vessels Pip 82(4):299–310. https://doi.org/10.1016/j.ijpvp.2004.08.008
6. Dong P, Zhang J, Bouchard PJ (2001) Effects of repair weld length on residual stress distribution. J Pressure Vessel Technol 124(1):74–80. https://doi.org/10.1115/1.1429230

7. George D, Smith DJ (2005) Through Thickness measurement of residual stresses in a stainless steel cylinder containing shallow and deep weld repairs. Int J Press Vessels Pip 82:279–287. https://doi.org/10.1016/j.ijpvp.2004.08.006
8. Lotsberg I (2016) Fatigue design of marine structures. Cambridge University Press, Cambridge
9. Link M (2021) Equinor: several factors behind faulty welds on Johan Castberg FPSO Hull. Available from: https://www.marinelink.com/news/equinor-several-factors-behind-faulty-486965#.YH4FKi90m_8.linkedin[cited 2021 29/09/2021];
10. Acevedo C, Drezet J-M, Nussbaumer A (2013) Numerical modelling and experimental investigation on welding residual stresses in large-scale tubular K-joints. Fatigue Fract Eng Mater Struct 36:177–185. https://doi.org/10.1111/j.1460-2695.2012.01712.x
11. Barsoum Z, Barsoum I (2009) Residual stress effects on fatigue life of welded structures using LEFM. Eng Fail Anal 16:449–467. https://doi.org/10.1016/j.engfailanal.2008.06.017
12. Bate SK et al (1998) A review of residual stress distributions in welded joints for the defect assessment of offshore structures. Offshore technology report. Vol. OTH 482. Sudbury: HSE Books
13. British Standard (2019) BS 7910 Guide to methods for assessing the acceptability of flaws in metallic structures: UK
14. American Petroleum Institute (2007) API RP 579–1/ASME FFS-1. Houston, TX: American Petroleum Institute; August 2007.: USA
15. British Energy Generation Ltd (2013) Procedure R6 revision 4, assessment of the integrity of structures containing defects. 2013: UK
16. Dong P et al (2014) On residual stress prescriptions for fitness for service assessment of pipe girth welds. Int J Press Vessels Pip 123–124:19–29. https://doi.org/10.1016/j.ijpvp.2014.07.006
17. Larsson M et al (2021) Experimental Residual stress investigation of weld joints fabricated at a close proximity in S420 structural steel. In Proceedings of 1st International Conference on Structural Damage Modelling and Assessment. Singapore: Springer Singapore. https://doi.org/10.1007/978-981-15-9121-1_26
18. Acevedo C, Nussbaumer A (2013) Effect of tensile residual stresses on fatigue crack growth and S-N curves in tubular joint in compression. Int J Fatigue 36:171–180. https://doi.org/10.1016/j.ijfatigue.2011.07.013
19. Larsson M, Larsson M, Ratnayake RM (2021) Investigation of fatigue strength behaviour in dual weld S420 Steel joints fabricated at a close proximity. In Proceedings of 1st International Conference on Structural Damage Modelling and Assessment. Singapore: Springer Singapore. https://doi.org/10.1007/978-981-15-9121-1_27
20. Acevedo C (2011) Influence of residual stresses on fatigue response of welded tubular K-joints. EPFL, Switzerland
21. Bhardwaj S, Ratnayake RMC (2022) Welding procedure qualification record (WPQR) for welds fabricated at proximity. The International Journal of Advanced Manufacturing Technology. https://doi.org/10.1007/s00170-022-09022-5
22. ENISO15614–1 Standard (2017) Specification and qualification of welding procedures for metallic materials — welding procedure test
23. Paradowska A et al (2006) Residual stress measurements by neutron diffraction in multi-bead welding. Physica B 385–386:890–893. https://doi.org/10.1016/j.physb.2006.05.241
24. Stuhr U et al (2005) Time-of-flight diffraction with multiple frame overlap Part II: the strain scanner POLDI at PSI. Nucl Instrum Methods Phys Res, Sect A 545:330–338. https://doi.org/10.1016/j.nima.2005.01.321
25. Arnold O et al (2014) Mantid—Data analysis and visualization package for neutron scattering and μ SR experiments. Nucl Instrum Methods Phys Res, Sect A 764:156–166. https://doi.org/10.1016/j.nima.2014.07.029
26. British Standards Institute (2019) Non-destructive testing — standard test method for determining residual stresses by neutron diffraction, in ISO 21432:2019: UK
27. Jacob A et al (2018) Residual stress measurements in offshore wind monopile weldments using neutron diffraction technique and contour method. Theoret Appl Fract Mech 96:418–427. https://doi.org/10.1016/j.tafmec.2018.06.001
28. Withers PJ, Bhadeshia HK, Withers PJ, Bhadeshia HK (2001) Residual stress. Part 1 – Measurement techniques. Materials Science and Technology 17(4): p. 355–365. https://doi.org/10.1179/026708301101509980
29. Song S, Dong P, Pei X (2015) A full-field residual stress estimation scheme for fitness-for-service assessment of pipe girth welds: Part I - Identification of key parameters. Int J Press Vessels Pip 126–127:58–70. https://doi.org/10.1016/j.ijpvp.2015.01.002
30. Dong P (2018) On repair weld residual stresses and significance to structural integrity. Welding in the World 62(2):351–362. https://doi.org/10.1007/s40194-018-0554-1
31. Song S, Dong P (2017) Residual stresses at weld repairs and effects of repair geometry. Sci Technol Weld Joining 22(4):265–277. https://doi.org/10.1080/13621718.2016.1224544
32. Alipooramirabad H et al (2015) Quantification of residual stresses in multi-pass welds using neutron diffraction. J Mater Process Technol 226:40–49. https://doi.org/10.1016/j.jmatprotec.2015.07.002
33. Kim S-H, Kim J-B, Lee W (2009) Numerical prediction and neutron diffraction measurement of the residual stresses for a modified 9Cr–1Mo steel weld. J Mater Process Technol 209:3905–3913. https://doi.org/10.1016/j.jmatprotec.2008.09.012
34. Stacey A et al (2000) Incorporation of residual stresses into the SINTAP defect assessment procedure. Eng Fract Mech 67:573–611
35. Bouchard PJ (2007) Validated residual stress profiles for fracture assessments of stainless steel pipe girth welds. Int J Press Vessels Pip 84(4):195–222. https://doi.org/10.1016/j.ijpvp.2006.10.006

Experimental and numerical investigation of residual stresses in proximity girth welds

Sachin Bhardwaj [1], Sigmund Kyrre Aas [2], R. M. Chandima Ratnayake [3]

[1,3] Department of Mechanical and Structural Engineering and Materials Science, University of Stavanger, N-4036 Stavanger, Norway

[2] Norwegian University of Science and Technology (NTNU), Faculty of Engineering, Department of Marine Technology, NO-7491 Trondheim,

chandima.ratnayake@uis.no

Abstract: International fabrication codes and standards provide minimum distance criteria for proximity welds, although rigorous justification is lacking. These distances are either based on practical experience or mutual agreement and are often left to the engineering judgment of contractors, inspection engineers, etc., especially in cases of repair welds fabricated in proximity to existing welds. Previous studies have shown high tensile residual stresses and altered mechanical and microstructural properties between proximity welds. This article focuses on numerical and experimental quantification of residual stresses in the proximity region by X-ray diffraction (XRD) and finite element method (FEM) thermo-mechanical models. Specimens were machine welded, then repair welded at distances of 5–15mm. A fair agreement in results was achieved between FEM and XRD. The most detrimental effect was observed at the weld root toe for the repair weld at 5 mm proximity, likely due to the high constraint and multi-axial stress state. These findings enable practitioners to propose technical justification and corrective actions while specifying minimum distance criteria for proximity welds.

Keywords: Residual stresses, thermo-mechanical, proximity repair welds, X-ray,

1. Introduction

Pipe replacement procedures are inevitable in high pressure piping structures. The causes vary and include high temperature creep effects, development of tensile residual stresses at weld toes, intersection of longitudinal welds with girth welds, internal corrosion and overlap of reinforcement of branch connections with existing welds [1]. These situations lead to the fabrication of repair welds in proximity to existing welds like welds of branch connections, nozzles, etc., during pipe replacement procedures. Failures due to repair weld proximity to existing welds have led to catastrophic incidents in structural offshore brace joints [2], nuclear power piping girth welds [3] and offshore floating structural members [4] due to development of deleterious tensile residual stresses at weld toe locations. International fabrication and repair codes lack clear consensus when it comes to deciding the minimum distance between welds as described in a previous review [5]. These fabrication codes lack consensus for deciding minimum proximity distance criteria, which is recommended either based on the thickness factor (four to five times) or diameter (one to one and a half times) the of the joining member. Repair procedures of fabrication codes are purely based on mutual agreement or some set arbitrary distance that is based on the operator's practical experience as stated in API 2200 [6] and DNV-OSF101[7], which are used in transportation pipelines and subsea pipe replacement guides, respectively.

Repair welds are widely used in replacement procedures to extend aging piping's life [8], which are often vulnerable to cracking due to stress corrosion cracking (SCC) at the weld root or at a distance away from weld toe locations. Tensile residual stress coupled with corrosive medium in pipe internal surfaces represents a risk for SCC cracking at weld root

locations [1]. Repair welds can develop further restraint in addition to the original restraint of girth welds, which can further develop harmful or beneficial residual stresses across the thickness of proximity regions [8, 9]. Increases in transverse residual stresses (perpendicular to the weld) have been observed by various researchers [3, 8–10] in repair regions of existing welds, which are important from a structural integrity perspective. Proximity regions that develop between repair and existing welds are subjected to multiaxial stress states due to the presence of additional restraints, which can increase the through thickness membrane and bending component as per stress decomposition theory [9]. Level 3 assessment of estimating welding-induced residual stresses (WRS) in structural integrity procedures of fitness for service codes [11–13] requires the use of nonlinear FEM results coupled with residual stress experimental measurements for defining residual stress profiles at a distance away from weld toe locations, which are currently practically non-existent or overly conservative [14, 15].

Changes in transverse residual stress profiles have been observed between offshore jacket brace joints and proximity butt welds in plates fabricated with a similar welding process in the past [16, 17]. Weld sequence and additional restraint due to the heat input of additional welds play important roles in estimating final WRS profiles [18]. We previously qualified the welding procedure between repair and existing girth welds [4] by welding with two different welding processes where high hardness and low Charpy energy values were recorded. Further development of high tensile axial residual stresses at mid thickness and towards the root region of proximity welds were observed between repair and existing welds by using neutron diffraction (ND) technique [19]. There is a lack of studies on the distribution of WRS around weld root and toe locations to estimate stresses on pipe outer and inner surfaces.

This study aimed to investigate how repair girth weld placement at set distances of 5, 10 and 15 mm from the existing weld impacts the residual stress distribution around weld toe and root regions. The thermo-mechanical-based finite element method (FEM) using ABAQUS was used to simulate the welding process and estimate residual stresses. Experimental validation was performed by using XRD to evaluate residual stresses at pipe outer and inner surfaces. The remainder of the paper is structured as follows: Sect. 2 presents the methodology. In Sect. 3, the results are presented and discussed. Finally, in Sect. 4, we draw our conclusions.

2. Methodology

2.1 Test specimens

Proximity girth welds were fabricated on structural steel grade S355 G14+N seamless pipe, with dimensions of 219.1 mm outside diameter and 8.18 mm thickness as shown in the schematic in Fig. 1. To simulate the practical scenario of proximity welds, an initial weld was welded with the tungsten inert gas (TIG) welding process. After maintaining the required weld proximity (WP) distance of 5, 10 or 15 mm between adjacent weld toes, a repair weld was fabricated with metal active gas (MAG) for the root pass, and Flux cored arc welding (FCAW) was used for the remaining passes. Details for the welding parameters and mechanical properties of the base and filler wire can be found in our previous work [4].

2.2 Residual stress measurements using X-Ray diffraction

WRS was measured using a Proto iXRD instrument on the inner and outer surfaces of the welded pipes. Stress calculations are done in Proto XRDWIN using the $\sin^2 \Psi$ method and 11 β angles. A β range of ± 20° was used for the outside of the pipe, while the inside was restricted to ± 16° due to collision with the pipe wall. A Cr cathode was used with a 1 mm circular aperture at 20 kV and 4 mA, which gives a penetration depth of about 4–5 µm [20]. Measurement locations were manually chosen as close to the roots as was feasible and at 3–5 mm intervals. The locations were programmed so that subsequent measurements could be obtained at the exact same points in both the axial and hoop directions. All

measuremnts were taken at the surface level of the pipe on the inner and outer surfaces, respectively.

2.3 Numerical model

In this study, a FEM-based numerical model was generated in ABAQUS [21] using the Qustom app plugin [22] which was used to develop automatic subroutines for multi-pass welds. In thermo-mechanical-based FEM models, temperature history output serves as input to mechanical models. Nodal temperature distribution is solved incrementally in mechanical models with time to satisfy equilibrium conditions [23]. It is important to mention here that an uncoupled thermo-mechanical simulation was used in this analysis, which generates separate thermal and mechanical models. Mechanical strains are estimated according to simulated heating and cooling times from a temperature distribution of existing and repair welds, which replicates the practical pipe replacement procedures. However, the effects of initial residual stresses were taken as negligible as reported by past research [8, 9]. Hence, WRS was measured after the completion of repair weld only.

2.2.1 Geometry

A 2D Axisymmetric model was built in ABAQUS from available macrographs of existing and repair welds. Three different scenarios of weld proximity (WP) distances of 5, 10 and 15 mm were maintained between adjacent weld toes as shown in Fig. 1 with a minimum element size of 0.15 mm maintained at HAZ and proximity regions. Mesh convergence study was performed and was found to be satisfactory as residual stresses profile did not change with increasing element size. Subsequently, repair welds were modelled according to an available macrograph from the welding qualification procedure record (WPQR) [4] at set proximity distances. Existing and repair welds were modelled simultaneously; however, during thermal analysis, repair weld was made inactive using the 'model change' feature in ABAQUS to develop automatic subroutines by use of the Qustom app plugin.

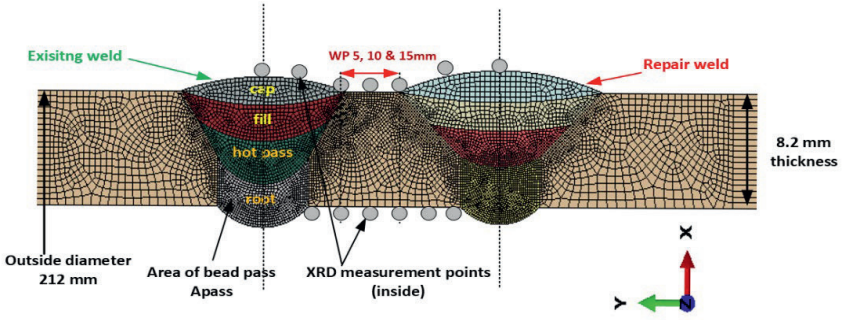

Fig. 1. Axisymmetric FEM model of existing and repair welds reproduced from weld macrographs showing XRD measurement locations

2.2.2 Material model

Temperature-dependent material and mechanical, material and hardening properties for the parent and weld metals were taken from Bhatti et al. [24] as also shown in Fig. 2a and b, respectively. Temperature-dependent mechanical and material properties are considered the same for the base and weld metal as per S355 grade. Thermal conductivity from temperature-dependent material properties [25] were doubled between melting and cut-off temperatures to take the enhanced convection effects of the molten weld pool into account [8]. The isotropic hardening law and rate-dependent power laws were used in this analysis without considering the effect of phase transformations [26] for base and weld materials as shown in Fig. 2b.

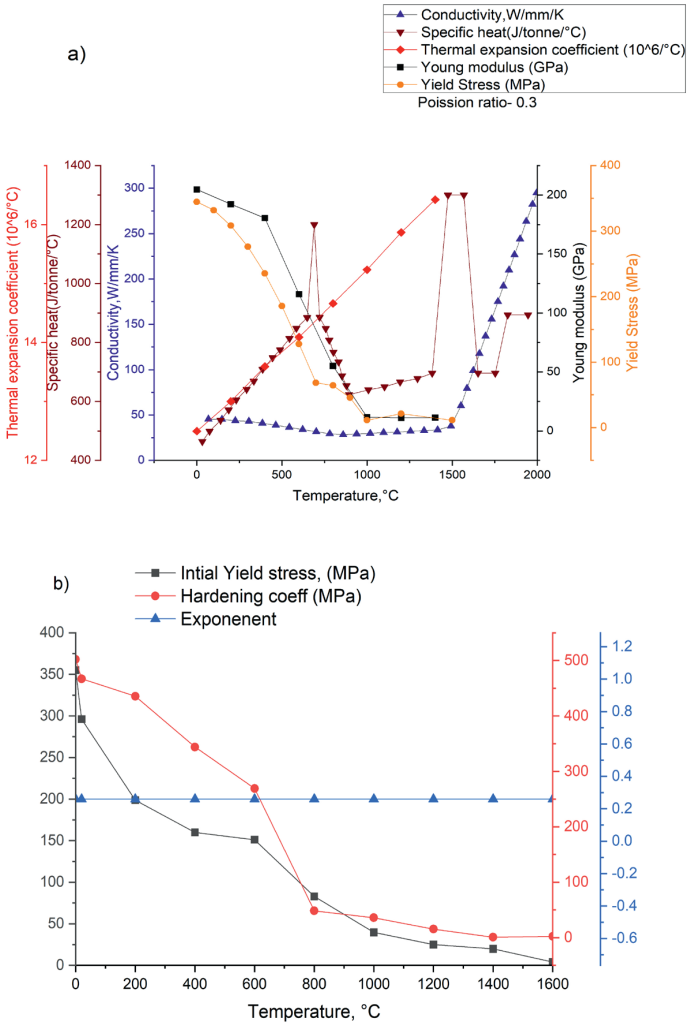

Fig. 2. S355 material temperature-dependent **a)** mechanical and material and **b)** hardening properties adopted from Bhatti et al. [24]

2.2.3 Heat source modelling

During thermal analysis, accurate estimation of linear heat input (Q) in J/mm in welding direction is important by approximating the area of the weld pass (A_{pass}) correctly as shown in Fig. 1. Goldak's double ellipsoid [27] fusion zone length parameters (c_r+ c_f) (i.e., rear and front part of the torch) were estimated by using Rosenthal's moving heat source solution for semi-infinite bodies [28]. Various researchers [9, 18, 29–33] have used a simplified model of heat flow analysis for estimating heat input in 2D or axisymmetric numerical models for residual stress estimations. Hold time t_{hold} determination can be estimated by deposited weld at specified melting temperature according to Equation (1). Determination of hold time and heat input to avoid overheating in the numerical model was performed by calculating weld pass area (A_{pass}) by using macrographs from WPQR, which we qualified in a previous study [4].

$$t_{hold} = \frac{c_r + c_f}{v} \qquad (1)$$

Linear heat approximation for each weld pass was performed analytically to estimate the torch length parameters and hold time as shown in Table 1. A detailed explanation for

linear heat input estimation and torch parameters can be found in Bhardwaj and Ratnayake [34]. The Qustom app plugin was used in ABAQUS, which can automatically import the defined geometry and can assign temperature-dependent properties to the relevant sections of the weld and parent metal. This plug-in can automatically generate and define weld passes by facilitating easy assignment of the weld bead sequence for each weld pass in multi-pass welds. In the bead assign section of this plugin, hold time can be calculated automatically by inserting analytically derived Goldak's parameters of front and rear (cr+ cf) parts of the torch. Similarly, weld bead laying sequence and corresponding cooling time can be inserted automatically.

DCAX4: A 4-node linear axisymmetric heat transfer quadrilateral element was used for thermal analysis in ABAQUS. Each weld pass was deposited at a melting temperature of 1500 °C and a cut-off temperature of 1200 °C until it reaches inter-pass from the WPQR. Surface film conditions were provided in the thermal model with a magnitude of 25 $Wm^{-2}K^{-1}$ corresponding to a still air environment for both sides across a thickness and radiation emissivity coefficient of 0.7. After the completion of each pass of the existing weld, sufficient cooling time was provided to the model to reach the ambient temperature conditions seen in Table 1. After its completion, repair weld beads were inserted into the model at set proximity distances of 5, 10 and15 mm according to the parameters mentioned in Table 1.

Table 1: Hold time and torch parameters for existing and repair welds.

Existing weld							
Weld pass	v **Travel speed mm/s**	**Q J/mm**	**Area of the bead A_{pass} (mm2)**	**Cr Rear length of torch (mm)**	**Cf Front length of torch (mm)**	t_{hold} **(s)**	**Cool down time (s)**
Root	1	913.9	21.99	1.91	0.67	2.58	1800
Hot pass	1.47	988.2	22.29	3.12	0.94	2.77	600
Fill	3.22	746.7	26.01	5.36	1.61	2.17	600
Cap	2.92	894.4	21.4	5.81	1.75	2.69	3600
Repair weld							
Weld pass	v **Travel speed mm/s**	**Q J/mm**	**Area of the bead A_{pass} (mm2)**	**Cr Rear length of torch**	**Cf Front length of torch**	t_{hold} **(s)**	**Cool down time (s)**
Root	1.52	736.0	28	0.70	2.34	2.00	900
Hot pass	5.9	650.3	20.93	2.47	8.23	1.81	600
Fill	5.48	640.6	27.69	2.47	8.22	1.95	600
Cap	4.28	794.2	30.13	2.30	7.66	2.33	3600

2.2.4 Mechanical model

The mechanical model was generated separately in ABAQUS in an uncoupled thermo-mechanical fashion after nodal temperature estimation was matched with available thermocouple data and macrographs from the available WPQR. In the mechanical model, suitable boundary conditions are provided to avoid rigid body motions and over-constraining of the model. In the mechanical analysis, melting temperature was capped to avoid excessively large thermal strains and cut-off temperatures were set in material properties as per Fig. 2b to avoid a large accumulation of plastic strains. CAX4: A 4-node bilinear axisymmetric quadrilateral element was used for mechanical analysis in ABAQUS. Boundary conditions were applied to eliminate all rigid body motions by restraint at the axial end of the pipe without affecting the stress solution. Residual stresses were measured with the XRD technique according to the locations mentioned in Fig. 1 between adjacent welds for all proximity distances on the outer and inner surface of the pipe, respectively.

3. Results and Discussion

The results of hoop and axial residual stress measured from XRD techniques were compared with FEM results for pipe outer and inner surfaces as shown in Figs. 3 and 5 respectively. The measurements were performed on the pipe's outer surface starting from the left side of the repair weld toe (WT-R) to the right toe of the existing weld (WT-E) and on the pipe's inner surfaces, i.e., between the repair and existing weld root toes for all proximity distances as previously shown in Fig. 1. Through thickness stress distribution at existing weld toe location is also presented in Figs. 4 and 6 for hoop and axial stress components respectively for all proximity distances.

3.1 Hoop residual stress: circumferential to weld direction

As shown in Fig. 3a and b, hoop residual stresses were presented for all WP distances starting from the repair weld towards the existing weld for the pipe's outer and inner surfaces, respectively. The figures show that hoop stresses at outer surface proximity regions are mainly compressive in nature. However, pipe inner surface stresses are mainly tensile in nature, starting from the weld toe WT-R (repair) to the WT-E (existing) weld.

3.1.1 Stress measured on the outside of the pipe

The XRD-measured points on the outside surface of the proximity region for 5 and 15 mm WP distances were found to be mainly compressive in nature, whereas 10 mm WPs were found to be on the tensile side as shown in Fig. 3a. The magnitude for 5 and 15 mm WP samples were found to be negative 20% of the yield strength of S355 material used in this study, whereas 10 mm WP was found to be positive 10% of yield strength. FEM results for 5, 10 and15 mm WPs showed the same decreasing trend between repair and existing welds, but their magnitude is overpredicted in contrast to XRD results. It is worth mentioning here that stresses estimated by FEM were overpredicted as the model used in this study does not consider the effect of phase transformations and temperature-dependent properties of filler wires of weld metal. Changes in the final developed profile at proximity regions (i.e., between adjacent welds) can be attributed to the additional restraint of the repair weld (i.e., due to an additional shrinkage effect) and tempering effect with decreasing distances between their weld toes as seen from the FEM results.

Hoop stresses measured at weld centre locations on pipe outer surfaces of repair welds are found to be tensile in nature due to natural restraint in pipe geometries. Generally, hoop stresses are found to be equal to the yield magnitude at weld centre locations and are balanced by compressive stresses on adjacent sides of the weld [35, 36]. Due to the sequence of repair welds being welded after the completion of existing welds, stresses found at weld centres of existing welds were found to be normalized or generally compressive in nature. A shrinkage zone-controlled plastic zone leads to the development of yield-level hoop residual stresses around weld toe regions as demonstrated by previous research [29–31, 34]. Due to the use of two different welding processes in simulating the conditions of repair and existing welds with varying heat inputs and sequences of welding, stresses developed at these regions are further normalized. Due to changes in morphology of final microstructure developed at proximity regions, as observed in WPQR of proximity welds micrographs, development of stress at an inter or intra-granular level can be considered the main reasons for changes in the final observed residual stress state.

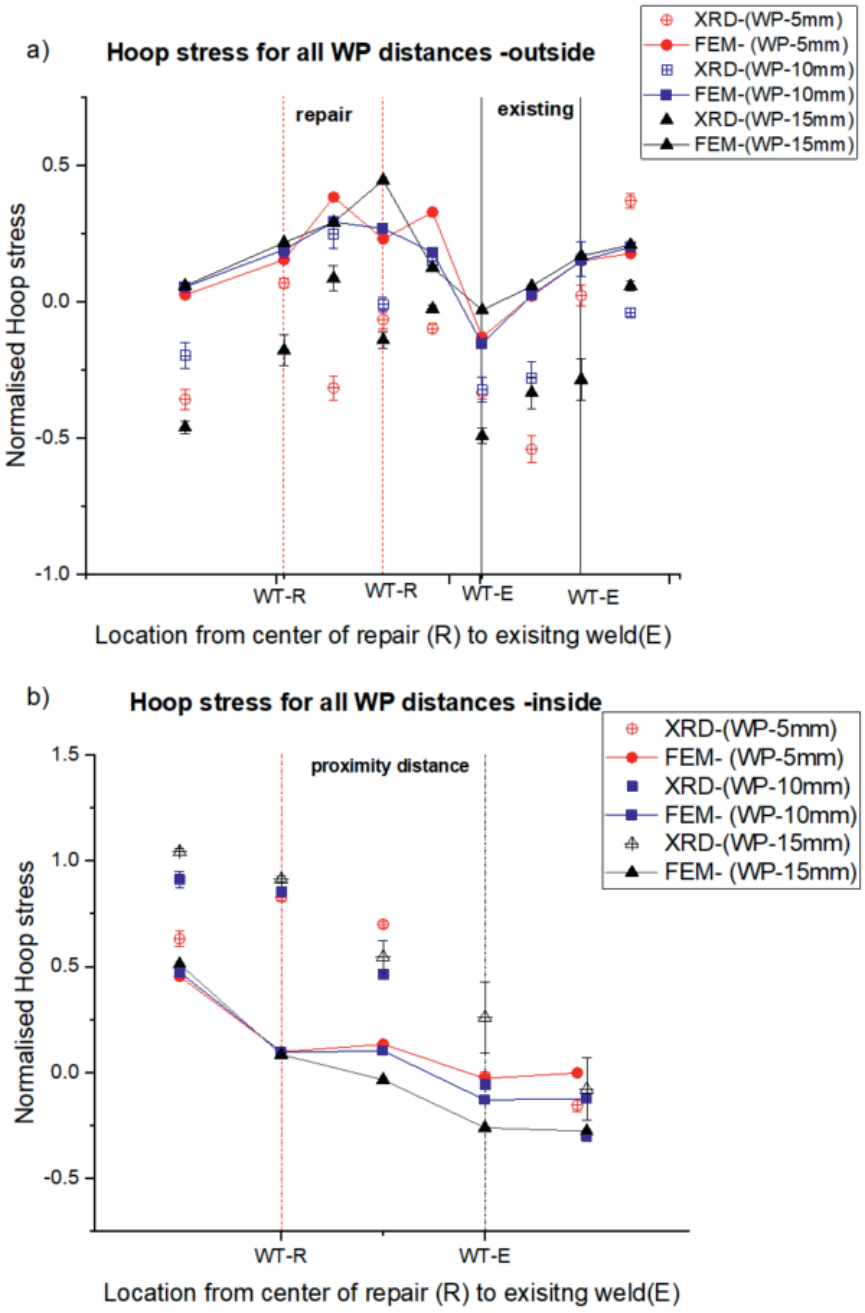

Fig. 3. FEM vs XRD comparison of normalized residual stresses on pipe **a)** hoop – outside **b)** hoop – inside for all proximity distances starting from the repair to the existing weld

3.1.2 Stress measured inside the pipe

Hoop stresses measured between two WT-R and WT-E locations on the pipe's inner surface by the XRD technique are presented in Fig. 3b. Repair welds exhibited tensile residual stresses equal to or greater than the yield strength of the material, i.e., S355 at WT-R locations, whereas these stresses were found to be converging towards compressive regions at WT-E locations. Stresses developed at proximity regions on pipes' inner surfaces for 5 mm WP from the XRD results were found to be of maximum magnitude,

i.e., around 50% yield stress of S355 steel used in this study, which can be attributed to the maximum restraint effect. FEM validation shows a fair agreement with the experimental results; however, the predicted stresses were underpredicted by 25%.

Stresses measured from XRD at WT-E root locations for 5mm WP distances are minimum at the weld root location due to the maximum compression effect of subsequent passes in a multi-pass weld, as observed by other researchers [35]. This high hoop tensile residual stress that developed at weld root toe locations can be deleterious to the structural integrity of piping, which are subjected to corrosive transport of fluid, creating a perfect environment for SCC cracking. Stresses measured at proximity regions for 5 mm WP show a global bending behaviour, i.e., compression on the outside and tension on the inside, as observed by previous researchers [8] for failures in power piping girth welds [37, 38]. Due to the multiaxial nature of residual stress developed at proximity regions, minimum distance criteria need to be standardized for non-stress-relieved welds to avoid the risk of SCC and reheat cracking.

3.1.3 Through thickness stress distribution: Existing weld vs repair weld

Fig. 4a presents the through thickness hoop stress distribution at the WT location of existing welds for all proximity distances. These FEM-based results are compared with the existing single weld (SW) stress state distribution without the presence of repair welds at proximity. It can be observed that original state of existing welds follows a tensile distribution on the outer surface and compression on the inner surface of the pipe. For 10 and 15 mm WP distances, hoop stress distribution exhibits almost the same trend with some changes due to the effect of decreasing proximities. For 5 mm WP, due to the maximum effect of restraint and an additional shrinkage effect, hoop stress distribution is changed and tensile stresses are estimated at pipe outer and inner surfaces at existing weld toes.

Stress linearized components based on the length scale-based characterization technique [39] and derived from stress decomposition theory is important from a structural integrity perspective. The decomposed components of the membrane and bending are beneficial in determining the fracture driving force in term of stress intensity factor (K). Membrane components provide maximum contributions in crack driving force followed by bending as demonstrated by various researchers in the past [3, 9, 39]. Fig. 4b presents the decomposed competent of membrane and bending for hoop stress for all WP distances at existing weld toe locations at pipe outer surfaces. It can be observed that the hoop-membrane component is the maximum for 5 mm WP in contrast to 10 and 15 mm WP in contrast to SW stress state, which was found to be the maximum. Higher membrane hoop stress exerts the maximum circumferential shrinkage force which can be deleterious to pressure-containing pipes as additional hoop component is developed in addition to natural hoop restraint in pipe girth welds. The hoop-bending component was found to be the maximum for the 15 mm WP distance and found to be comparable with existing SW original state, which implies increased radial restraint.

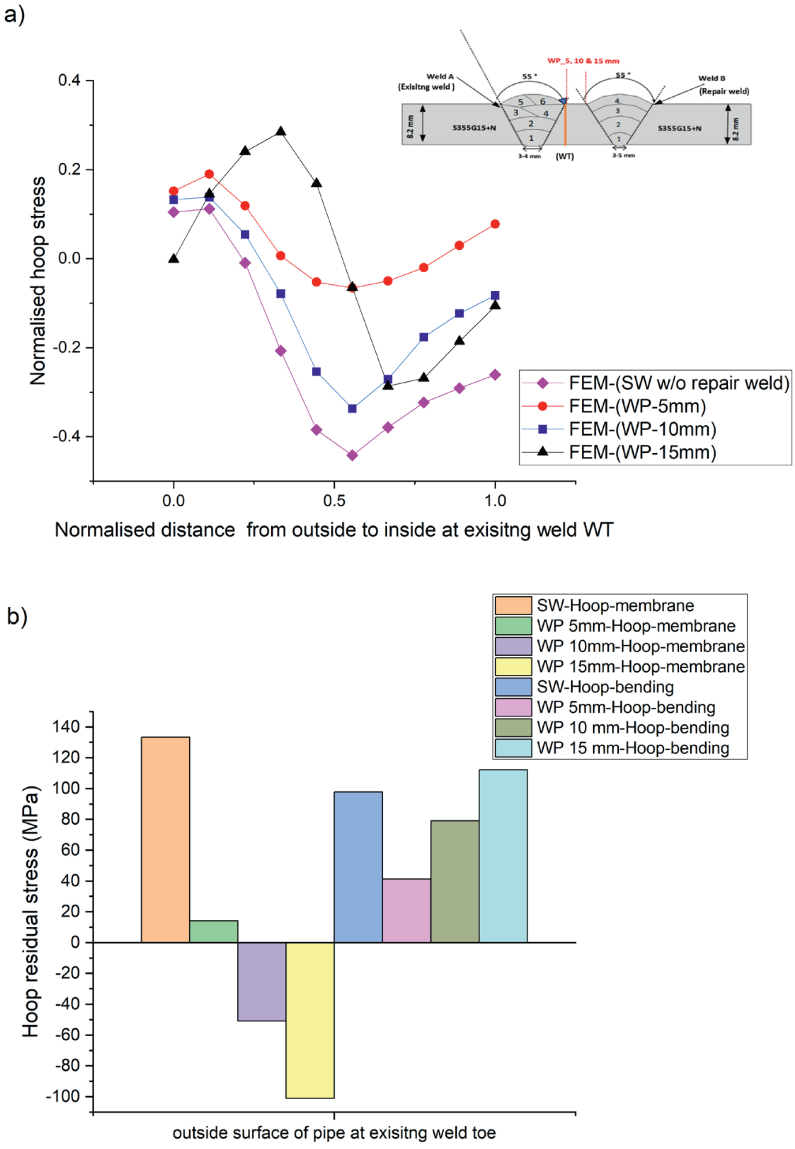

Fig. 4. Hoop stress distribution **a)** through thickness at existing weld toe location **b)** hoop stress linearized components from FEM for all proximity distances

3.2 Axial residual stress: perpendicular to weld direction

As shown in Fig. 5a and b, axial residual stress distribution is presented for all WP distances starting from the repair weld towards the existing weld on pipe outer and inner surfaces. It can be observed that axial stresses change from compressive to tensile and vice versa starting from the repair to the existing weld on pipes' outer and inner surfaces, respectively.

3.2.1 Stress measured on the outside of pipes

WRS measured by the XRD technique for all WP distances were found to be compressive at the weld centre location of repair welds and shift towards tensile regions at existing weld centre locations as shown in Fig. 5a. Stresses measured at the proximity region were found to be compressive from the XRD technique for all proximity distances and found between negative 50% and 70% magnitude of the yield stress for the S355 material. FEM results were estimated to be in reasonable agreement, except weld centre locations. This can be attributed to the use of S355 temperature-dependent mechanical properties for weld metal locations of repair and existing welds in FEM models.

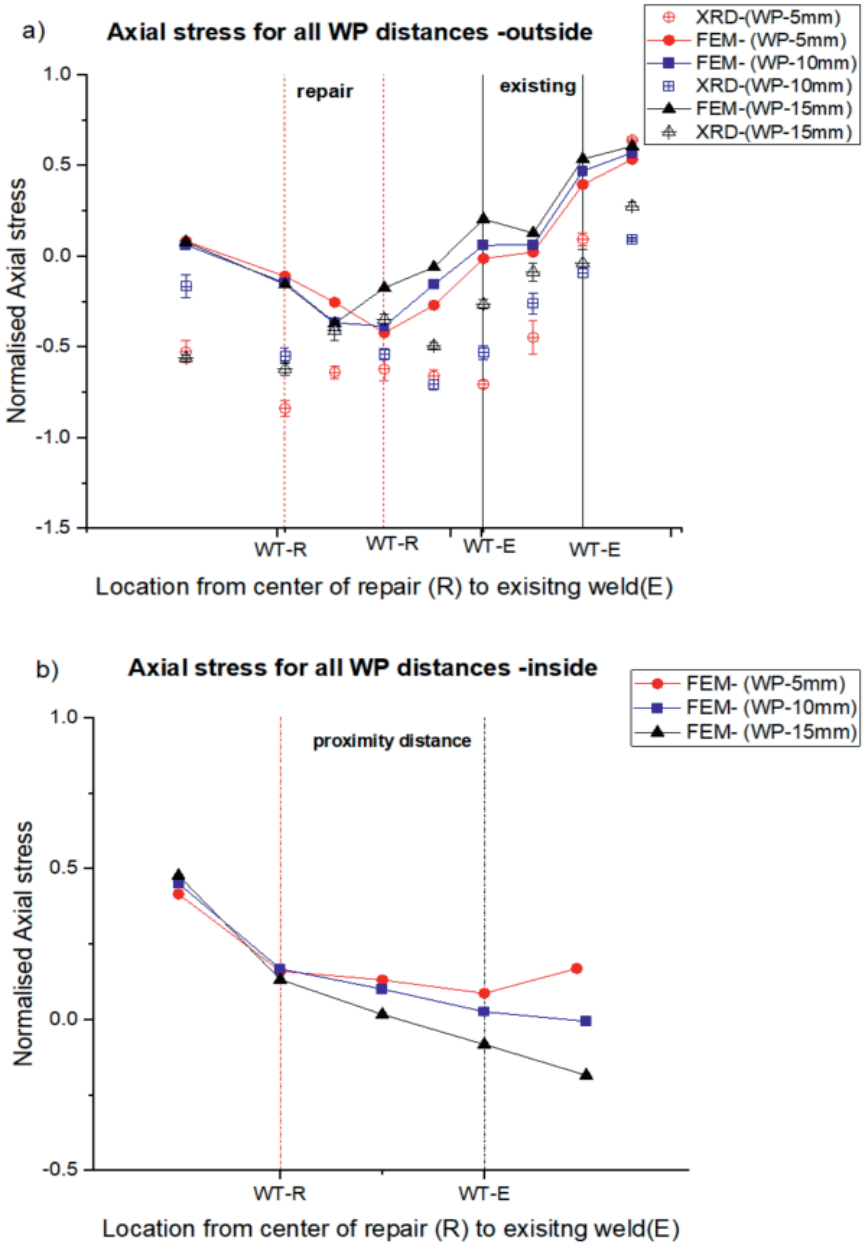

Fig. 5. FEM vs XRD comparison of normalized residual stresses on pipe **a)** axial-inside **b)** axial-inside surface (FEM only) for all proximity distances starting from the repair to the existing weld

Axial stress distribution is primarily affected by the mismatch in axial strains and due to different expansion and contraction properties of filler wires used in the fabrication of repair and existing welds. This mismatch is compensated by plastic straining of repair welds and proximity regions when compared with elastic deformation of the parent metal as noticed by Bouchard [37] while studying the overlapping repair weld length effect on the existing weld. Song and Dong [8] made a similar observation while deciding repair length optimum size, i.e., maximum possible length, but width should be as narrow as possible, and its depth as shallow as possible.

3.2.2 Stress measured inside the pipe

Axial residual stresses estimated at pipe inner surfaces from the FEM study were found to be tensile at the repair weld root toe location and moving toward a zero-stress state or compression at the existing weld root toe as shown in Fig. 5b. For the 5 mm WP distance, tensile stresses were observed at weld root toe locations of existing welds in contrast to compressive stresses found at 10 and 15 mm WPs. This can be attributed to maximum restraint at WP 5 mm distance and the multi-axial stress state developed at proximity regions. Tensile axial residual stress was also observed at root toe locations of existing and repair welds at 6 mm depth from the top of the weld cap by neutron diffraction experiments [19]. Axial residual stresses contribution is important for determining crack driving parameters for components subjected to axial loadings; hence their estimation is important for determining the minimum distance for repair weld placement in piping subjected to corrosive mediums.

3.2.3 Through thickness stress distribution: Existing weld vs repair weld

Fig. 6a presents through thickness axial stress distribution for all proximity distances compared with the existing single weld (SW) stress distribution without the presence of repair welds in proximity. It can be observed that the original state of SW follows a distribution of a self-balancing state with compression on the outer surface balanced by tension at mid thickness followed by compression on the inner surfaces of pipe. The same observation was noticed for 10 and 15 mm WP distances; however, for 5mm WP, tensile axial stresses were estimated at weld root toe locations of existing weld toe locations. Tensile 10% and 20% compression S355 yield was estimated by FEM at pipes' inner and outer surfaces, respectively for 5 mm WP. 20% compression can be attributed to maximum tempering and interaction taking place between weld toe of repairs and existing welds in contrast to 10 and 15 mm WP. At pipe inner surfaces, tensile stresses were observed in contrast to 10 and 15 mm WP due to the maximum effect of restraint and multi-axial stress developed at proximity regions.

The membrane component in the axial direction was found to be negligible [15, 30] for different r/t geometries unless final assembly welds have restraints. Stress decomposed factors of axial residual stress at pipe outer surfaces are presented in Fig. 6b where the membrane component for 5 mm WP was found to be higher than 10 and 15 mm WP and comparable with the SW axial component. The bending component was found highest for 15 mm WP in contrast to 5 and 10 mm WP. Macrographs of 15 mm WP generated from WPQR in a previous study [4] displayed maximum distortion in axial or transverse directions in contrast to 5 and 10 mm WP. This can cause high primary and secondary bending stresses, which are deleterious to pipe welds subjected to axial loading conditions under repeated loading conditions leading to fatigue failures.

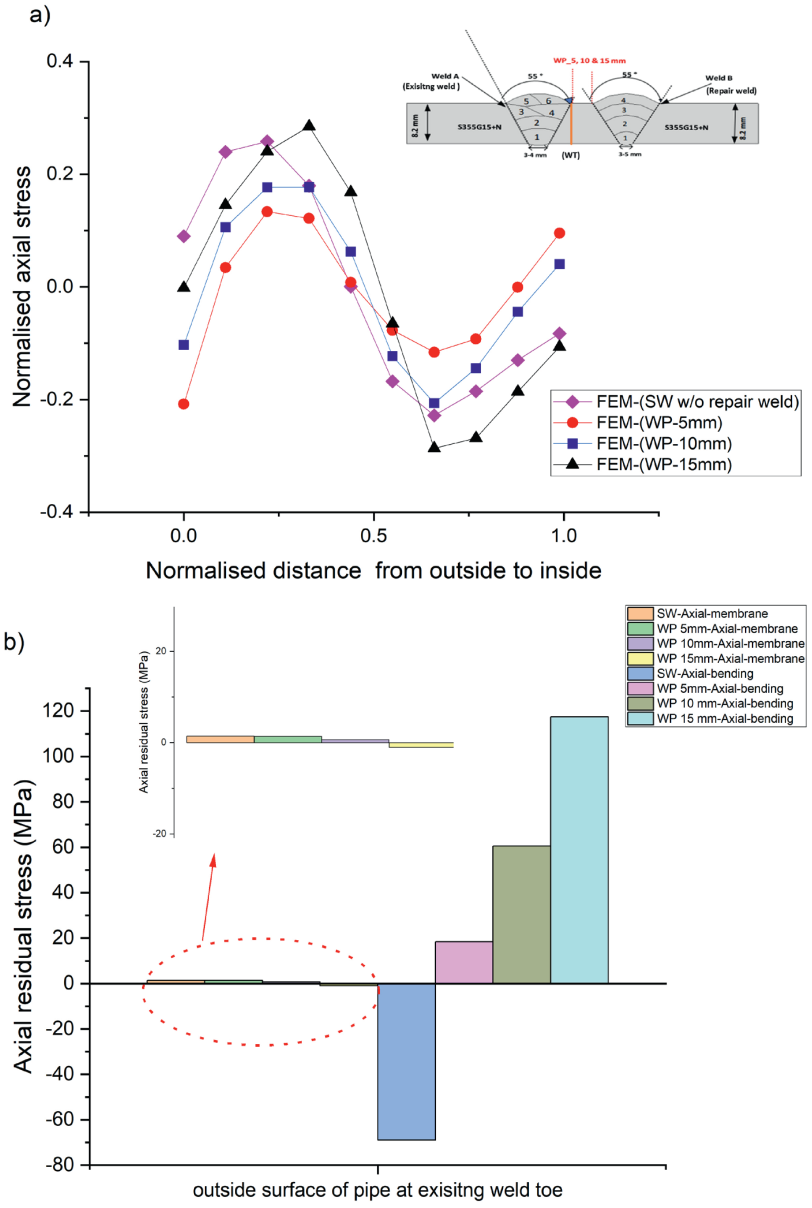

Fig. 6 Axial stress distribution **a)** through thickness at existing weld toe locations **b)** axial stress linearized components from FEM for all proximity distances

4. Conclusion

In this article, numerical and experimental investigations were conducted to estimate welding-induced residual stress between weld toes of repair girth welds placed at set proximity distances to an existing girth weld. XRD measurements were conducted by using a Proto iXRD® compact instrument at SINTEF/NTNU/IMT, Norway on pipe outer and inner surfaces, respectively. These measurements were validated with a FEM-based thermo-mechanical model in ABAQUS® and were found to have a fair agreement with the experimental results. This case study was an extension of a previously qualified

welding procedure qualification record and residual stress measurement by neutron diffraction between proximity welds on a structural steel S355 grade pipe. Residual stresses were quantified using the stress decomposition technique for determining the through thickness stress state profile and highlights the contribution of hoop and axial decomposed components of membrane and bending which are useful in estimating stress intensity factors due to residual stress used in crack assessment procedures. The major findings of this study are reported below:

- Residual stress distribution between repairs and existing weld toes on pipes' outer surfaces are strongly influenced by the distance maintained from their weld toe as a maximum tempering effect was noticed in the hoop and axial directions for 5 mm proximity due to the closest interaction of adjacent weld toes.
- The residual stress distribution on pipe inner surfaces between adjacent weld root toes exhibits the development of harmful tensile stress formation at existing weld root toes which can be deleterious to SCC and reheat cracking in aging welds of power and process piping's structures.
- The sequence and restraint of repair weld fabrication in proximity to existing welds were identified as major factors in determining final residual stress development of tension at existing weld toe locations at pipe outer and inner surfaces by using the XRD technique.
- FEM models were found to have a reasonably fair agreement with measured XRD results. Variations in results can be attributed to a lack of temperature-dependent mechanical properties for filler metals, type of hardening model and the exclusion of phase transformations in FEM models.
- Linear 2D heat input approximation and Rosenthal's moving heat source solution for avoiding overheating problems and estimating Goldak's torch parameter, respectively in thermal models, from weld macrographs have proven to be an effective technique for estimating residual stresses in FEM.
- An increase in the decomposed component of membrane stress by stress decomposition theory in the hoop and axial directions for the closest proximity distance was identified as an important technique for identifying important parameters for determining fracture driving forces used in structural integrity procedures for cracks in welds.
- In deciding minimum distance criteria for the placement of repair welds in proximity to existing welds, residual stress profile estimation at distances where they completely vanish from weld toe locations need to be recommended based on repair weld geometry i.e., radius to thickness ratio, heat input of the repair welding process and the sequence of welding leading to additional restraints.

Further validation with an FEM-based numerical model considering the effect of metallurgical and phase transformations needs to be developed during the defect assessment procedures of welds.

Acknowledgments: We would like to acknowledge the support of SINTEF Ocean/Structural engineering and NTNU/IMT, Norway for providing free access to the Proto iXRD instrument for measuring residual stresses. We would also like to acknowledge the support of Qustom apps, USA for providing free access to their plugin that we used for modelling welds in ABAQUS.

Authors' contributions: **Sachin Bhardwaj:** Conceptualization, Experimentation, Investigation, Methodology, Visualization, Writing – original draft, Writing – review and editing, Data analysis; **Sigmund Kyrre Aas:** Experimentation, Investigation, Analysis, Writing – review and editing **R.M. Chandima Ratnayake:** Conceptualization, Formal analysis, Review and editing, Funding acquisition, Project administration, Supervision

Funding: The research was fully funded by the Norwegian Ministry of Education (Internal PhD project No. IN-12168). This work was carried out as part of a PhD research project, performed at the University of Stavanger, Norway.

Availability of data and material: All data generated and analysed during this research are included in this published article.

Code availability: Not applicable.

Declarations

Ethics approval	Not applicable.
Consent to participate	Not applicable.
Consent for publication	Not applicable.
Conflict of interest	The authors declare no competing interests.

5. References

1. Antaki GA (2003) Piping and pipeline engineering: design, construction, maintenance, integrity, and repair. Marcel Dekker, New York
2. Lotsberg I (2016) Fatigue Design of Marine Structures. Cambridge University Press, Cambridge
3. Song S, Dong P (2014) Residual Stresses in Weld Repairs and Mitigation by Design. In: ASME 2014 33rd International Conference on Ocean, Offshore and Arctic Engineering
4. Bhardwaj S, Ratnayake RMC (2022) Welding procedure qualification record (WPQR) for welds fabricated at proximity. Int J Adv Manuf Technol
5. Bhardwaj S, Ratnayake RMC (2020) Challenges due to Welds Fabricated at a Close Proximity on Offshore Structures, Pipelines, and Piping: State of the Art. In: ASME 2020 39th International Conference on Ocean, Offshore and Arctic Engineering
6. Institute AP (2015) API 2200 Repairing Hazardous Liquid Pipelines. API: USA
7. DNVGL, DNV-OS-F101 (2013) In: Submarine Pipeline Systems. DNV: Norway
8. Song S, Dong P (2017) Residual stresses at weld repairs and effects of repair geometry. Sci Technol Weld Join 22(4):265–277
9. Dong P (2018) On repair weld residual stresses and significance to structural integrity. Weld World 62(2):351–362
10. Dong P, Zhang J, Bouchard PJ (2001) Effects of Repair Weld Length on Residual Stress Distribution. J Press Vessel Technol 124(1):74–80
11. American Petroleum Institute, API (2007) RP 579-1/ASME FFS-1. Houston, TX: American Petroleum Institute; August 2007.: USA
12. British Energy Generation Ltd (2013) Procedure R6 Revision 4, assessment of the integrity of structures containing defects. UK
13. British Standard, BS (2019) 7910 Guide to methods for assessing the acceptability of flaws in metallic structures: UK
14. Dong P et al (2014) On residual stress prescriptions for fitness for service assessment of pipe girth welds. Int J Press Vessels Pip 123-124:19–29.

15. Bhardwaj S, Ratnayake RMC (2020) Residual stress estimation in defect assessment procedures at weld toe and away locations on girth welds: Review of key parameters. Theor Appl Fract Mech 102848
16. Acevedo C, Nussbaumer A (2013) Effect of tensile residual stresses on fatigue crack growth and S-N curves in tubular joint in compression. Int J Fatigue 36:171–180
17. Larsson M et al (2021) Experimental Residual Stress Investigation of Weld Joints Fabricated at a Close Proximity in S420 Structural Steel 357–376
18. Brickstad B, Josefson BL (1998) A parametric study of residual stresses in multi-pass butt-welded stainless steel pipes. Int J Pressure Vessels Pip 75(1):11–25
19. Bhardwaj S et al (2022) Experimental investigation of residual stress distribution on girth welds fabricated at proximity using neutron diffraction technique. Int J Adv Manuf Technol 121(5):3703–3715
20. Hauk V (1997) 2 - X-ray diffraction. Structural and Residual Stress Analysis by Nondestructive Methods. In: Hauk V (ed) Elsevier Science, Amsterdam, pp 17–65.
21. ABAQUS (2020) User's manual Version 7
22. Qustomapps (2019) Qustom weld plug in ABAQUS
23. Yaghi A, Becker AA (2005) State of the art review - weld simulation using finite element methods. Glasgow: NAFEMS2005.
24. Bhatti AA et al (2015) Influence of thermo-mechanical material properties of different steel grades on welding residual stresses and angular distortion. Mat Des (1980–2015) 65:878–889
25. Barsoum Z, Lundbäck A (2009) Simplified FE welding simulation of fillet welds – 3D effects on the formation residual stresses. Eng Fail Anal 16(7):2281–2289
26. Zhu J, Khurshid M, Barsoum Z (2019) Accuracy of computational welding mechanics methods for estimation of angular distortion and residual stresses. Weld World 63(5):1391–1405
27. Goldak JA, Akhlaghi M (2005) Computational Welding Mechanics. Comput Weld Mech 1–321
28. Rosenthal D (1946) The theory of moving sources of heat and its application to metal treatments. ASME, Cambridge
29. Pei X, Song S, Dong P (2015) An Analytical Method for Estimating Welding-Induced Plastic Zone Size for Residual Stress Profile Development. In: ASME 2015 Pressure Vessels and Piping Conference
30. Song S, Dong P, Pei X (2015) A full-field residual stress estimation scheme for fitness-for-service assessment of pipe girth welds: Part I – Identification of key parameters. Int J Press Vessels Pip 126–127:58–70
31. Song S, Pei X, Dong P (2015) An Analytical Interpretation of Welding Linear Heat Input for 2D Residual Stress Models. In: ASME 2015 Pressure Vessels and Piping Conference

32. Yaghi A et al (2010) A Comparison Between Measured and Modeled Residual Stresses in a Circumferentially Butt-Welded P91 Steel Pipe. J Press Vessel Technol 132
33. Bhardwaj S, Ratnayake RMC (2021) Comparison Between Shrinkage Strain and FEM Thermo-Mechanical Method for Estimation of Welding Induced Residual Stresses. In: ASME 2021 40th International Conference on Ocean, Offshore and Arctic Engineering
34. Bhardwaj S Ratnayake RMC (2021) Estimation of Welding-Induced Plastic Zone Size and Residual Stress Levels: Linear Heat Input Approximation. In: ASME 2021 40th International Conference on Ocean, Offshore and Arctic Engineering
35. Alipooramirabad H et al (2015) Quantification of residual stresses in multi-pass welds using neutron diffraction. J Mater Process Technol 226:40–49
36. Stacey A et al (2000) Incorporation of residual stresses into the SINTAP defect assessment procedure. Eng Fract Mech 67:573_611
37. Bouchard PJ et al (2005) Measurement of the residual stresses in a stainless steel pipe girth weld containing long and short repairs. Int J Press Vessels Pip 82(4):299–310
38. Gandy D, Findlan S, Viswanathan R (2001) Weld Repair of Steam Turbine Casings and Piping—An Industry Survey. J Press Vessel Technol 123
39. Dong P (2008) Length scale of secondary stresses in fracture and fatigue. Int J Press Vessels Pip 85:128–143